Mekelle University

Ethiopian Institute of Technology Mekelle (EiT-M)
School of Mechanical and Industrial Engineering
Automation and Control Chair

Postgraduate Program in Mechatronics Engineering

A Thesis Submitted to Automation and Control Chair in Partial Fulfillment of the Requirements for the Master of Science Degree in Mechatronics Engineering

By: Binyam Tadros

Advisor: Dr Beteley Teka (PhD)

Design of Fuzzy logic controller to series active variable geometry suspension system of automobile vehicle using full car model

(With preview road profile information)

October 2024

THESIS ACCEPTANCE APPROVAL

This is to certify that Mr. Binyam Tadros has incorporated all comments forwarded by the internal and external examiners and the chairperson during the thesis defense.

Members of the Examination Board

Nebyat G/gziabhier	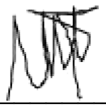	05/04/2025
Name of the Chairman	Signature	Date
Dr. Tsegay Tesfay		05/04/2025
Name of the Internal Examiner	Signature	Date
Dr. Riessom Weldegiorgis	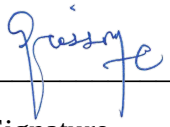	05/04/2025
Name of the External Examiner	Signature	Date

Confirmation: Automation and Control Chair

Nebyat G/gziabhier	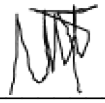	05/04/2025
Name of the Chair Head	Signature	Date

CANDIDATE'S DECLARATION

I declare that this written submission represents my ideas in my own words and where others' ideas or words have been included, I have adequately cited and referenced the sources. I also declare that I have adhered to all principles of academic honesty and integrity and have not misrepresented or fabricated or falsified any idea/data/fact/source in my submission. I understand that any violation of the above will cause disciplinary action by the Institute and can also invoke penal action from the sources which have thus not been properly cited or from whom proper permission has not been taken when needed.

Name of the Candidate: Mr. Binyam Tadros

Signature: _____

Date: _____

ADVISOR'S DECLARATION

This is to certify that the above declaration made by the candidate is correct to the best of my knowledge and the thesis is adequate for the award of the degree of Master of Science in Mechatronics Engineering

Advisor: Dr. Beteley Teka (PHD)

Signature: _____

Date: _____

ACKNOWLEDGEMENT

I would like to take this opportunity to thank God for being my strength and guide in writing of this thesis as well as in general in my life. Without the Almighty of God, I would not have had the wisdom or the physical ability to do so.

I would like to express my sincere appreciation and gratitude to my thesis advisor Dr. Beteley Teka for his guidance, patience, and encouragement. My pursuit of a master's degree was profoundly based upon his character and integrity. He was devoting much time to read my work over and over again and gave me a valuable comment, hence I would like to take this opportunity to thank and let them know I have great respect.

Finally, I must express my very profound gratitude to my parents for providing me with unfailing support and continuous encouragement throughout my years of study and through the process of researching and writing this thesis. This accomplishment would not have been possible without you, my family. Thank you

ABSTRACT

Recent advancements in electro-mechanical active suspensions are presenting new opportunities, showcasing numerous benefits over traditional passive and semi-active systems, while also overcoming the significant drawbacks of other active solutions. This thesis introduces fuzzy logic controller with perfect preview information to improve the performance of Series Active Variable Geometry Suspension (SAVGS), which enhances conventional independent passive or semi-active suspensions by actively regulating the suspension geometry through an electro-mechanical actuator. The research work explores the benefits of this suspension type and provides an in-depth analysis of its simplest form. Additionally, it offers insights into the design process, including liberalized full-car modeling and selection. A control system designed to manage pitch and roll attitude of the chassis is also discussed. Simulation results demonstrate the viability of the proposed system as the fuzzy logic controller (FLC) is developed using MATLAB-Simulink for the SAVGS improves the suspension system, with various performance metrics (Passenger Ride Comfort, Suspension Safety, and Road Handling) evaluated at different speed for Road disturbance. The performance response at 20 kilometer per hour shows improvement in all the performance metrics, like in Passenger ride comfort is reduced in Vertical acceleration by 41.67% with reduced pitch and roll acceleration, Suspension safety is reduced in suspension deflection by 49.1% in front and 43.1% in rear sides with reduced velocity, and in road handling the tire deflection reduces by 46.3% at front and 36.9% at the rear sides of the car.

Keywords: Fuzzy logic controller, SAVGS, variable geometry, active suspension, mechatronics.

TABLE OF CONTENT

Contents

TABLE OF FIGURES

LISTS OF TABLES

LISTS OF ABRIBATION

FLC……Fuzzy logic control

SAVGS……. Series active variable geometry suspension

$H\infty$ ……H-infinity control

$H2$ ……H-control

LQR……...Linear quadratic regulator

LQG……. Linear quadratic Gaussian

PMSM……. permanent magnet synchro's machine

Kg……Kilogram

M_1 or M_s ……. Mass of car body or sprung mass

M_2 or M_u ……. Mass of wheel or Unsprang mass

M_{uf} ……...Front Mass of wheel or Unsprang mass

M_{ur} ……...Rear Mass of wheel or Unsprang mass

Zr……Road profile

X_w or Zu ……. …...Wheel displacement

X_s or Zs ……. Car body displacement

K_a ……...Stiffness of Car body spring

K_t ……...Stiffness of tire

C_a or Ceq ……...Damper

C…….....Front damping

b_r…….....Rear damping

I_P…….....Pitch moment of inertia

I_r…….....roll moment of inertia

T_f…….....Front treat

T_r…….....Rear treat

a……...Distance from center of mass to front wheel

b……...Distance from center of mass to front wheel

$Zcmc$……Center of mass of sprung mass

K_f ……..…...Stiffness of car body sprung of front

K_r …….. Stiffness of car body sprung of rear

K_{tf} ……...Stiffness of front tire

K_{tr} ……...Stiffness of rear tire

CHAPTER 1

INTRODUCTION

1.1 Introduction

Suspension systems are mainly classified as passive, semi active and active suspension. Their main role is to mitigate vibration resulting from uneven road surfaces. Passive suspension utilizes oil dampers and recognizes them for their affordability, reliability, and stable performance. In contrast, semi active suspension uses dampers that can adjust their characteristics based on electrical inputs, offering some control over damping forces, though generally falling short of the performance levels seen in active systems. Active suspension applies external force from the actuator that attenuates most of the transmitted vibration. Active suspension has superior performance over passive and semi active suspension systems, but they are expensive, high-power consumption and may not be reliable or failsafe and mostly uses hydraulic force as external force.

The series active variable geometry suspension is a single or double link rotary introduced to the spring damper unit, while the other end of the link is connected to the chassis[1]. As its name indicates the single link is implemented in series with the former passive components. The single link is driven by a rotor electromechanical actuator to provide force on the passive suspension strut [1][2]. The SAVGS has been considered as potential improvement to active suspension because small increment in the sprung mass, no increment in the unsprang mass, performance improvement, failsafe operation and low power demand[3].

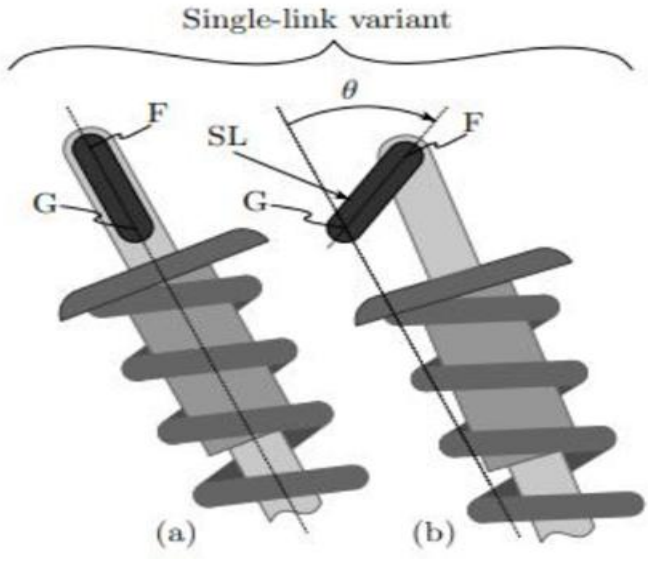

Figure1.1 : single link SAVGS concept[3]

As seen from the above figure 1.1: the mechanical links in these SAVGS variants connect point G in the chassis to point F in the upper end of the link SD through revolute joints. When there is no actuation torque the SL remains in equilibrium position (a). another configuration is reached when torque is applied on point G (b)[3].

The current research focuses on mechatronics systems from Bose's proprietary technology to linear electromechanical actuators. It is the time to see fully electric vehicles with mechanical solution to active suspension system. Because electric vehicles are used widely due to their green energy source.

1.1.1 Technological advancement

The realm of mechatronics is experiencing substantial advancement in suspension technologies, particularly with the rise of electric vehicles. Researchers are investigating sophisticated preview active control strategies designed to predict road conditions, thus minimizing the effects of disturbance on vehicle dynamics use various techniques, including radar, ultrasonic, and cameras are employed for effective road profile information gathering. Several control methods, such as robust approaches (H∞, H2) and intelligent techniques like fuzzy logic and neural networks have been explored to enhance suspension performance[4].

Preview information to control suspension is focused on using the road profile irregularity ahead of the vehicle. This information helps to predict the actuation force ahead and apply the force in prefect timing which means decrease the effect of disturbance on wheel contact area. There are different methods of gathering preview information such as ultrasonic, radar beams, cameras and reflected light.

The control force derived from mathematical model and preview road data has been investigated in active suspension for different controller methods. Analysis within a four-degree freedom model suggests that LQG control and Kalman filtering can significantly improve active suspension system when integrated with preview data. Additionally, both H∞ and H2 control strategies artificial intelligent controller methods like fuzzy logic and neural networks have shown considerable promise in enhancing vehicle dynamics.

The efficiency of active suspension system is growing compared to passive system when used with and without preview information from sensor. The LQG and stochastic optimal control controller are used to improve efficiency by controlling vibration from random road excitation and calculating force ahead of the road respectively[5].

Whereas a full car active suspension system exploited in the H∞ and H2 techniques were used to improve vehicle dynamic criteria. Robust H∞ preview control was investigating for an active system with look ahead sensor [4]. It is obvious the fuzzy control technique plays an active role to designing system controller to generate actuation force. This methodology does not need accurate models of the system but is highly dependent on fuzzy rule base[6].

The series active variable geometry suspension is used to compensate between semi active and active suspension while, giving superior performance from semi active suspension and avoiding the main disadvantage of active suspension system.

1.2 MOTIVATION

The development of the SAVGS aligns with current aspect in the vehicle industry which emphasize hybridization and electrification, which are essential for reducing vehicle weight, particularly in electric vehicles where battery mass presents a significant challenge.

1.3 Problem statement

The series active variable geometry suspension plays a significant role in closing the drawbacks of passive, semi active and active suspensions systems. It addresses the efficiency limitation of both passive and semi active suspensions. while overcoming the drawbacks commonly associated with active suspension system such as mass and energy demand.

Currently cars have much electric power to drive the car and facilities the other systems on the car. So that it is better to use electromechanical actuator to drive the suspension system of electric cars like SAVGS and we must control it very precisely.

1.4 objective

1.4.1 General objective

To design a fuzzy logic controller for the series active variable geometry suspension that utilizes preview information, aimed at enhancing passenger comfort and vehicle handling using full car model.

1.4.2 Specific objective

The specific objectives are

- To develop a full car mathematical model of passive suspension system.
- Create mathematical dynamic model of the series active variable geometry suspension system
- Design fuzzy logic controller to determine the necessary actuation force for SAVGS
- Assess SAVGS performance through MATLAB-Simulink computer simulation and compare it with traditional passive suspension system.

1.5 scope of the thesis

This thesis focuses on building a model for the SAVGS and design fuzzy logic control base when assumed accurate preview information, thereby refining the broader scope of suspension system research.

1.6 limitation

The thesis on series active variable geometry suspension (SAVGS) system and fuzzy logic controller were simulated under idealized conditions. The model employed is primarily linear, which may not fully capture the nonlinear dynamics inherent in real world vehicle suspension systems, especially under extreme road conditions or high-speed variations. Another limitation of the thesis assumes perfect and instantaneous sensor measurement, without accounting for potential sensor noise delays, which could impact the system responsiveness in practical application. The limitations suggest that further experimental validation is needed to verify the findings and refine the controller for real world conditions.

In this research the design FLC is limited to using only five triangular membership functions; it doesn't compare with different membership function types and with extended number of membership functions. Additionally, there is no comparisons of different controller design approaches only the FLC is selected as it is robust and good for systems having uncertainty, vagueness, and it could compensate the nonlinearity behaviors of the SAVGS system as we use the liberalizes model of SAVGS.

1.7 thesis organization

The structure of this thesis is organized as follows: starting as introduction from this chapter it flows as; Chapter 2: literature review and methodology

This chapter provides a compressive review of existing literature on vehicle suspension systems. Control strategies and fuzzy logic controllers. Chapter 3: system modeling; In this chapter, the mathematical models for both passive and SAVGS systems are developed for full-car model based on Newtons law. Chapter 4: controller design; This chapter discusses design and implementation of the fuzzy logic controller (FLC) for SAVGSS in MATLAB.

Chapter 5: simulation and result; Simulation results are presented in this chapter, comparing the performance of the passive suspension system with the SAVGS system controlled by FLC using Key performance metrics. Chapter 6: conclusion and recommendation; The final chapter summaries' the findings and discusses the limitations of the study and provides recommendation for future work.

CHAPTER 2

LITERATURE REVIEW AND METHEDOLOGY

2.1 Literature Review

The active suspension system includes an actuator and sensor and control unit that can input force and displacement to the passive suspension system. In the control process, the active suspension system adjusts the output of active suspension actuator according to real time changes of the road input and vehicle status. There by canceling the influence of the road and obtaining a good shock absorption effects while controlling the height and altitude[7].

The SAVGS system is a new family of electromechanical active suspension which significantly surpasses passive and semi-active suspensions while avoiding the primary drawbacks of alternative solution used in high performance sport cars[1]. The feasibility of single link series active variable geometry suspension has been confirmed by conducting experiments on quarter car test rigs which reduces suspension deflection and vertical acceleration[3].

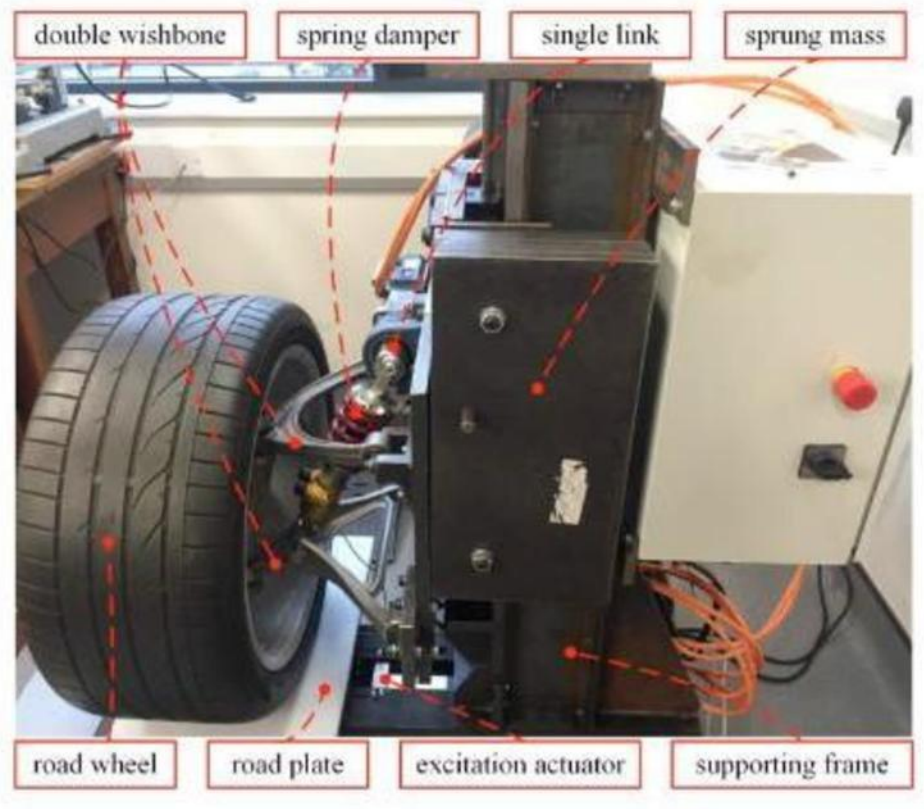

Figure 2.1 : The SAVGS quarter car test rig[2]

In almost all full car models the researchers use mechanical modification to both front corners of double wishbone suspension with single link attached to upper ends of spring damper unit, while both rear corner suspensions remain in original alignment[2].the linearzed model of full car dynamics has been used to improve chassis vertical acceleration and suspension performance while small mass increment with respect to passive suspension systems[2].

Since the research work focuses on control systems for academic purposes, I prefer to use linearized full car model with all corners of the vehicle modified with single link series active variable geometry suspension increase performance in all aspects. As mentioned on introduction fuzzy logic control is becoming familiar to control vehicles suspension system over other control systems. For example, fuzzy logic controls outperform linear quadratic regulator control in reducing the acceleration of the sprung mass when the suspension system is modeled using a two degree of freedom linear time invariant quarter car model [8]. The ride comfort and handling stability performance of the active suspension surpass the passive one when uncertainty due nonlinearity on controller is approximated by fuzzy logic control and robustness of the controller reduced by adaptive controller[7].

The preview information has significant importance on improving ride comfort and vehicle stability. The preview information is used to control disturbances input from the road to the tire contact patch. This uses various sensing techniques like radar beams, reflected light, ultrasonic and cameras to obtain information about the road profile ahead of the vehicle[9].

Preview active control suspension involves the acquisition and use of information concerning the road profile ahead of the vehicle integrates mathematical model between the preview signals and the controller for estimated the control force have been investigated with active suspension for wide range of controller techniques.

The road input can be provided for a vehicle in advance by using an optical sensor to preview the front terrain and suspension parameters can be adjusted before a corresponding moment to keep the body as smooth as possible and thus improve ride comfort and handling stability this shows that the ride comfort and handling stability surpass the passive suspension[10]. Preview information was also used to control active seat suspension intended for use in vehicles with suspension of wheel used as preview data to the control action[9].

2.2 Fuzzy Logic Controller

Fuzzy logic control (FLC) is an advanced control methodology that mimics human reasoning to manage complex systems. Unlike traditional controllers which rely on precise mathematical models, fuzzy logic controllers leverage linguistic variables and human-like decision making processes. This approach is especially beneficial when dealing with systems where exact modeling is challenging, enabling intuitive control that adapts the system uncertainties and nonlinearity. We can discuss the key concepts and relating to this study as follows having concepts based on references[19] [20][21][22][23].

Key Concepts in Fuzzy Logic Control

1. **Fuzzy sets and Membership Functions:** Traditional set theory is binary- an element is either a member of a set or isn't. Fuzzy set theory, introduced by Lofti A.Zedah, expands on this concept by allowing partial membership, which is defined by a *membership function*. This function assigns degree of membership, ranging from 0 (not a member) to 1 (full member), thus enabling elements to partially belong to multiple sets. For example, temperatures can be classified/ranges "Could", "Warm", and "Hot" with varying degree of membership, allowing for smooth transition and flexible control.
2. **Fuzzy Rules and Linguistic Variables:** fuzzy logic controls use a set of IF-THEN riles based on linguistic terms (e.g. "IF speed is High THEN breaking should be Strong") rather than precise numerical values. These rules are formulated by the experts or derived from experience, incorporating human expertise directly into the control processes. This rule-based approach enables FLCs to handle complex systems without requiring a detailed mathematical model.
3. **Inference and Defuzzification:** The fuzzy inference process combines the rules and evaluates the input condition to produce fuzzy outputs. Then defuzzification converts these fuzzy outputs back into precise control actions. Common defuzzification methods includes centroid and weighted average approaches, which translates the fuzzy results into specific, actionable commands.

Historical Development and Applications

In 1975, Mamdani and colleagues expanded on Zadeh's fuzzy set theory to develop a practical fuzzy logic controller for a steam engine model. This work demonstrated that FLCs could be successfully applied to real-world systems, paving the way for broader adoption. Since then, fuzzy control has been implemented in numerous consumer products and industrial applications, such as:

- **Consumer Electronics**: Washing machines, air conditioners, and other appliances use fuzzy logic to optimize performance based on variable conditions.
- **Automotive Systems**: Fuzzy logic controls various car functions, from transmission to braking systems, improving comfort and stability.
- **Elevator Control**: Fuzzy algorithms manage elevator speeds and stops based on load and demand, enhancing efficiency.
- **Suspension Systems**: Fuzzy logic controllers have been applied to vehicle suspension systems, as in the study by Patil et al., where an FLC improved ride comfort and stability by dynamically adjusting suspension forces.

Fuzzy Logic for Suspension Systems

In automotive applications, particularly in suspension systems, fuzzy logic controllers are effective because they can adjust in real-time to changing road conditions and driving scenarios without needing a precise mathematical model.

For example, Patil et al. designed a fuzzy logic controller for a quarter-car suspension model, improving chassis stability and ride comfort by adjusting damping forces based on vehicle movement and road feedback.

Advantages of Fuzzy Logic Control

- **Human-Like Reasoning**: FLCs replicate human thought processes, making them intuitive for complex systems.
- **No Need for Exact Models**: Unlike traditional controllers, FLCs do not require exact mathematical modeling and make them suitable for non-linear or uncertain systems.
- **Smooth and Adaptive Control**: The partial membership function allows for smooth transitions between control states, improving adaptability to varying conditions.

In conclusion, Fuzzy logic controllers provide a flexible and adaptive approach to managing complex, non-linear systems by incorporating human reasoning and expertise into control logic. With applications spanning from household products to complex industrial systems, FLCs represent a robust solution for scenarios where traditional mathematical models fall short. The success of fuzzy control in areas such as automotive suspension underscores its potential for enhancing comfort, stability, and safety in dynamically changing environments.

2.3 Methodology

To increase understanding about the suspension system (passive, semi active and active) I will conduct a literature review on an existing suspension including series active variable suspension. Also find the standards to measure performance parameters of suspension for the designed system. So, in doing this proposed thesis it is considered to combine different sections, which are developed to increase the performance of vehicle suspension in different places to come up with best research. In general, in order to come up with good design of fuzzy logic controller to series active variable geometry suspension system of automobile vehicle using full car model following steps are followed.

As stated in the following flow chart, after reviewing research gaps and having the linearized mathematical full car model of the SAVGS will be found in differential dynamic equations. Having the model of the SAVGS system we use FLC to control actuation force using rule base as foundation. The controller will be implemented using MATLAB toolbox. Finally, it will be simulated using MATLAB-Simulink environment to design the system. At the end, the result will be interpreted, compared and discussed with the passive suspension system.

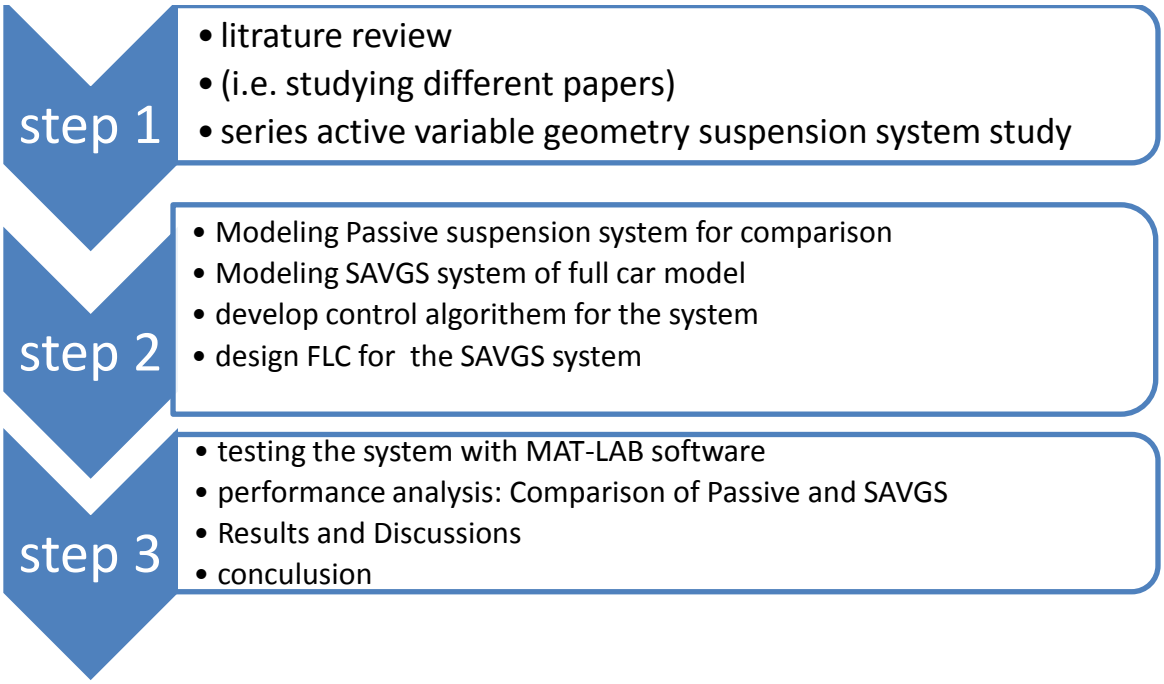

How modeling will do: The model's development is grounded on Newton's laws of motion, providing the systematic approach to capturing the dynamics of the suspension system. So using this principle we start with the Quarter-car Schematic model of passive and SAVGS and will Extend this model to Full-car Passive and SAVGS System models respectively by having basic Consideration and incorporating the Roll and pitch motions.

How FLC Designing and Simulations will done: The design approach of a fuzzy logic controller (FLC) for the Series Active Variable Geometry Suspension (SAVGS) system follows starting from identifying the control objective first and follow with assessments of the existing passive suspensions system performance for taken performance matrices and observing or having data how the error and error rates of the desired response goes using MATLAB-Simulink simulation software. Having the simulation results will help us to develop the Rule-Bases of the FLC by observing the input and output behaviors of the suspension system. Here the developed Mathematical model of the dynamic linear differential state equation of the full-car SAVGS system will be implemented on MATLAB-Simulink environment with designed FLC in MATLAB fuzzy tool box and then simulated to see how the performance criteria's are meet or not depending on the taken three performance matrices which detailed in the controller design section.

Finally, the simulation results will be compared and discussed for the designed FLC controller algorithm based on the performance matrices.

CHAPTER 3

SYSTEM MODELING AND ANALAYSIS

3.1 Introduction

This chapter provides foundational insights into the mathematical modeling of series active variable geometry suspension system (SAVGS) with in full car model. By developing the dynamic mathematical model that captures the input-output relationships, readers gain a deeper understanding of the dynamic system behavior. Initially a non-linear multi-body model constructed in different studies was revised for use in numerical simulations. From this, a linearzed equivalent mathematical model is derived and serves as a base for synthesizing a fuzzy logic control (FLC) scheme, which will be detailed in the following chapter.

The chapter begins with the discussions on developing mathematical modeling for both passive and active suspension (SAVG) systems in quarter-car modeling and laying the groundwork for understanding suspension dynamics. This will lead to extending to the full-car model and setting the stage for comprehensive examination of the (SAVG) system.

3.2 Full-Car Mathematical Modeling of Passive suspension System

In full-car modeling, the car body (sprung mass) is permitted to experience rolling and pitching motion. The suspension system links this car body to the four distinct tires or wheel (Unsprang mass) at the front left and right, rear left and right wheels. Each wheel is free to move vertically or ‘bounce’ relative to the sprung mass and representing the dynamic interaction between the car body and the wheels.

The model’s development is grounded on Newton’s laws of motion, providing the systematic approach to capturing the dynamics of the suspension system. Based on these principles, a mathematical model of the full-car suspension is derived using the framework provided in [1][3][4] as a foundational reference. This model serves for analyzing the interactions between the car’s body and suspension system under various dynamic conditions.

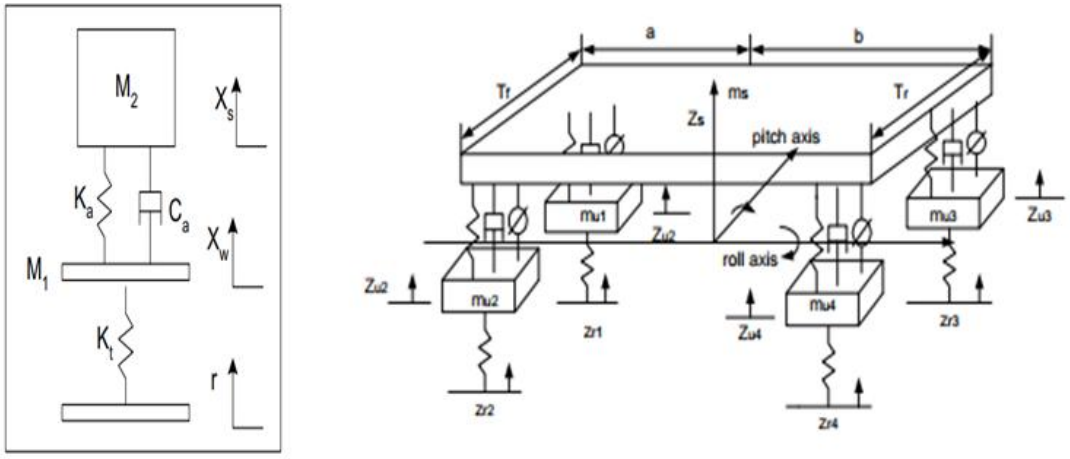

(a) (b)

Figure 3.1 : Passive Suspension system block diagram for a) Quarter-Car Model b) Full-Car Model[11]

To drive the mathematical equation for the quarter-car model, we'll start by applying Newton's second law to the primary component of the system and beginning with the sprung mass $M1$ of the car body supported by the suspension system) and considering the dynamics of the Unsprang mass (the wheel and other connected parts).

In the quarter-car model, the suspension system is represented by a single spring and damper connecting the sprung mass M1 and Unsprang mass M2 which interacts with the road through a tire modeled as a spring.

action of motion for sprung mass

- Xs vertical displacement of sprung mass (M1)
- Xw vertical displacement of Unsprang mass (M2)

Given the suspension spring constant Ka and Damping coefficient, Ca we can apply Newton's law for the sprung mass (M1), considering the force acting on due to the suspension system.

The equation for $M1$ is:

$$M_1\ddot{X} = -K_a(X_s - X_w) - C_a(\dot{X}_s - \dot{X}_w) \quad (3.1)$$

Here:

- $K_a(X_s - X_w)$ is the force exerted by the suspension system
- $C_a(\dot{X}_s - \dot{X}_w$ is the force exerted by the damping element of the suspension

Equation of motion for Unsprang mass ($M2$):

For the Unsprang mass 2, we need to consider both the suspension system and the tire's interaction with the road surface. Let:

- Kt be the tire stiffness
- Xr be the road surface displacement (or disturbance)

The equation for $M2$ is:

$$M_2\ddot{X} = K_a(X_s - X_w) + C_a(\dot{X}_s - \dot{X}_w) - K_t(X_w - X_r) \quad (3.2)$$

Here:

- $K_a(X_s - X_w)$ And $C_a(\dot{X}_s - \dot{X}_w$ represents the force exerted by the suspension spring and damper on mass M_2 .
- $K_t(X_w - X_r)$ As force exerted by the tire compresses or stretches relative to road surface.

These two equations together describe the quarter-car model's dynamic behavior and capturing the interaction between sprung and unsprang mass through the suspension system and the contact with the road through the tire stiffness.

To derive the mathematical model for full-car passive suspension system, will extend the quarter-car model to account for the roll and pitch dynamics of the car body. In this setup the car body (Sprung mass) is represented by Ms that can undergo vertical (heave), roll, and pitch movements. The four unsprung masses ($Muf1, Muf2, Mur3, Mur4$) represent front left and right, rear left and right wheels respectively.

Assumptions and definitions:

- Let's Zs represents vertical displacement of the car body (sprung mass Ms
- Zuf1, Zuf2, Zur3, Zur4 represents the vertical displacement of each wheel (unsprung mass)
- The suspension spring constants are $Kf1, Kf2$ and $Kr3, Kr4$ for front left and right, rear left and right respectively
- The damping coefficients are $Cf1, Cf2, Cr3, Cr4$.
- Tire stiffness constants are $Kt1, Kt2, Kt3, Kt4$.
- Road displacement at each wheel is $Zr1, Zr2, Zr3, Zr4$

- The distance from the car's center of mass (COM) to each wheel is defined as a, b, Tf, Tr:
  - T_f: half-width of car (from the car COM to the left or right front side)
  - T_r: half-width of car (from the car COM to the left or right rear side)
  - a: the distance from COM to the front axle
  - b: the distance from COM to the rear axle

The car body can pitch (rotation about the lateral axis with moment of inertia I_{ry}) and roll (about the longitudinal axis with moment of inertia I_{rx})

So, let:

- θ_s be the pitch angle
- φ_s be the roll angle

Equation of motion for sprung mass (car body)

The motion of the car body (sprung mass) involves vertical, pitch and rolling movements. Using the Newton's second law the vertical (heave) motion, pitch moment, and roll moments are as follow:

1. Vertical (Heave) motion:

   $M_s\ddot{Z}_s = -\sum_i K_{fi}(Z_{si} - Z_{ui}) + C_{fi}(\dot{Z}_{si} - \dot{Z}_{ui})$

   (3.3)

   Here (Z_{si}) represents the vertical displacement velocity contribution due to pitch and roll motion at each corner, and it is defined as:

$Z_{s1} = Z_s + T_f\varphi_s + a\theta_s$ $\dot{Z}_{s1} = \dot{Z}_s + T_f\dot{\varphi}_s + a\dot{\theta}_s$

(3.4)

$Z_{s2} = Z_s + T_f\varphi_s - a\theta_s$ $\dot{Z}_{s2} = \dot{Z}_s + T_f\dot{\varphi}_s - a\dot{\theta}_s$

(3.5)

$Z_{s3} = Z_s - T_r\varphi_s + b\theta_s$ $\dot{Z}_{s3} = \dot{Z}_s - T_r\dot{\varphi}_s + b\dot{\theta}_s$

(3.6)

$Z_{s4} = Z_s - T_r\varphi_s - b\theta_s$ $\dot{Z}_{s4} = \dot{Z}_s - T_r\dot{\varphi}_s - b\dot{\theta}_s$

(3.7)

So it will be:

$$M_s\ddot{Z}_s = -K_{f1}(Z_{s1} - Z_{u1}) - C_{f1}(\dot{Z}_{s1} - \dot{Z}_{u1}) - K_{f2}(Z_{s2} - Z_{u2}) - C_{f2}(\dot{Z}_{s2} - \dot{Z}_{u2}) - K_{f3}(Z_{s3} - Z_{u3}) - C_{f3}(\dot{Z}_{s3} - \dot{Z}_{u3}) - K_{f4}(Z_{s4} - Z_{u4}) - C_{f4}(\dot{Z}_{s4} - \dot{Z}_{u4}) \quad (3.8)$$

Then substituting $Z_{si}\ and\ \dot{Z}_{si}$ as defined in the above to the equation.

2. Pitch motion:

The pitch equation of moment around the car center of mas is:

$$I_{ry}\ddot{\theta}_s = -a\left(K_{f1}(Z_{s1} - Z_{u1}) + C_{f1}\left(\dot{Z}_{s1} - \dot{Z}_{u1}\right)\right) - a\left(K_{f2}(Z_{s2} - Z_{u2}) + C_{f2}\left(\dot{Z}_{s2} - \dot{Z}_{u2}\right)\right) + b\left(K_{f3}(Z_{s3} - Z_{u3}) + C_{f3}\left(\dot{Z}_{s3} - \dot{Z}_{u3}\right)\right) + b\left(K_{f4}(Z_{s4} - Z_{u4}) + C_{f4}\left(\dot{Z}_{s4} - \dot{Z}_{u4}\right)\right)$$

(3.9)

3. Roll motion:

The roll moment of equation about the car center of mass is:

$$I_{rx}\ddot{\varphi}_s = -T_f\left(K_{f1}(Z_{s1} - Z_{u1}) + C_{f1}\left(\dot{Z}_{s1} - \dot{Z}_{u1}\right)\right) + T_f\left(K_{f2}(Z_{s2} - Z_{u2}) + C_{f2}\left(\dot{Z}_{s2} - \dot{Z}_{u2}\right)\right) - T_r\left(K_{f3}(Z_{s3} - Z_{u3}) + C_{f3}\left(\dot{Z}_{s3} - \dot{Z}_{u3}\right)\right) + T_r\left(K_{f4}(Z_{s4} - Z_{u4}) + C_{f4}\left(\dot{Z}_{s4} - \dot{Z}_{u4}\right)\right)$$

(3.10)

Equation of motion for each unsprung mass

For each unsprung mass M_{ui} using newton's second law of motion and considering the suspension and tire forces, we have:

$$M_{ui}\ddot{Z}_{ui} = K_{fi}(Z_{si} - Z_{ui}) + C_{fi}\left(\dot{Z}_{si} - \dot{Z}_{ui}\right) - K_{ti}(Z_{ui} - Z_{ri})$$

(3.11)

So, for each corner it will be:

$$M_{u1}\ddot{Z}_{u1} = K_{f1}(Z_{s1} - Z_{u1}) + C_{f1}\left(\dot{Z}_{s1} - \dot{Z}_{u1}\right) - K_{t1}(Z_{u1} - Z_{r1})$$

$$M_{u2}\ddot{Z}_{u2} = K_{f2}(Z_{s2} - Z_{u2}) + C_{f2}\left(\dot{Z}_{s2} - \dot{Z}_{u2}\right) - K_{t2}(Z_{u2} - Z_{r2})$$

$$M_{u3}\ddot{Z}_{u3} = K_{f3}(Z_{s3} - Z_{u3}) + C_{f3}\left(\dot{Z}_{s3} - \dot{Z}_{u3}\right) - K_{t3}(Z_{u3} - Z_{r3})$$

$$M_{u4}\ddot{Z}_{u4} = K_{f4}(Z_{s4} - Z_{u4}) + C_{f4}\left(\dot{Z}_{s4} - \dot{Z}_{u4}\right) - K_{t4}(Z_{u4} - Z_{r4})$$

These equations together from 3.3 to 3.11 form a comprehensive model of the full-car passive suspension system and capturing the vertical (heave), roll, and pitch dynamics of the car body, as well as the vertical motion of each wheel. This model serves as basis for comparing passive system's performance with that of series active variable geometry suspension (SAVGS) system.

With the following assigned state variables in Table 3.1 and definition of each state variable we can form the state equation below.

Table 3.1: Full-car model state variables

$X_1 = \varphi_s$	$X_8 = \dot{\varphi}_s$
$X_2 = \theta_s$	$X_9 = \dot{\theta}_s$
$X_3 = Z_s$	$X_{10} = \dot{Z}_s$
$X_4 = Z_{u1}$	$X_{11} = \dot{Z}_{u1}$
$X_5 = Z_{u2}$	$X_{12} = \dot{Z}_{u2}$
$X_6 = Z_{u3}$	$X_{13} = \dot{Z}_{u3}$
$X_7 = Z_{u4}$	$X_{14} = \dot{Z}_{u4}$

Table 3.2: Full-car State variable definitions

Variables	Definitions
φ_s	Roll angle
$\dot{\varphi}_s$	Roll rate
θ_s	Pitch angle
$\dot{\theta}_s$	Pitch rate
Z_s	Vertical displacement
$\dot{Z}_s$	Vertical velocity
Z_{u1}	Vertical displacement of front right wheel
$\dot{Z}_{u1}$	Vertical velocity of front right wheel
Z_{u2}	Vertical displacement of front left wheel
$\dot{Z}_{u2}$	Vertical velocity of front left wheel
Z_{u3}	Vertical displacement of rear right wheel
$\dot{Z}_{u3}$	Vertical velocity of rear right wheel
Z_{u4}	Vertical displacement of rear left wheel
$\dot{Z}_{u4}$	Vertical velocity of rear left wheel

The state space form can be written as in equation 3.12 and the above differential dynamic equations can be rewritten as state equations as shown below.

$$\dot{X}(t) = AX(t) + f(t) \tag{3.12}$$

$\dot{X}_1 = \dot{\varphi}_s \; is \; X_8$

$\dot{X}_2 = \dot{\theta}_s \; is \; X_9$

$\dot{X}_3 = \dot{Z}_s \; is \; X_{10}$

$$\dot{X}_4 = \dot{Z}_{u1}\ is\ \ X_{11}$$

$$\dot{X}_5 = \dot{Z}_{u2}\ is\ \ X_{12}$$

$$\dot{X}_6 = \dot{Z}_{u3}\ is\ \ X_{13}$$

$$\dot{X}_7 = \dot{Z}_{u4}\ is\ \ X_{14}$$

$$\dot{X}_8 = \ddot{\varphi}_s\ \approx [-T_f\left(K_{f1}\left((X_3 + T_f X_1 + aX_2) - X_4\right) + C_{f1}\left((X_{10} + T_f X_8 + aX_9) - X_{11}\right)\right) + T_f\left(K_{f2}\left((X_3 - T_f X_1 + aX_2) - X_5\right) + C_{f2}\left((X_{10} - T_f X_8 + aX_9) - X_{12}\right)\right) - T_r\left(K_{f3}((X_3 + T_r X_1 - bX_2) - X_6) + C_{f3}((X_{10} + T_r X_8 - bX_9) - X_{13})\right) + T_r\left(K_{f4}((X_3 - T_r X_1 - bX_2) - X_7) + C_{f4}((X_{10} - T_r X_8 - bX_9) - X_{14})\right)]/I_{rx}$$

$$\dot{X}_9 = \ddot{\theta}_s \approx [-a\left(K_{f1}\left((X_3 + T_f X_1 + aX_2) - X_4\right) + C_{f1}\left(\left((X_{10} + T_f X_8 + aX_9) - X_{11}\right)\right)\right) - a\left(K_{f2}\left((X_3 - T_f X_1 + aX_2) - X_5\right) + C_{f2}\left((X_{10} - T_f X_8 + aX_9) - X_{12}\right)\right) + b\left(K_{f3}((X_3 + T_r X_1 - bX_2) - X_6) + C_{f3}((X_{10} + T_r X_8 - bX_9) - X_{13})\right) + b\left(K_{f4}((X_3 - T_r X_1 - bX_2) - X_7) + C_{f4}((X_{10} - T_r X_8 - bX_9) - X_{14})\right)]/I_{ry}$$

$$\dot{X}_{10} = \ddot{Z}_s \approx [-K_{f1}\left(\left(X_3 + T_f X_1 + aX_2\right) - X_4\right) - C_{f1}\left(\left(X_{10} + T_f X_8 + aX_9\right) - X_{11}\right) - K_{f2}\left(\left(X_3 - T_f X_1 + aX_2\right) - X_5\right) - C_{f2}\left(\left(X_{10} - T_f X_8 + aX_9\right) - X_{12}\right) - K_{f3}((X_3 + T_r X_1 - bX_2) - X_6) - C_{f3}\left((X_{10} + T_r X_8 - bX_9) - X_{13}\right) - K_{f4}\left((X_3 - T_r X_1 - bX_2) - X_7\right) - C_{f4}\left((X_{10} - T_r X_8 - bX_9) - X_{14}\right)]/M_s$$

$$\dot{X}_{11} = \ddot{Z}_{u1} \approx [K_{f1}\left(\left(X_3 + T_f X_1 + aX_2\right) - X_4\right) + C_{f1}\left(\left(X_{10} + T_f X_8 + aX_9\right) - X_{11}\right) - K_{t1}(X_4 - Z_{r1})]/M_{u1}$$

$$\dot{X}_{12} = \ddot{Z}_{u2} \approx [K_{f2}\left(\left(X_3 - T_f X_1 + aX_2\right) - X_5\right) + C_{f2}\left(\left(X_{10} - T_f X_8 + aX_9\right) - X_{12}\right) - K_{t2}(X_5 - Z_{r2})]/M_{u2}$$

$$\dot{X}_{13} = \ddot{Z}_{u3} \approx [K_{f3}((X_3 + T_r X_1 - bX_2) - X_6) + C_{f3}((X_{10} + T_r X_8 - bX_9) - X_{13}) - K_{t3}(X_6 - Z_{r3})]/M_{u3}$$

$$\dot{X}_{14} = \ddot{Z}_{u4} \approx [K_{f4}\left((X_3 - T_r X_1 - bX_2) - X_7\right) + C_{f4}\left((X_{10} - T_r X_8 - bX_9) - X_{14}\right) - K_{t4}(X_7 - Z_{r4})]/M_{u4}$$

3.3 Mathematical modeling and Model Analysis of SAVGS

In this study, Series active variable geometry suspension (SAVGS) system is used as an advanced mechanism within mechatronic suspension system, aiming to enhance vehicle

handling, stability, and comfort. The SAVGS concept has recently gained attention and was initially studied and proposed in earlier works ([12]-[13]). Here the concept is adapted and extended with a linearized model for application in both quarter-car and full-car settings.

3.3.1 Model Analysis and SAVGS Concept

SAVGS concept overview:

The SAVGS system introduces a unique approach to suspension dynamics by incorporating additional active components that alter the geometry of the suspension system in real time. Unlike conventional passive suspension systems, which rely solely on spring-damper to control the vertical motion of the wheel and car body, the SAVGS system adds an active linkage in between the spring-damper unit and the vehicle chassis.

Mechanism of SAVGS system in quarter-car model:

As shown in figure 3.2 below the SAVGS system is initially applied to a quarter-car model with a double-wishbone suspension. In this configuration:

- The spring-damper element is connected to the points E and F.
- The active component is introduced as single-link mechanisms between points of F and G.

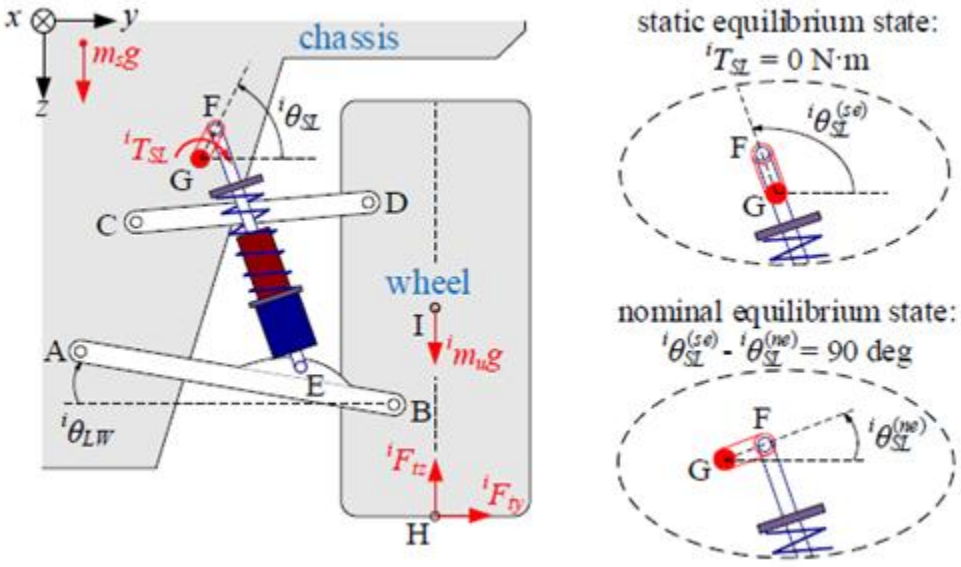

Figure 3.2: The SAVGS in quarter-car with double-wishbone suspension schematic diagram [3].

The active component between points F and G is designed to change the suspension geometry through actuation. By adjusting the position or angle of the linkage in real time, the system can modify the effective motion characteristics of the suspension without changing the properties of spring or damper itself. This geometry adjustment allows for fine-tuning of the suspension's response to various driving conditions, achieving a balance between comfort and handling performance.

As the image shows the schematic of series active variable geometry suspension (SAVGS) system applied to a quarter-car model which is the same concept to full-car model with a double-wishbone suspension. Here's a breakdown the key elements and their roles in SAVGS setups as discussed in[9]:

1. **Suspension Linkages:**
   - Points A, B, C, D, E, F, and G indicate the key points in the suspension geometry. The setup includes double-wishbone linkage, which provides a stable connection between the chassis and the wheel.
2. **Spring and Damper:**
   - The spring-damper unit connects points E and F. This unit provides the passive suspension force, which resists vertical movements of the wheel, helping to absorb shocks from the road surface.
3. **Active geometry adjustment (points F and G):**
   - The critical feature of SAVGS is the introduction of an active single-link mechanism between points F and G. This link can change its angle or position, actively modifying the suspension geometry in real time. By adjusting the angle θ_{sl} of the link F and G, the system changes the suspensions dynamic responses.
4. **Equilibrium States:**
   - The schematic includes two configurations:
     - Static equilibrium state: Here the angle $\theta_{sl}^{(se)}$ results in zero net torques (i.e. $iT_{sl} = 0$) on the suspension link F-G.
     - Nominal equilibrium state: In this state the angle $\theta_{sl}^{(ne)}$ differs from the static equilibrium angle by 90 degrees (i.e. $\theta_{sl}^{(se)} - \theta_{sl}^{(ne)} = 90\ deg$), which changes effective geometry of the suspension system.
5. **Force and moments:**
   - iT_{sl} Represents the torques applied to adjust the angle of the active link.
   - $iF_{TE}\ and\ iF_{Ty}$ Are the forces acting on point E due to the interaction of the wheel and the suspension system?
   - Gravitational forces are represented as $M_s g$ for the chassis and $m_u g$ for the wheel.

In conclusion the rotation of the single link, with respect to the pivot joint 'G' operates within the range of $\Delta\theta_{sl}^{i} \in [0\ 180]\ deg$, where $\Delta\theta_{sl}^{i}$ defined as $\Delta\theta_{sl}^{i} = \Delta\theta_{sl}^{(se)i} - \Delta\theta_{sl}^{i}$. Therefore, if the road wheel is assumed fixed $\Delta\theta_{sl}^{i} = 0$ (which is corresponding to static equilibrium position) leads to the lowest chassis height, while$\Delta\theta_{sl}^{i} = 180$. The chassis is lifted up by the maximum amount. Additionally, both variation of spring-damper forces and vertical tire forces are most sensitive to the rotation of single-link at about the nominal equilibrium state $\Delta\theta_{sl}^{i} = 0$([9].

This SAVGS setup allows the suspension system to dynamically adjust in response to road conditions or driving demands. By actively controlling the angle θ_{sl}^{i}, the system can vary the suspension spring and damping characteristics. This adaptability helps to improve ride comfort, handling, and stability by adjusting the suspension responses in real time.

In the concept of modeling and control, this configuration provides flexibility in designing control strategies that adjust geometry actively, based on the input's vehicle speed, road profile and driver commands. The quarter-car SAVGS model can be extended to full-car setup, where each wheel would have the same configuration, allowing for coordinated control of the vehicles vertical, pitch, and roll dynamics.

3.3.2 Linear equivalent mathematical model of SAVGS

The linear equivalent model for full-car SAVGS which accounts for main SAVGS non-linearity basically can be used for control design strategies. Here the non-linear setup for quarter-car model is linearized and will be extended to full-car SAVGS model with basic considerations, which will be discussed letter in this subsection. The modeling is adapted extended based on reference and the quarter-car suspension is linearized according to procedures detailed in which extended to full-car model [3][14] and the schematic diagram on figure 3.3 shows it below.

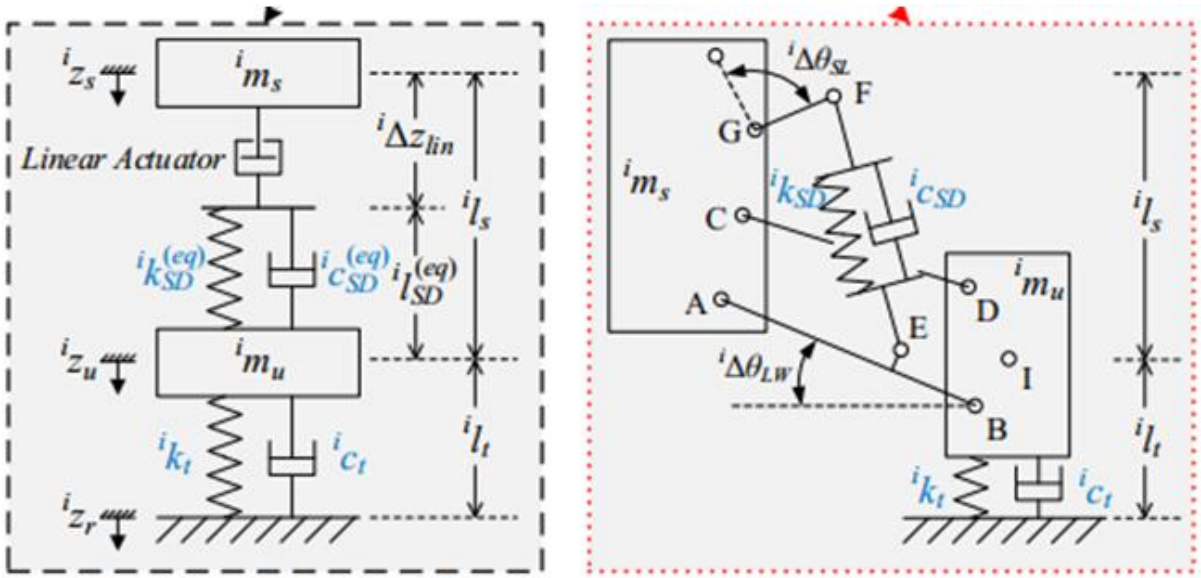

Figure3.3: Quarter-car schematic model of SAVGS [3]

The linear equivalent model shown on the left uses a spring-damper and actuator setup which is simplified compared to the non-linear multi-body on the right. Note here the function i_{α} to be seen is crucial for:

1. **Converting rotational motion** ($i_{\omega_{sl}}$) in the non-linear model into vertical displacement ($i_{\Delta Z_{lin}}$) in the linear model, which will be discussed later in full-car model detailed.
2. **Addressing the geometric nonlinearities** of the SAVGS which are compensated by control system to maintain desired dynamics.

General dynamic state equation representation of linear equivalent model:

Based on the setup shown in figure 3.3 the linearzed SAVGS system can be expressed in dynamic state equations. Here is the outline for the state variables, inputs, and the dynamic state equations.

State variables let's define the following variables for the linear equivalent model.

1. Sprung mass position and velocity
   - (i_{Z_s}) position of sprung mass (chassis)
   - ($i_{\dot{Z}_s}$) Velocity of sprung mass
2. Unsprung mass position and velocity
   - (i_{Z_u}) Position of unsprung mass (wheel)
   - ($i_{\dot{Z}_u}$) velocity of unsprung mass
3. Linear equivalent position and velocity
   - ($i_{\Delta Z_{lin}}$) Actuator displacement
   - ($i_{\Delta \dot{Z}_{lin}}$) Actuator velocity

Generally having actuator force ($i_{f_{act}}$) and road disturbance (i_{Z_r}) as an input, and the vertical position (i_{Z_s}) of sprung and unsprung mass position (i_{Z_u}), the suspension deflection ($i_{l_s} = i_{Z_s} - i_{Z_u}$) , tire deflection ($i_{l_t} = i_{Z_u} - i_{Z_r}$), velocity, and (roll ($\ddot{\theta}_s$) and pitch ($\ddot{\varphi}_s$) accelerations in case of full-car model) as an output we can have the following dynamic model equations.

1. The sprung mass dynamics: Using Newton's second law

$$m_s i_{\ddot{Z}_s} = -Ksd\left(i_{Z_s} - i_{Z_u} - i_{\Delta Z_{lin}}\right) - Csd(i_{\dot{Z}_s} - i_{\dot{Z}_u} - i_{\Delta \dot{Z}_{lin}})$$
(3.13)

2. The unsprung mass dynamics:

$$m_u i_{\ddot{Z}_u} = Ksd\left(i_{Z_s} - i_{Z_u} - i_{\Delta Z_{lin}}\right) + Csd\left(i_{\dot{Z}_s} - i_{\dot{Z}_u} - i_{\Delta \dot{Z}_{lin}}\right) - Kt\left(i_{Z_u} - i_{Z_r}\right) - Ct(i_{\dot{Z}_u} - i_{\dot{Z}_r})$$
(3.14)

3. The actuator dynamics: assuming it's a linear force input

$$m_{act} i_{\ddot{Z}_{lin}} = i_{f_{act}} - Ksd\left(i_{Z_s} - i_{Z_u} - i_{\Delta Z_{lin}}\right) - Csd(i_{\dot{Z}_s} - i_{\dot{Z}_u} - i_{\Delta \dot{Z}_{lin}})$$
(3.15)

Now to extend the quarter-car SAVGS to a full-car SAVGS model, we need to account for additional dynamics introduced by the full-car movements. Specially, a full-car model includes:

1. **Four suspensions and tires:** each wheel (front left and right, rear left and right) has its own suspension, tire dynamics, and SAVGS components.
2. **Three degrees of freedom (DOF) in the chassis:** Unlike the quarter-car model that primarily focuses on vertical motion, a full-car model typically includes:
   - Vertical motion (Z_s) represents the vertical position of the chassis center of mass (CMC).
   - Pitch (θ_s) represents rotation around the lateral axis
   - Roll (φ_s) represents rotation around the longitudinal axis

General approach to for extending the model:

To build the dynamic state equation representation of full-car SAVGS system considering the figure 3.4 below and to construct the state dynamic equations, lets analyze each component, including pitch rotation and the relationships between sprung and unsprung mass, and develop the linearized equations of motion for each state.

Defining States: for a full car with a suspension system like SAVGS the state vector typical includes:

1. Vertical position and velocity of the car body (sprung mass), $Z_{s1}, Z_{s2}, Z_{s3}, Z_{s4}$ and their derivatives
2. Vertical position and velocity of the wheel (Unsprung mass), $Z_{u1}, Z_{u2}, Z_{u3}, Z_{u4}$ and their derivatives
3. Roll (φ_s) and Pitch (θ_s) angle of the car body and their derivatives

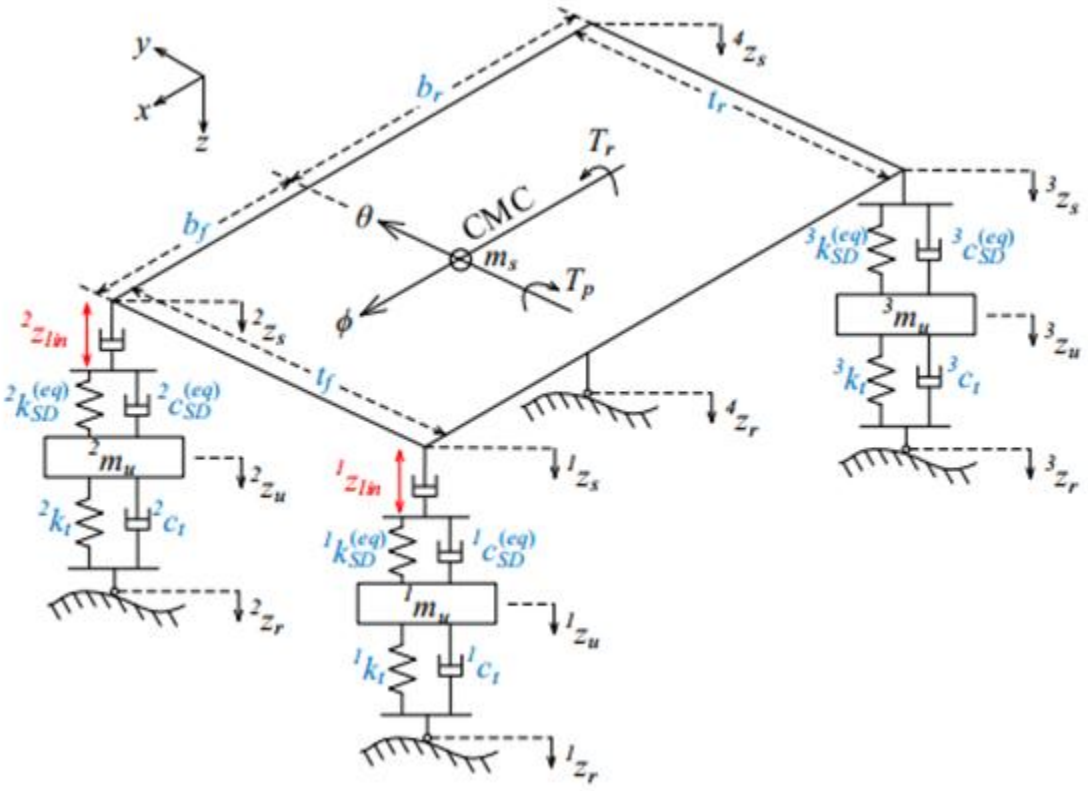

Figure 3.4: Linearized Full-car SAVGS schematic diagram[5]

System assumptions and parameters:

- (M_s): sprung mass of the car body (central chassis)
- (M_{ui}): unsprung mass of each wheel
- ($K_{sD}^{(eq)}$ and $C_{sD}^{(eq)}$): equivalent spring and damper constants of the SAVGS
- (K_{ti} and C_{ti}): Tire stiffness and damping
- ($i_{l_s} = i_{Z_u} - i_{Z_s}$): Suspension deflection (the difference between unsprung and sprung mass vertical displacement)

- ($i_{l_t} = i_{Z_r} - i_{Z_u}$): Tire deflection (the difference between road surface and unsprung mass vertical displacement)
- The vertical position of the chassis at each corner (Z_{si}) is linearzed as:

$$Z_{s1} = Z_{cmc} - b_f\theta_s - 0.5T_f\varphi_s$$

$$Z_{s2} = Z_{cmc} - b_f\theta_s + 0.5T_f\varphi_s$$

$$Z_{s3} = Z_{cmc} + b_r\theta_s - 0.5T_r\varphi_s$$

$$Z_{s4} = Z_{cmc} + b_r\theta_s + 0.5T_r\varphi_s$$

- The load transfer due to the driving event of acceleration/breaking and cornering is equivalent with virtual pitch and roll torques Tp and Tr acting on the vehicle chassis are included in the exogenous disturbances.

Finally, now the dynamics of linearzed full-car model of SAVGS can be described as follows.

Equations of motion

The dynamics starts from the linear equivalent spring-damper force at each corner of the car, given as:

$$F^{eq}_{(sD)i} = K^{eq}_{(sD)i}\left(l_{si} - Z_{(lin)i}\right) + C^{eq}_{(sD)i}(\dot{l}_{si} - \dot{Z}_{(lin)i})$$

(3.16)

The equivalent spring stiffness ($K^{eq}_{(sD)i}$) and damping coefficient ($C^{eq}_{(sD)i}$) are function with respect to the two independent variables of (θ^i_{lw}) and (θ^i_{sl}) for front and rear axles ($i = 1, 2, 3, and\ 4$), while solely related to the rear axle ($i = 3\ and\ 4$), satisfying

$$K^{eq}_{(sD)i} = \frac{dF^{eq}_{(sD)i}}{dl_{si}} = \frac{d(F_{(sd)i}\frac{dl_{(sD)i}}{dl_{si}}}{dl_{si}}, C^{eq}_{(sD)i} = (\frac{dl_{(sD)i}}{dl_{si}})^2 C_{(s)i}$$

Where $F_{(sd)i}$ the actual spring force while $F^{eq}_{(sD)i}$ is the linear equivalent spring force that is vertically acting between the chassis and the road wheel. The linear equivalent actuator has the same power output as the actual rotary actuator, such as:

$$T_{(sl)i}\delta\theta_{(sl)i} - F^{eq}_{(sD)i}\delta Z_{(lin)i} = 0$$

and as discussed previously here the functions i_α that convert $i_{\omega_{sl}}\ to\ i_{Z_{lin}}$

are derived as: $i_\alpha = i_\alpha\left(\theta_{(lw)i}, \theta_{(sl)i}\right) = \frac{\dot{Z}_{(lin)i}}{i_{\omega_{sl}}} = \frac{\partial \dot{Z}_{(lin)i}}{\partial \theta_{(sl)i}}$

Where a function $\alpha = \dot{Z}_{(lin)i}/\omega_{sl}$ ($\dot{Z}_{(lin)i}$ is the speed of linear actuator and ω_{sl} is the actual rotary actuator speed of the single link) is introduced to compensate the overall suspension geometric nonlinearity and to bridge the linear equivalent model and the nonlinear multi-body model. According to the suspension geometry relationship, the function α, the linear equivalent stiffness Keq and damping Ceq can be derived and they are all with respect to the single-link angle $\theta_{(sl)i}$ and the lower wishbone angle $\theta_{(lw)i}$ as plotted in figure 3.5 below the equivalent values can be approximated to a constant with values at their nominal equilibrium state (Keq=31400 N/m and Ceq=N/(m/s)), shown as the red points in the middle and right plots in the figure 3.5 respectively, while the function α is simplified as a parabolic function against $\theta_{(sl)i}$ only shown in the left side as its variation with respect to $\theta_{(lw)i}$ is very small [3][9].

Further the parameter α, that accounts for the geometric nonlinearity of the SL and which is a function of wheel travel and SL angle, can be computed through approximated with installation ration R_{SD} as:

$$\dot{Z}_{lin} = -\frac{1}{R_{SD}}\frac{\partial l_{SL}}{\partial \theta_{SL}}\dot{\theta}_{SL} \;\rightarrow\; \alpha = -\frac{1}{R_{SD}}\frac{\partial l_{SL}}{\partial \theta_{SL}}$$

$$\dot{Z}_{lin} = -\frac{1}{R_{SD}}\frac{\partial l_{SL}}{\partial \theta_{SL}}\frac{\partial \theta_{SL}}{\partial t}$$

$$\dot{Z}_{lin} = -\frac{1}{R_{SD}}\frac{\partial l_{SL}}{\partial t} = -\frac{1}{R_{SD}}\frac{\partial (Z_u - Z_S)}{\partial t} = -\frac{1}{R_{SD}}(\dot{Z}_u - \dot{Z}_S)$$

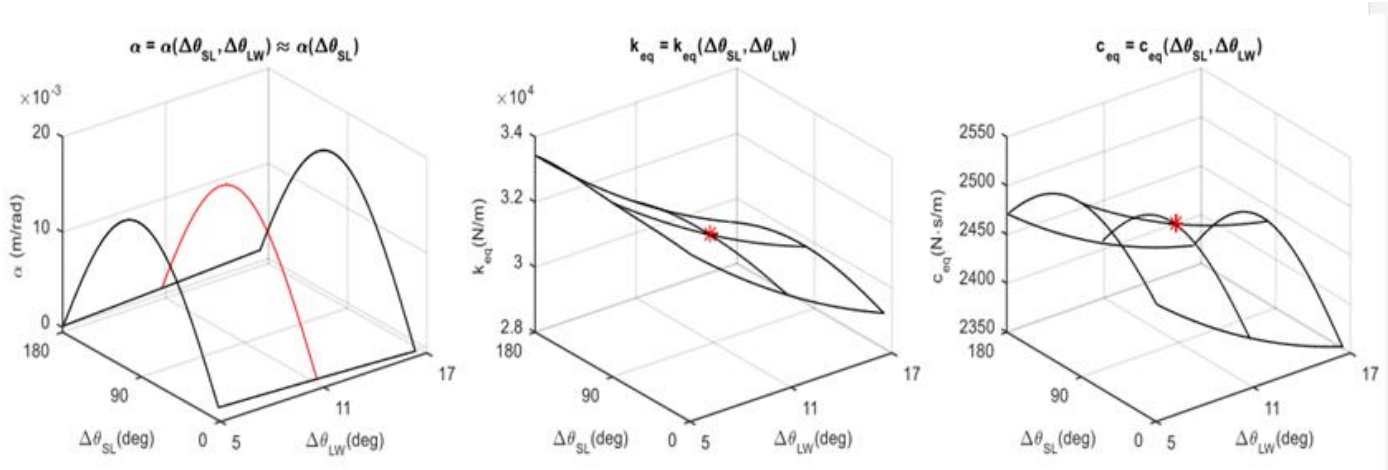

Figure 3.5: The full-car prototype SAVGS nonlinear characteristics.

And the other force is the vertical tire forces at each road wheel corner are given as:

$$F_{(tz)i} = K_{(t)i} l_{(t)i} + C_{(t)i} \dot{l}_{(t)i} \quad (3.17)$$

Having those basic forces applied to the SAVGS system now we can have the dynamic state equations that describe the full-car SAVGS.

1. **Vertical Dynamics of sprung mass:**
   The vertical motion of the car body (sprung mass) at each corner to the center of mass (cmc) based on Newton's second law is given as:

   $$M_s \ddot{Z}_{cmc} = \sum_i F^{eq}_{(sD)i} + f_{(act)i} \quad (3.18)$$

2. **Vertical dynamics of unsprung mass:**
   The vertical motion at each corner of unsprung mass (road wheel) applying newton's second law:
   $$M_{ui} \ddot{Z}_{ui} = F_{(tz)i} - F^{eq}_{(sD)i} \quad (3.19)$$
3. **Pitch and Roll dynamics:**
   Pitch ($\boldsymbol{\theta_s}$): the rotational motion about the y-axis (front to back axis), according to the balance of pitching motion of moments:
   $I_y \ddot{\theta}_s = 0.5T_f\left(F^{eq}_{(sD)2} - F^{eq}_{(sD)1}\right) + 0.5T_r\left(F^{eq}_{(sD)4} - F^{eq}_{(sD)3}\right) + 0.5T_p(f_{(act)1} + f_{(act)2} + f_{(act)3} + f_{(act)4})$
   (.20)
   Roll ($\boldsymbol{\varphi_s}$): the rotational motion about the x-axis (side to side axis), according to the balance of rolling motion of moments:
   $I_x \ddot{\varphi}_s = -b_f\left(F^{eq}_{(sD)2} + F^{eq}_{(sD)1}\right) - b_r\left(F^{eq}_{(sD)4} + F^{eq}_{(sD)3}\right) + 0.5T_r(f_{(act)1} - f_{(act)2} + f_{(act)3} - f_{(act)4}$
   (3.21)
   Where I_x and I_y are the rolls and pitches moment of inertias with respect to the CMC respectively.

Combing (3.16) -(3.21) and vertical position of the chassis at each corner (Z_{si}) the state space equation of linear equivalent full-car model of SAVGS can be formed, with the state vector X, output Y, and input U being:

$$X^T = \left[\dot{Z}_{cmc} \;\; \dot{\theta}_s \;\; \dot{\varphi}_s \;\; \dot{Z}_{ui} \;\; \dot{l}_{si} \;\; \dot{l}_{ti}\right]$$

$$Y^T = [\ddot{Z}_{cmc} \;\; l_{si} \;\; l_{ti}]$$

$$X^T = \left[\ Z_{ri} \quad Z_{(lin)i}\right]$$

The derived differential dynamic equations are re-written as follows for each case of the above general forms by substituting each parameter to be used for simulation as follows, with parameter values given in table 3.3 below.

Table3.3: Full-car SAVGS parameters [4]

Parameters	Symbol	Axle	Value	Unit
Total/Sprung mass	m/m_s	-	1134/1325	kg
Wheelbase/CMC height	$b_f + b_r/h_{CMC}$	-	2265/457	mm
Track width	t_f/t_r	F/R^a	1405/1430	mm
Weight distribution	-	F/R	53/47	%
Spring stiffness	k_{SD}	F/R	60.0/20.7	KN/m
Damping coefficient	c_{SD}	F/R	5000/4000	N/(m/s)
Tire stiffness	k_t	F/R	275	kN/m
Tire damping	c_t	F/R	300	N/(m/s)
Installation ratio	R_{SD}	F/R	0.72/0/88	-
Single-link length	l_{SL}	F/R	11/-	mm
PMSM model	-	F/R	SGM7J	-
Gear ratio	G_{bgx}	F/R	50/-	-
PMSM rated power	P_{act}	F/R	750/-	W
PMSM rated torque	T_{act}	F/R	2.39/-	N.m

The Vertical car body (sprung mass) motion:

$$M_s\ddot{Z}_{cmc} = F^{eq}_{(sD)1} + F^{eq}_{(sD)2} + F^{eq}_{(sD3} + F^{eq}_{(sD)4} + f_{(act)1} + f_{(act)2} + f_{(act)3} + f_{(act)4}$$

$$M_s\ddot{Z}_{cmc} = K^{eq}_{(sD)1}\left(l_{s1} - Z_{(lin)1}\right) + C^{eq}_{(sD)1}(\dot{l}_{s1} - \dot{Z}_{(lin)1}) + K^{eq}_{(sD)2}\left(l_{s2} - Z_{(lin)2}\right) + C^{eq}_{(sD)2}(\dot{l}_{s2} - \dot{Z}_{(lin)2}) + K^{eq}_{(sD)3}\left(l_{s3} - Z_{(lin)3}\right) + C^{eq}_{(sD)3}(\dot{l}_{s3} - \dot{Z}_{(lin)3}) + K^{eq}_{(sD)4}\left(l_{s4} - Z_{(lin)4}\right) + C^{eq}_{(sD)4}(\dot{l}_{s4} - \dot{Z}_{(lin)4}) + f_{(act)1} + f_{(act)2} + f_{(act)3} + f_{(act)4}$$

$$M_s\ddot{Z}_{cmc} = K^{eq}_{(sD)1}\left(Z_{u1} - (Z_{cmc} - b_f\theta_s - 0.5T_f\varphi_s) - Z_{(lin)1}\right) + C^{eq}_{(sD)1}\left(\dot{Z}_{u1} - \left(\dot{Z}_{cmc} - b_f\dot{\theta}_s - 0.5T_f\dot{\varphi}_s\right) - \dot{Z}_{(lin)1}\right) + K^{eq}_{(sD)2}\left(Z_{u2} - (Z_{cmc} - b_f\theta_s + 0.5T_f\varphi_s) - Z_{(lin)2}\right) + C^{eq}_{(sD)2}\left(\dot{Z}_{u2} - \left(\dot{Z}_{cmc} - b_f\dot{\theta}_s + 0.5T_f\dot{\varphi}_s\right) - \dot{Z}_{(lin)2}\right) + K^{eq}_{(sD)3}\left(Z_{u3} - (Z_{cmc} + b_r\theta_s - 0.5T_r\varphi_s) - Z_{(lin)3}\right) + C^{eq}_{(sD)3}\left(\dot{Z}_{u3} - \left(\dot{Z}_{cmc} + r\dot{\theta}_s - 0.5T_r\dot{\varphi}_s\right) - \dot{Z}_{(lin)3}\right) + K^{eq}_{(sD)4}\left(Z_{u4} - \left(Z_{cmc} + b_r\theta_s + 0.5T_r\varphi_s\right) - Z_{(lin)4}\right) + C^{eq}_{(sD)4}\left(\dot{Z}_{u4} - \left(\dot{Z}_{cmc} + b_r\dot{\theta}_s + 0.5T_r\dot{\varphi}_s\right) - \dot{Z}_{(lin)4}\right) + f_{(act)1} + f_{(act)2} + f_{(act)3} + f_{(act)4}$$

The Pitch rotational moments:

$$I_y\ddot{\theta}_s = 0.5T_f\left(F^{eq}_{(sD)2} - F^{eq}_{(sD)1}\right) + 0.5T_r\left(F^{eq}_{(sD)4} - F^{eq}_{(sD)3}\right) + 0.5T_p(f_{(act)1} + f_{(act)2} + f_{(act)3} + f_{(act)4})$$

$$I_y\ddot{\theta}_s = 0.5T_f\left(\left(K^{eq}_{(sD)2}\left(l_{s2} - Z_{(lin)2}\right) + C^{eq}_{(sD)2}\left(\dot{l}_{s2} - \dot{Z}_{(lin)2}\right)\right) - \left(K^{eq}_{(sD)1}\left(l_{s1} - Z_{(lin)1}\right) + C^{eq}_{(sD)1}\left(\dot{l}_{s1} - \dot{Z}_{(lin)1}\right)\right)\right) + 0.5T_r\left(\left(K^{eq}_{(sD)4}\left(l_{s4} - Z_{(lin)4}\right) + C^{eq}_{(sD)4}\left(\dot{l}_{s4} - \dot{Z}_{(lin)4}\right)\right) - \left(K^{eq}_{(sD)3}\left(l_{s3} - Z_{(lin)3}\right) + C^{eq}_{(sD)3}\left(\dot{l}_{s3} - \dot{Z}_{(lin)3}\right)\right)\right) + 0.5T_p(f_{(act)1} + f_{(act)2} + f_{(act)3} + f_{(act)4})$$

$$I_y\ddot{\theta}_s = 0.5T_f\left(\left(K^{eq}_{(sD)2}\left(Z_{u2} - (Z_{cmc} - b_f\theta_s + 0.5T_f\varphi_s) - Z_{(lin)2}\right) + C^{eq}_{(sD)2}\left(\dot{Z}_{u2} - (\dot{Z}_{cmc} - b_f\dot{\theta}_s + 0.5T_f\dot{\varphi}_s) - \dot{Z}_{(lin)2}\right)\right) - \left(K^{eq}_{(sD)1}\left(Z_{u1} - (Z_{cmc} - b_f\theta_s - 0.5T_f\varphi_s) - Z_{(lin)1}\right) + C^{eq}_{(sD)1}\left(\dot{Z}_{u1} - (\dot{Z}_{cmc} - b_f\dot{\theta}_s - 0.5T_f\dot{\varphi}_s) - \dot{Z}_{(lin)1}\right)\right)\right) + 0.5T_r\left(\left(K^{eq}_{(sD)4}\left(Z_{u4} - (Z_{cmc} + b_r\theta_s + 0.5T_r\varphi_s) - Z_{(lin)4}\right) + C^{eq}_{(sD)4}\left(\dot{Z}_{u4} - (\dot{Z}_{cmc} + b_r\dot{\theta}_s + 0.5T_r\dot{\varphi}_s) - \dot{Z}_{(lin)4}\right)\right) - \left(K^{eq}_{(sD)3}\left(Z_{u3} - (Z_{cmc} + b_r\theta_s - 0.5T_r\varphi_s) - Z_{(lin)3}\right) + C^{eq}_{(sD)3}\left(\dot{Z}_{u3} - (\dot{Z}_{cmc} + r\dot{\theta}_s - 0.5T_r\dot{\varphi}_s) - \dot{Z}_{(lin)3}\right)\right)\right) + 0.5T_p(f_{(act)1} + f_{(act)2} + f_{(act)3} + f_{(act)4})$$

The Roll rotational moments:

$$I_x\ddot{\varphi}_s = -b_f\left(F^{eq}_{(sD)1} + F^{eq}_{(sD)2}\right) - b_r\left(F^{eq}_{(sD)3} + F^{eq}_{(sD)4}\right) + 0.5T_r(f_{(act)1} - f_{(act)2} + f_{(act)3} - f_{(act)4}$$

$$I_x\ddot{\varphi}_s = -b_f\left(\left(K^{eq}_{(sD)1}\left(l_{s1} - Z_{(lin)1}\right) + C^{eq}_{(sD)1}\left(\dot{l}_{s1} - \dot{Z}_{(lin)1}\right)\right) + \left(K^{eq}_{(sD)2}\left(l_{s2} - Z_{(lin)2}\right) + C^{eq}_{(sD)2}\left(\dot{l}_{s2} - \dot{Z}_{(lin)2}\right)\right)\right) - b_r\left(\left(K^{eq}_{(sD)3}\left(l_{s3} - Z_{(lin)3}\right) + C^{eq}_{(sD)3}\left(\dot{l}_{s3} - \dot{Z}_{(lin)3}\right)\right) + \left(K^{eq}_{(sD)4}\left(l_{s4} - Z_{(lin)4}\right) + C^{eq}_{(sD)4}\left(\dot{l}_{s4} - \dot{Z}_{(lin)4}\right)\right)\right) + 0.5T_r(f_{(act)1} - f_{(act)2} + f_{(act)3} - f_{(act)4}$$

$$I_x\ddot{\varphi}_s = -b_f\left(\left(K_{(sD)1}^{eq}\left(Z_{u1} - (Z_{cmc} - b_f\theta_s - 0.5T_f\varphi_s) - Z_{(lin)1}\right) + C_{(sD)1}^{eq}\left(\dot{Z}_{u1} - (\dot{Z}_{cmc} - b_f\dot{\theta}_s - 0.5T_f\dot{\varphi}_s) - \dot{Z}_{(lin)1}\right)\right) + \left(K_{(sD)2}^{eq}\left(Z_{u2} - (Z_{cmc} - b_f\theta_s + 0.5T_f\varphi_s) - Z_{(lin)2}\right) + C_{(sD)2}^{eq}\left(\dot{Z}_{u2} - (\dot{Z}_{cmc} - b_f\dot{\theta}_s + 0.5T_f\dot{\varphi}_s) - \dot{Z}_{(lin)2}\right)\right)\right) - b_r\left(\left(K_{(sD)3}^{eq}\left(Z_{u3} - (Z_{cmc} + b_r\theta_s - 0.5T_r\varphi_s) - Z_{(lin)3}\right) + C_{(sD)3}^{eq}\left(\dot{Z}_{u3} - (\dot{Z}_{cmc} + r\dot{\theta}_s - 0.5T_r\dot{\varphi}_s) - \dot{Z}_{(lin)3}\right)\right) + \left(K_{(sD)4}^{eq}\left(Z_{u4} - (Z_{cmc} + b_r\theta_s + 0.5T_r\varphi_s) - Z_{(lin)4}\right) + C_{(sD)4}^{eq}\left(\dot{Z}_{u4} - (\dot{Z}_{cmc} + b_r\dot{\theta}_s + 0.5T_r\dot{\varphi}_s) - \dot{Z}_{(lin)4}\right)\right)\right) + 0.5T_r(f_{(act)1} - f_{(act)2} + f_{(act)3} - f_{(act)4}$$

The vertical unsprung mass dynamics at each corner:

At wheel one;

$$M_{u1}\ddot{Z}_{u1} = F_{(tz)1} - F_{(sD)1}^{eq}$$

$$M_{u1}\ddot{Z}_{u1} = K_{(t)1}l_{(t)1} + C_{(t)1}\dot{l}_{(t)1} - \left(K_{(sD)1}^{eq}\left(l_{s1} - Z_{(lin)1}\right) + C_{(sD)1}^{eq}\left(\dot{l}_{s1} - \dot{Z}_{(lin)1}\right)\right)$$

$$M_{u1}\ddot{Z}_{u1} = K_{(t)i}(Z_{r1} - Z_{u1}) + C_{(t)i}\left(\dot{Z}_{r1} - \dot{Z}_{u1}\right) - \left(K_{(sD)1}^{eq}\left(Z_{u1} - (Z_{cmc} - b_f\theta_s - 0.5T_f\varphi_s) - Z_{(lin)1}\right) + C_{(sD)1}^{eq}\left(\dot{Z}_{u1} - (\dot{Z}_{cmc} - b_f\dot{\theta}_s - 0.5T_f\dot{\varphi}_s) - \dot{Z}_{(lin)1}\right)\right)$$

At wheel two;

$$M_{u2}\ddot{Z}_{u2} = F_{(tz)2} - F_{(sD)}^{eq}$$

$$M_{u2}\ddot{Z}_{u2} = K_{(t)2}l_{(t)2} + C_{(t)2}\dot{l}_{(t)2} - \left(K_{(sD)2}^{eq}\left(l_{s2} - Z_{(lin)2}\right) + C_{(sD)2}^{eq}\left(\dot{l}_{s2} - \dot{Z}_{(lin)2}\right)\right)$$

$$M_{u2}\ddot{Z}_{u2} = K_{(t)2}(Z_{r2} - Z_{u2}) + C_{(t)2}\left(\dot{Z}_{r2} - \dot{Z}_{u2}\right) - \left(K_{(sD)2}^{eq}\left(Z_{u2} - (Z_{cmc} - b_f\theta_s + 0.5T_f\varphi_s) - Z_{(lin)2}\right) + C_{(sD)2}^{eq}\left(\dot{Z}_{u2} - (\dot{Z}_{cmc} - b_f\dot{\theta}_s + 0.5T_f\dot{\varphi}_s) - \dot{Z}_{(lin)2}\right)\right)$$

At wheel three;

$$M_{u3}\ddot{Z}_{u3} = F_{(tz)3} - F_{(sD)3}^{eq}$$

$$M_{u3}\ddot{Z}_{u3} = K_{(t)3}l_{(t)3} + C_{(t)3}\dot{l}_{(t)3} - \left(K^{eq}_{(sD)3}\left(l_{s3} - Z_{(lin)3}\right) + C^{eq}_{(sD)3}\left(\dot{l}_{s3} - \dot{Z}_{(lin)3}\right)\right)$$

$$M_{u3}\ddot{Z}_{u3} = K_{(t)3}(Z_{r3} - Z_{u3}) + C_{(t)3}\left(\dot{Z}_{r3} - \dot{Z}_{u3}\right) - \left(K^{eq}_{(sD)3}\left(Z_{u3} - (Z_{cmc} + b_r\theta_s - 0.5T_r\varphi_s) - Z_{(lin)3}\right) + C^{eq}_{(sD)3}\left(\dot{Z}_{u3} - (\dot{Z}_{cmc} + b_r\dot{\theta}_s - 0.5T_r\dot{\varphi}_s) - \dot{Z}_{(lin)3}\right)\right)$$

At wheel one;

$$M_{u4}\ddot{Z}_{u4} = F_{(tz)4} - F^{eq}_{(sD)4}$$

$$M_{u4}\ddot{Z}_{u4} = K_{(t)4}l_{(t)4} + C_{(t)4}\dot{l}_{(t)4} - \left(K^{eq}_{(sD)4}\left(l_{s4} - Z_{(lin)4}\right) + C^{eq}_{(sD)4}\left(\dot{l}_{s4} - \dot{Z}_{(lin)4}\right)\right)$$

$$M_{u4}\ddot{Z}_{u4} = K_{(t)4}(Z_{r4} - Z_{u4}) + C_{(t)4}\left(\dot{Z}_{r4} - \dot{Z}_{u4}\right) - \left(K^{eq}_{(sD)4}\left(Z_{u4} - (Z_{cmc} + b_r\theta_s + 0.5T_4\varphi_s) - Z_{(lin)4}\right) + C^{eq}_{(sD)4}\left(\dot{Z}_{u4} - (\dot{Z}_{cmc} + b_r\dot{\theta}_s + 0.5T_r\dot{\varphi}_s) - \dot{Z}_{(lin)4}\right)\right)$$

These dynamic differential state equations above will be implemented with MATLAB-Simulink function designed and will be simulated to observe the SAVGS system response which will be compared with the passive suspension system. The implemented MATLAB-Simulink function designed is shown in appendixes' B.

3.4 preview and road profile modeling

Generally, the roads shape and condition vary in different places. The variations exist between different places as well as within the same location such as highway and city streets. And this road surface irregularity represents the main disturbing function to either a passenger's comfort in car or car components. It is important to predict or have preview information about the road profile to car dynamic response using a realistic road model; however, such a model may be difficult to develop.

Therefore, in this study sinusoidal road profile is employed with two different constant forward velocities to simulate the performances of a car suspension model in MATLAB-Simulink environment. Sinusoidal form is one of the commonly used inputs in research, the response of the suspension system in time domain is easily seen. The sinusoidal input here provides an easy way understanding of a car suspension system performance by experiencing a car bump, pothole or both at the same time. A simple model of the vertical road displacement such a bump disturbance on wheel or tire, resulting from a single road bump was presented in reference [28]. And modeled here as a road disturbance as $Zr(t)$ for front wheel of a full car model. The sinusoidal used in this study is assumed to be a single bump, to get a clearer visual understanding of the suspension model performances.

Smoothed Bump Profile: The road height corresponding to the smoothed bump event considered in the present work is given by the following expression:

$$Z_{rf(t)} = \begin{cases} \frac{a}{2}\left(1 - \cos 2\pi \frac{v}{w} t\right), & t_f \le t \le t_{2f} \\ 0, & t \ge \frac{w}{v} \end{cases}$$

Where a is the bump amplitude, w is the width of bump (such that wavelength of the bump) of the road profile experienced by the front and rear wheels during a car travel with velocity, t_f And t_{2f} are the time start and end for the front wheel of a car experienced by the bump, and the time end, t_{2f} is given by: $t_{2f} = t_f + \frac{w}{v}$

In which $v = 20\frac{km}{h} and\ v = 50\frac{km}{h}$ is the forward speed, while the maximum bump height $a = 0.05\ m$ and bump width $w = 3\ m.$ To evaluate the pitch and roll mitigation, the Fuzzy logic controlled SAVGS full-car system only experiences a bump disturbance at the wheels of the vehicle. The bump profile parameters are taken from reference [2cheng] and the time start for the sinusoidal input at front wheel, t_f of a car is assumed 0.5 second during time simulation, t. The time domain analysis of a Full car suspension model is carried out for two different constant forward velocities given above.

The front and rear wheels of a car assumed experienced the same road profile (and only one); therefore, road disturbance for rear wheel, Zrr(t) is found by time delay, t_d as:

$$Zrr(t) = Zrf(t - t_d)$$

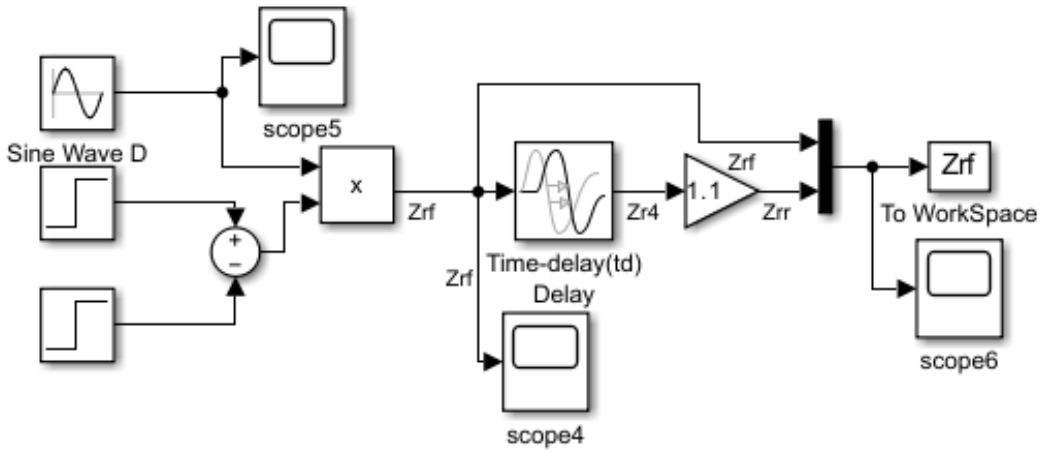

(a)

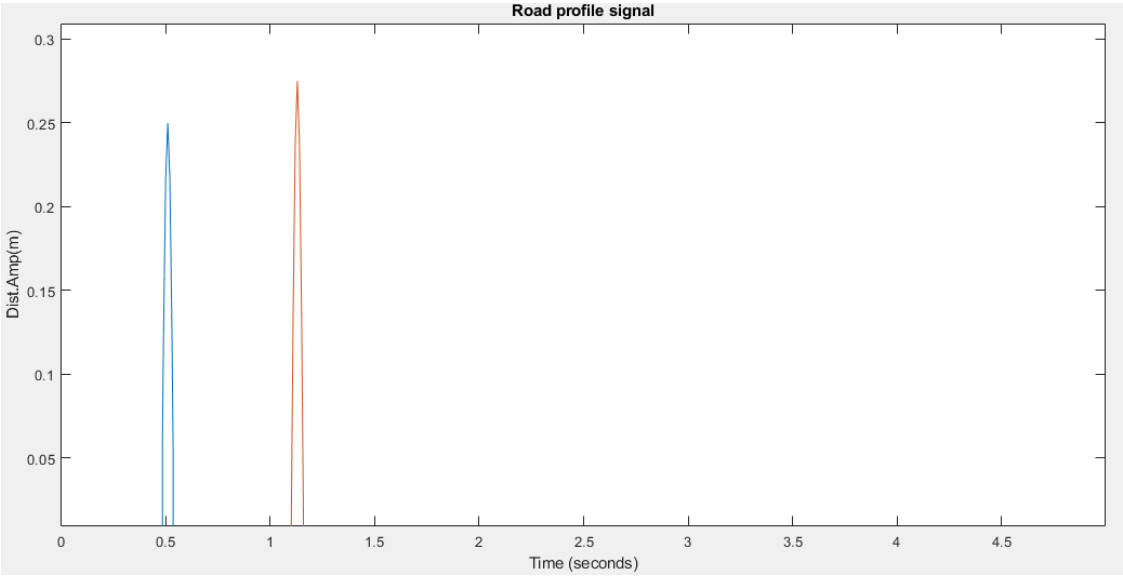

(b)

Figure 3.6: Road profile a) Sine wave signal Simulink model, b) sinusoidal bump as road input disturbance

3.4.1 Preview/Predictive Road Profile Handling in Simulink

To implement a scenario in Simulink where the road profile is known in advance before the wheels reach it, it can be modeled in predictive approach. This allows the system to adjust suspension settings before encountering the actual bump or road feature. Predictive control in vehicle suspension systems involves adjusting the suspension settings in anticipation of road disturbances.

By knowing the road profile in advance, such as from GPS data or pre-mapped road information, the suspension can be optimized before the vehicle encounters bumps or potholes. This proactive approach enhances ride comfort and vehicle stability, particularly on roads with known irregularities.
The smoothed bump profile used in this study is mathematically represented as seen in the above and to simulate the predictive handling of a known road profile, the following steps are taken:

1. Create a Pre-Defined Road Profile in MATLAB:
First, the road profile is generated in MATLAB as a time series. This represents the displacement the vehicle will experience when reaching the bump.

MATLAB
```
% Define the road profile as a pre-calculated vector
  a = 0.05; % Bump amplitude in meters
  w = 3; % Bump width in meters
  v = 20 / 3.6; % Vehicle speed in m/s
  t = 0:0.01:2; % Time vector
```

```
Zrf = (a/2) (1 - cos (2pi v / w *t)); % Road profile
save ('road Profile. Mat', 't', 'Zrf'); % Save profile in MATLAB for later use
```

2. Load and Apply the Road Profile in Simulink:
In the Simulink model, load the pre-defined road profile from the MATLAB workspace using a "From Workspace" block or a "MATLAB Function" block. Use a "MATLAB Function" block to simulate the suspension system's response to the profile, with the time of application slightly ahead of the actual bump to simulate predictive control.

MATLAB

```
Function Zpred = predictive Road Profile(t, leadTime)
    load ('roadProfile.mat', 't', 'Zrf');
    Zpred = interp1(t, Zrf, t + leadTime, 'linear', 'extrap'); % Shift profile by leadTime
end
```

Then finally connect this function to the input of the suspension model. The `leadTime` parameter ensures that the system anticipates the bump, allowing it to adjust the suspension in advance.

CHAPTER 4

CONTROLLER DESIGN AND ANALYSIS

4.1 General introduction

The chapter focuses on designing fuzzy logic controller (FLC) for series active variable geometry suspension (SAVGS) system in a full-car model. Before creating an active suspension (SAVG) controller, simulation of passive suspension system is conducted to understand the full-car suspension dynamics and identify design requirements for FLC. Here section 4.2 introduces performance evaluation criteria for the suspension system followed by the design of FLC in section 4.3.

In this study, sensors measure the vertical displacement and velocity at the front and rear sprung mass points. The active suspension system (SAVG) uses this data to adjust actuator forces, modifying suspension stiffness, spring rate, and shock absorber damping to improve ride quality. The FLC controller, based on Mamdanian-type fuzzy logic, stabilizes vehicle bounce and tire deflection, maintaining values to zero for smooth driving. Expert knowledge and prior research inform the FLC design and enhances suspension performance.

4.2 Performance evaluation criteria for suspension system

The three main performance evaluation criteria for suspension system discussed in this section are:

1. **Passenger Ride Comfort:** Ensuring a smooth and comfortable ride by minimizing vibrations and jolts transmitted to the passengers, discussed later in this section based on reference [15][16].
2. **Suspension Safety:** protecting the vehicle's structure and suspension components by limiting excessive suspension travel and impacts, discussed later in this section based on reference [17].
3. **Road Handling:** maintaining good contact between tire and the road surface to ensure stability and control, especially during maneuvers or over uneven surfaces, discussed later in this section based on reference [18].

These criteria are critical in assessing and designing an effective suspension system and here's a summary of the detailed performance evaluation criteria for the suspension system:

Passenger Ride Comfort: this is affected by the car's roll, pitch, and vertical motions, primarily from road disturbances affecting the sprung mass and the vertical motion, especially the amplitude and acceleration of the sprung mass has the most significant impact on the comfort. Additionally pitch and roll accelerations are crucial due to the coupled behavior of the front and rear wheels in a full-car model like SAVGS systems.

From these, the top reasons that vibrations cause discomfort for passengers are sprung mass amplitude (Z_{cmc}) and acceleration ($\ddot{Z}_{cmc}$), pitch acceleration ($\ddot{\theta}_s$), and the rolling acceleration ($\ddot{\varphi}_s$) motion are included here as an evaluation parameter for passenger ride comfort criteria.

Suspension Safety: To ensure passenger comfort, it's essential to isolate the car's sprung masses from road disturbances, ideally absorbing them in the unsprung masses, in which suspension deflection/travel (the vertical distance between the sprung and unsprung masses) must be limited to avoid structural damage on the vehicle. Suspension velocity is also considered to protect the suspension system's physical components, as excessive travel and velocity (i.e. vibrations) can cause damage to the system. The main reasons that vibration causes structural damage to the suspension system is suspension deflection/travel ($l_{si} = Z_{(s)i} - Z_{(u)i}$) and velocity ($\dot{l}_{si} = \dot{Z}_{(s)i} - \dot{Z}_{(u)i}$) at the front and rear wheel drives are included here as an evaluation parameters criterion for the structural safety of the suspension system.

Road Handling: road handling is the car's ability to maintain tire contact with the road during maneuvers such as cornering, breaking, or accelerating. The tire deflection/travel

($l_{ti} = Z_{(r)i} - Z_{(u)i}$) (difference between the road and suspension movement at front and rear wheel) is critical for handling and impacts safety by prevention loss of control, which could lead to accidents. Therefore, these parameters should be included here as an evaluation parameter for the safety of the ride.

These criteria provide a comprehensive basis for designing an active suspension system (SAVGS) focused on comfort, structural integrity, and handling.

4.3 Fuzzy Logic Controller Design

The general block diagram which can be used as closed loop control structure with FLC is shown below in figure 4.1. The diagram illustrates the structure of the Fuzzy Logic Controller (FLC)-based closed-loop control system for a full-car series active variable geometry suspension (SAVGS) system model.

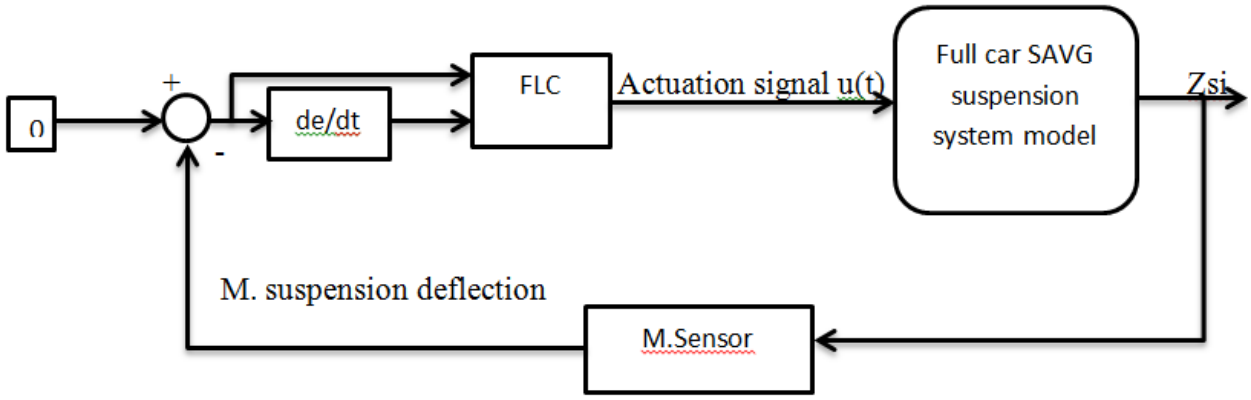

Figure 4.1: Closed-Loop FLC for SAVGS system control

Here's a breakdown of how this FLC is designed and functions:

1. **Inputs to the FLC:** the fuzzy logic controller is structured with mamdani-type fuzzy structure with two inputs.
   The two FLC input variables are:
   - Suspension Deflection (Z_{si}): this represents the displacement of the suspension system.
   - Rate of Change of Suspension Deflection ($\frac{dZ_{si}}{dt}$): this captures the velocity of suspension movements, providing information on how quickly the deflection is changing.
2. **FLC Architecture:** A mamdani-type fuzzy controller is used, known for handling complex, nonlinear effectively by applying fuzzy rule bases. The membership functions for the inputs are mainly triangular for simplicity, manipulation and for smooth transitions. Hence this design choice simplifies computation while maintaining effective control.

3. **Output of FLC:** the output variable from the FLC is actuation signal u(t) (actuating force $f_{(act.i)}$). This signal adjusts the actuator in the SAVGS system, modifying the suspension system's behavior in real time. The actuation adjusts/changes (($Z_{(lin)i}$) of the SAVGS system at each corner to improve performance in response to the suspension and tire deflection of the system.
4. **Closed-Loop Control Process:** the system is set up in closed-loop structure, where the FLC continuously receives feedback on suspension deflection from sensors (labeled as "M. sensor" on the diagram). This feedback loop allows the FLC to continuously adjust suspension in real time to improve/optimize ride comfort, safety, handling, and stability.

This FLC-based system is designed to provide precise and responsive control over the SAVG suspension system, leveraging fuzzy logic to handle complex, dynamic interactions within the suspension. The setup enables real-time adjustments that help maintain optimal vehicle dynamics and enhance the overall driving experience in this design.

Hence the SAVGS system has high nonlinear, parameter uncertainty and vagueness. The Fuzzy logic Controller is first designed to overcome these problems, with the basic structure of closed loop Fuzzy Control System is shown below I figure 4.2.

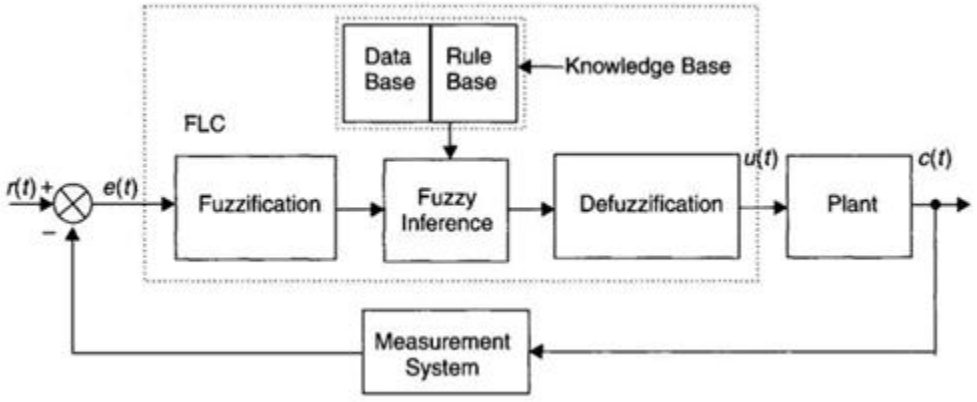

Figure 4.2: Closed-loop Fuzzy Logic Controller Structure[19].

The illustrated structure of the Fuzzy logic controller (FLC) in the above figure4.1 and 4.2, within a closed-loop system is used for controlling Series active variable geometry suspension (SAVGS) system in a full-car model. Let's breakdown each components of FLC system shown in the diagram, concepts based on references [22][25].

1. **Input (Error Calculation):** The system calculates the error signal, $e_{(t)i}$, which represents the difference between the desired vertical displacement ($r_{(t)i} = 0$) and actual displacement ($Z_{(s)i}$) at each sprung mass endpoints of the vehicle (front and rear part). These errors are used as input to the FLC, helping it to make adjustments based on how far the system is from the desired state.

2. **Fuzzification:** The fuzzification block converts the crisp error signals $e_{(t)i}$, as well as their rate of changes $\frac{de_{(t)i}}{dt}$ front and rear parts, into fuzzy values. This involves mapping the input values to a set of linguistic variables, such as "small," "medium," or "large," according to predefined membership functions. This step translates numerical data into fuzzy sets that can be used in fuzzy logic operations.
3. **Knowledge Base (Data Base and Rule Base)**: The data base stores the definition of membership functions for each fuzzy set, defining how input will be categorized (e.g. what range of error corresponds to "small," "medium," etc.). The rule-base contains a set of IF-THEN rules based on expert knowledge. Each rule determines how the system response to the various combination of inputs. For example, a rule might say, "IF the error is Large and the rate of error change is Positive THEN apply a strong corrective force". Together, these components allow the FLC to make decisions similar to how a human operator would, based on experience and judgment rather than precise mathematical equations/model.
4. **Fuzzy Inference:** This block applies the fuzzy rules from the rule-bases to the fuzzified inputs to determine fuzzy outputs; this involves evaluating each rule and combining the outputs of activated rule. The result is a set of fuzzy outputs that represent the appropriate control actions for the system. These outputs reflect the controller's suggested adjustments based on the current error conditions.
5. **Defuzzification:** In this step, the fuzzy outputs are converted back to crisp values that can be applied as control signal. Common methods of defuzzification include centroid or weighted average techniques. The resulting crisp value is a single output signal, u(t) (i.e f_{act}), that represents the actuator force needed to correct the suspension's displacement.
6. **Output (Actuation):** The crisp control signal u(t) is sent to the Plant (in this case, the suspension system), where it adjusts the actuator forces applied to the drive wheels. This control action aims to bring the vehicle's suspension closer to the desired state, improving ride comfort and stability by reducing vertical displacements.
7. Feedback Loops: the measurement system continuously monitors the suspension's actual displacement and sends feedback to calculate the error signals ($e_{(t)i}$). This feedback enables the FLC to dynamically adjust its control actions based on real-time changes in the system's behavior, making it robust to parameter uncertainties and non-linearities

So now in designing a Fuzzy Logic Controller (FLC) for the Active Vehicle Suspension System (SAVGS), the process consists of three main stages: **Fuzzification, Fuzzy Inference, and Defuzzification**. Here's a closer look at each of these stages and the design considerations associated with them taken in the design processes, having concepts based on references [24][21][25][23][26].

Fuzzification Processes

As discussed, the fuzzification stage is responsible for mapping crisp input signals (like the suspension deflection error $e_{(t)i}$ and its rate of changes $\frac{de_{(t)i}}{dt}$ at each corner of the SAVGS) into fuzzy sets. These inputs are transformed into corresponding linguistic variables using fuzzy sets and membership functions.

- **Design Consideration in Fuzzification:**
  - **Number of inputs:** in the SAVGS model, typically we need two inputs for each FLC at front and rear side; i.e $e_{(t)i}$ and $\frac{de_{(t)i}}{dt}$ (rate of error change). Note here the two inputs are taken as most of the time the FLC that emulates PD controller will be required to minimize the error and error rates.

  - **Size of Universe of Discourse:** the universe of discourse defines the possible range of input values. For example, if the expected range of error is from -10 to 10, then the universe of discourse should cover this range. The range is often chosen to ensure the FLC can handle the system's maximum expected variability (saturation levels).

  - **Number and Shape of Fuzzy sets:** The number of fuzzy sets (e.g., Negative Big (NB), Negative Medium (NM), Zero (Z), Positive Medium (PM), Positive Big (PB)) and their shapes (triangular, trapezoidal, Gaussian) are crucial. Typically, most of the time 5-7 fuzzy sets are used to balance granularity with computational simplicity.

In conclusion, fuzzification transforms crisp inputs into fuzzy values that can be used by the inference engine. The decision on the number of sets, their shape, and range will affect the system's sensitivity and response smoothness.

Fuzzy Rule-Base

The fuzzy rule-base is a set of rules in the form of "IF-THEN" statements that define how the system should respond to various input conditions. The rules are created based on expert experience, knowledge of the system, and sometime using empirical data's.

- **Structure of Fuzzy Rules:** Each rule relates linguistic variables for the error and its rate of changes to output linguistic variables representing the actuation force (f_{act}), an example rule might be: IF $e_{(t)i}$ is Positive Medium (PM) AND $\frac{de_{(t)i}}{dt}$ is Negative Medium (NM), THEN f_{act} is Positive Medium (PM). The rules cover all possible combinations of the input fuzzy sets, ensuring that the controller can respond to any situation within the input range.

- **Source of Rule Development:** This are based on:
    - **Physical Laws:** For example, knowledge about how a vehicle suspension should behave based on physics laws can guide rule formations.
    - **Data from Exciting Controller:** Data from conventional controllers (like PD or PID) can help define rules.
    - **Expert Knowledge:** Operators with experience in suspension systems may provide heuristic rules based on observed system behavior.

The fuzzy rule base captures the decision-making logic of the controller.

Fuzzy Inference

The fuzzy inference process applies the rule base to the fuzzified inputs to determine fuzzy output values. This process involves:

- **Membership Function:** Fuzzy inference involves in determining/calculating the degree of membership for each rule.
- **Logic Operation:** Logic operations **(AND, OR)** are applied to combine the input condition in each rule. Typically, the min-max or product-sum methods are used for these operations to be done.
- **Aggregation:** The outputs from each rule are combined into a single fuzzy set representing the controller suggested action.

The result of fuzzy inference is a fuzzy output set that contains information from all applicable rules which is activated at the time.

Defuzzification Processes

Defuzzification converts the fuzzy output set from the inference stage into a single crisp output as actuation signal ($f_{act},\ \ $) which can be applied as a control action. The main defuzzification methods include:

- **Largest of Maximum (LoM), Middle of Maximum (MoM), and Smallest of Maximum (SoM):** This method focuses on the highest points on aggregated membership functions, selecting a single crisp value based on the peak of the output fuzzy set. If the output has a plateau, they pick the leftmost, center, or rightmost point of the plateau, respectively.
- **Center of Area (Centroid method):** This is the most popular method of defuzzification. It calculates the centroid or "center of gravity" of the aggregated output fuzzy set and returns this as crisp output values. The centroid method considers the entire shape of fuzzy output set, making it sensitive to the contribution from all applicable rules. This is beneficial for smoother, more balanced control, and safety as it accounts for both the rule with the highest output value and the rules that contribute a wider area.

4.3.1 Design approach of FLC

The design approach for the Series Active Variable Geometry Suspension (SAVGS) system using a fuzzy logic controller (FLC) follows a structured process. Here's a summary of the key steps:

Step1: Analyze Passive Suspension System: Begin by examining the behavior of existing passive suspension system. This involves simulating the system response under various conditions, using the current parameters for the sprung mass at both front and rear endpoints of the car. Then observe the key matrices, such as the sprung mass displacement, error signal, and response time for both the front and rear suspension. This analysis provides insights into how the system currently handles road disturbance and helps identify areas for improvements.

Step2: Define Control objectives: Based on the observed performance, set control objective for the FLC design. Common control objectives in suspension system includes minimizing displacement and vibration of sprung mass, improve ride comfort, and enhancing road handling. The control objectives should address limitations found in the passive suspension system such as reducing excessive vibrations of suspension system or improving response time of the system.

Step3: Design Fuzzy Logic Controller (FLC): replaces the simple nonlinear feedback system with a FLC to handle the systems nonlinearity and complexity. Configure the FLC to use the error values and their rate of change as input variables, capturing real-time deviation in suspensions performance. These inputs provide information on suspension deflection and tire deflection for both front and rear endpoints. Set up the knowledge base, including the fuzzy sets, membership functions, and a rule base tailored to the suspension control objectives. The rule base should be designed based on observed system behavior, expert knowledge, and any performance criteria previously defined.

Step4: Configure Fuzzification and Defuzzification: Choose appropriate fuzzification and defuzzification methods. Fuzzification involves in converting input signals (error and error rate) into fuzzy values, while defuzzification converts will transform the fuzzy output from the FLC into a crisp control signal. Decide on membership function type (e.g Triangular, Trapezoidal) and the universe of discourse for each variable to ensure smooth and responsive control.

Step5: Test and Iterate: Simulate the SAVGS system with the FLC in place to observe the new system behavior and compare it to the passive suspension response. Measure the system's performance based on defined criteria ride comfort, suspension safety, and road handling. Adjust the rule-base, membership function, or control parameters as needed based on simulation result to fine-tune the FLC improve its effectiveness in meeting the control objective.

This design approach allows the FLC to handle the SAVG suspension system's nonlinearity and parameter uncertainty, creating a robust controller that enhances the vehicle's ride quality and

handling under varying conditions. The FLC's reliance on fuzzy logic, rather than precise mathematical models, also makes it more adaptable to real-world complexities.

4.4 Full-Car Passive Suspension System Simulation

In this subtopic, it focuses on simulating a full-car Suspension system to analyze its response using MATLAB-Simulink. The objective is to understand the car's behavior under road disturbance, which will inform the design of FLC for an active suspension SAVG system. The key parameters observed in the simulation are:

- **Vertical Displacement** at the front ($l_{si} = Z_{(s)i} - Z_{(u)i}$) 0where i=1, 2 and rear ($l_{si} = Z_{(s)i} - Z_{(u)i}$) where i=3, 4 sprung mass endpoints.
- **Vertical Velocity** at the front ($\dot{l}_{si} = \dot{Z}_{(s)i} - \dot{Z}_{(u)i}$) where i=1, 2 and rear (($\dot{l}_{si} = \dot{Z}_{(s)i} - \dot{Z}_{(u)i}$) where i=3, 4 endpoints.

Roll of MATLAB-Simulink

MATLAB/Simulink is used as the primary tool for this simulation. Developed by MathWorks, MATLAB/Simulink is a software package for modeling, simulating, and analyzing multi-domain dynamical systems.

For modeling, MATLAB/Simulink provides a graphical user interface (GUI) that allows users to construct models as block diagrams representing formulated equations (such as differential equations). Additionally, users can customize and create new blocks in MATLAB/Simulink and simulate them to observe system responses [29][30]. Furthermore, the concepts for MATLAB used here are based on references [30][32][34]. It allows for:

1. **Graphical Modeling:** The suspension system can be represented with block diagrams in Simulink, which enables a visual approach to modeling differential equations.
2. **Customization:** Custom blocks can be created to better represent specific system requirements.
3. **Real Time Parameter Adjustment:** Simulink allows for real-time adjustments to parameters and displays results through scopes, making it easy to analyze system responses interactively.

The Simulation setup

The full-car passive suspension system model is created in Simulink, representing the car's dynamics when traveling at a constant speed of 20 km/hr over a bump in the road, which is

modeled as a sinusoidal input. The system's state-space model, derived in Chapter 3, is used to capture the car's suspension dynamics.

So before designing FLC lets run full car passive suspension system and observes the nature of the system response which will support the FLC design and the MATLAB-Simulink block diagram full car passive suspension system without controller is shown below in figure 4.3.

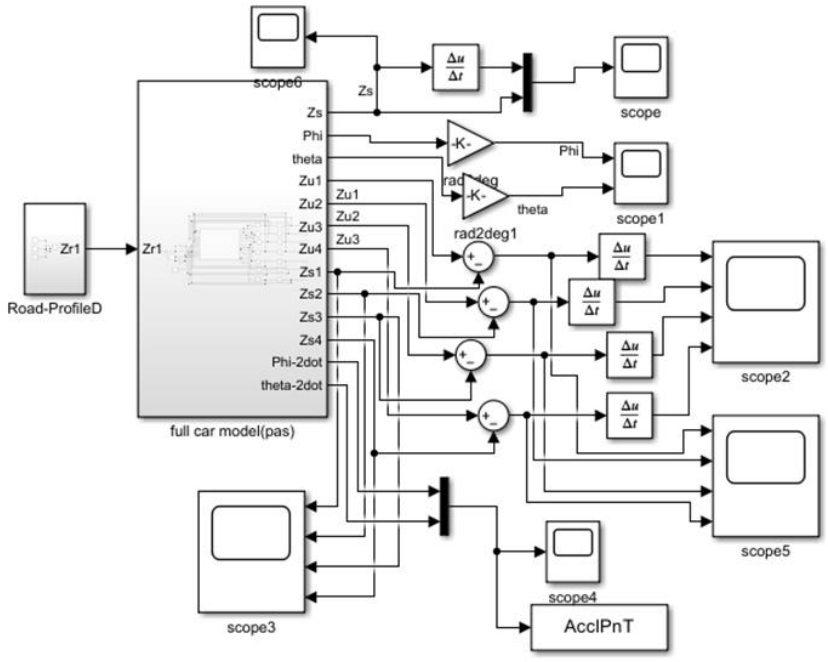

Figure 4.3: Full-Car Passive Suspension system MATLAB-Simulink Block diagram.

Observing Passive Suspension System

The purpose of this simulation is to observe how the passive suspension system reacts to road disturbance, specifically:

- The range of vertical displacement error ($e_{(t)i}$) and its rates ($\frac{de_{(t)i}}{dt}$) for both the front and rear endpoints of the vehicle.
- The system performance matrices (e.g., the degree of oscillations or deviations from desired (vertical displacement ($r_{(t)i} = 0$)) positions) that would inform the design of an active controller.

This analysis provides into crucial insights into:

1. **Defining the Universe of Discourse:** Determining the expected range for input variables (displacement error and its rate) to configure the FLC's input membership functions.
2. **Control Output Requirements:** Understand the range of the actuator force $f_{(act)i}$ signal needed at the front and rear drive wheels to maintain stability and ride comfort.

The full car passive suspension system response of vertical displacement error and error rate is shown below in figure 4.4.

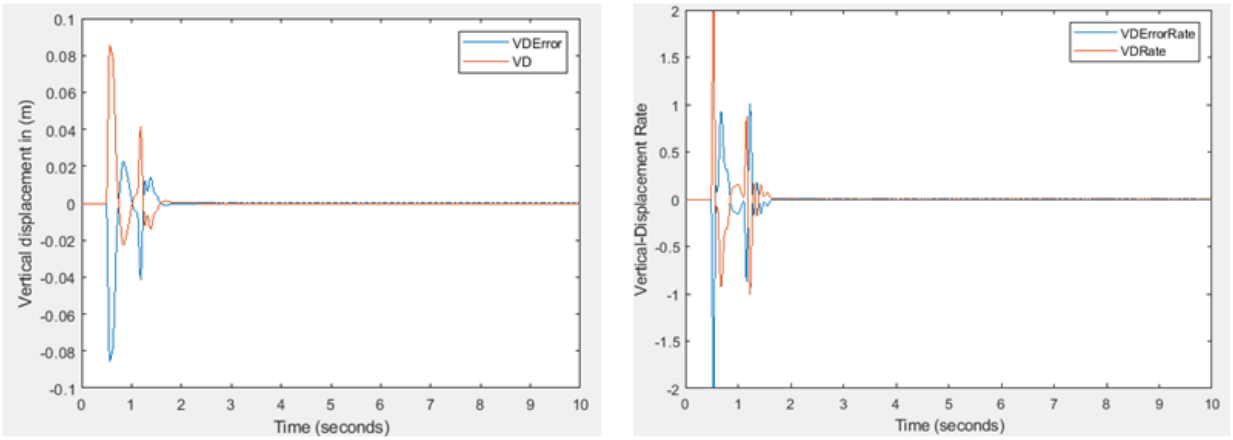

(a) (b)

Figure 4.4: a) vertical displacement and error response, b) vertical rate (velocity) response and at front sprung mass endpoint of a full car passive suspension system.

Next Steps: With the observed results from the passive suspension system response, the design of FLC can proceed. The identified ranges of displacement error and rate at the front and rear endpoints will help set up the fuzzy sets for the FLC inputs, which are critical for controlling the actuator forces in the active suspension system. This process provides a solid foundation for the FLC to enhance ride comfort, safety, and road handling.

4.4.1 Design Approach of Fuzzy Logic Controller (FLC) In SAVGS system

To design a fuzzy logic controller for the suspension (SAVGS), it is essential to understand the system's input-output behavior and establish rule-base that ensure optimal performance, particularly in terms of minimizing settling time, reducing undershoot, and maintaining a small steady-state error, some concepts in this subsection are seen in references [27][22].

Input Consideration for FLC Design

In this design, the key inputs to the FLC are:

1. Vertical displacement error, $e_{(t)i}$ for both front and rear sides
2. Rate of Vertical Displacement error (velocity), $\frac{de_{(t)i}}{dt}$ for both front and rear sides

For effective control, the system's response is divided into four primary scenarios:

- Input Negative with Negative Slope

- Input Negative with Positive Slope
- Input Positive with Negative Slope
- Input Positive with Positive Slope

These scenarios help in formulating rules that guide the FLC in applying appropriate control action based on both the error and its rates of change.

Universe of Discourses and Membership Function

Based on the Passive suspension system's response, the range (Universe of discourse) for each variable are:

- Error: $e_{(t)} = [-1\ 1]$
- Error Rate: $\frac{de_{(t)}}{dt} = [-1\ 1]$
- Actuating signal (force $f_{(act)i}$) $f_{(act)} = [-100\ 100]$

The input and output universes of discourse are each divided into five overlapping fuzzy sets, with the linguistic variables:

- Positive Big (PB)
- Positive Medium (PM)
- Zero (Z)
- Negative Medium (NM)
- Negative Big (NB)

Each Fuzzy variable has a degree of membership between 0 (not an element) and 1 (full member) allowing for partial membership and smooth transition.

For simplicity and computational efficiency, Triangular membership functions are chosen for the inputs (Vertical displacement error and its rate) and the output actuation signal (force). The triangular membership function is defined as:

$$\mu = \max\left[\min\left(\frac{x - x_1}{x_2 - x_1}, \frac{x_3 - x}{x_3 - x_2}\right), 0\right]$$

Where:

- x are the crisp input values
- $x_1, x_2\ and\ x_3$ are left end, peak and right end points on the corresponding crisp universe, respectively.

Fuzzy Rule-Base

The FLC's Rile-base contains 25 rules to cover the possible combinations of error and error rate inputs. Each rule takes the form of an "IF-THEN" statement such as:

- IF: $e_{(t)}$ is PM AND $\frac{de_{(t)}}{dt}$ is NM THEN Actuation signal $f_{(act)}$ is PM

These rules are constructed using a combination of knowledge from physical laws, data from existing controllers, and heuristic knowledge from experts and reviewing previous studies with different controllers.

Fuzzy Inference and Defuzzification

The Mamdani-type Fuzzy inference system was chosen due to its ease of use and wide acceptance, as it closely aligns with human reasoning using linguistic variables. This method involves:

1. **Clipping:** The output membership functions at the rule strength for each rule will be done.
2. **Aggregating:** All fuzzy set into an output distribution will be done as discussed previously in this chapter.
3. **Defuzzifying:** The output distribution to produce a crisp actuation signal (force) using the centroid method, which calculates center of area under the aggregated fuzzy set output.

Implementation and Membership Function Design

The vertical displacement error ($e_{(t)}$) and its rate ($\frac{de_{(t)}}{dt}$) are the two inputs to the FLC, while the actuation signal (force $f_{(act)}$) is the output. These variables are divided into five fuzzy sets based on the output response of the passive suspension system and used in the design. Using the MATLSB-Simulink fuzzy logic tool boxes, triangular membership functions are defined for each case of input and output. The membership function editor in Simulink allows for adjusting the range and shape of these fuzzy sets. The designed FLC, shown in figure 4.5, utilizes two inputs and one output to control the SAVGS system effectively and figure 4.6 shows all the membership functions used.

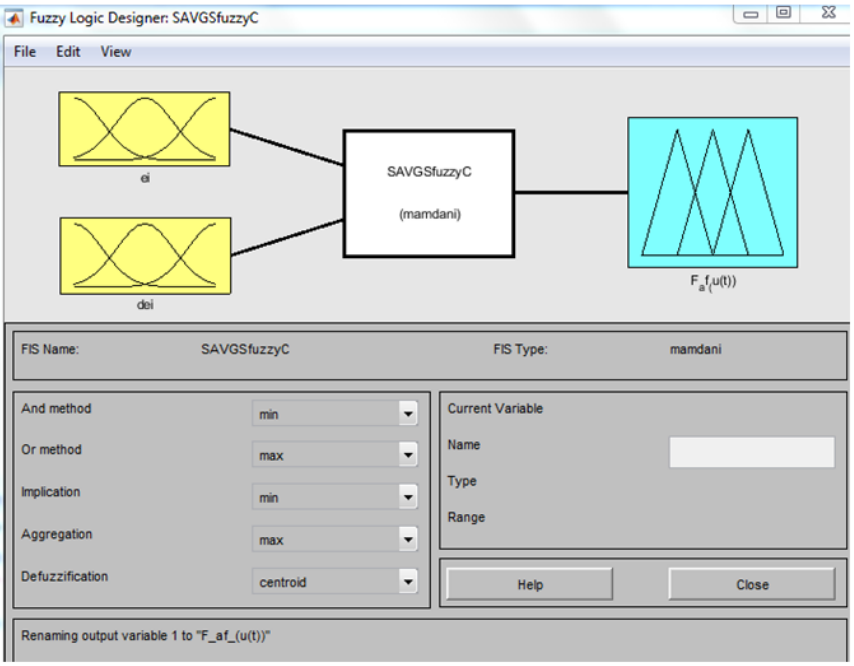

Figure 4.5: Overall Fuzzy logic Structure of the Input and output

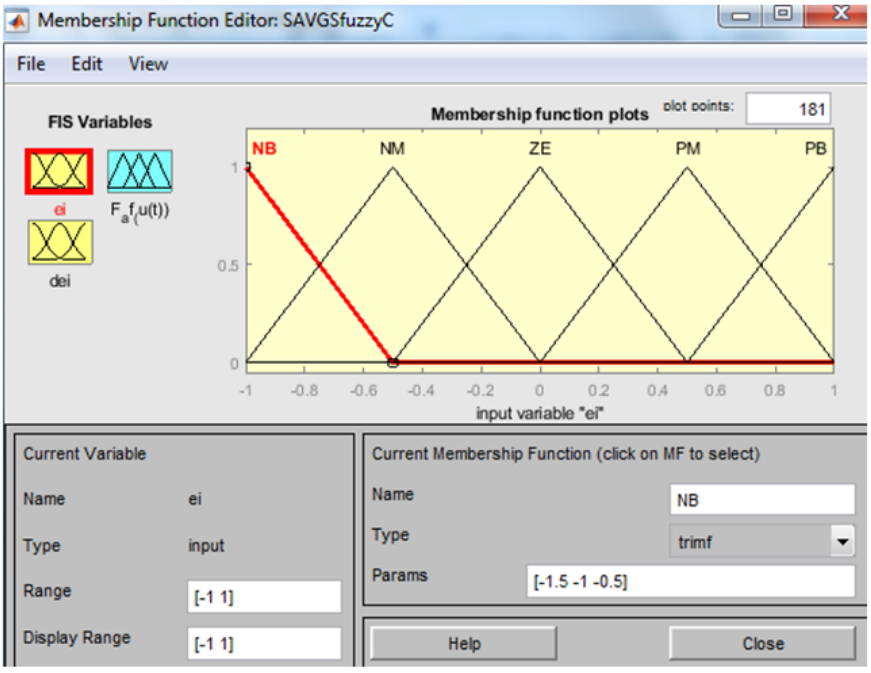

(a)

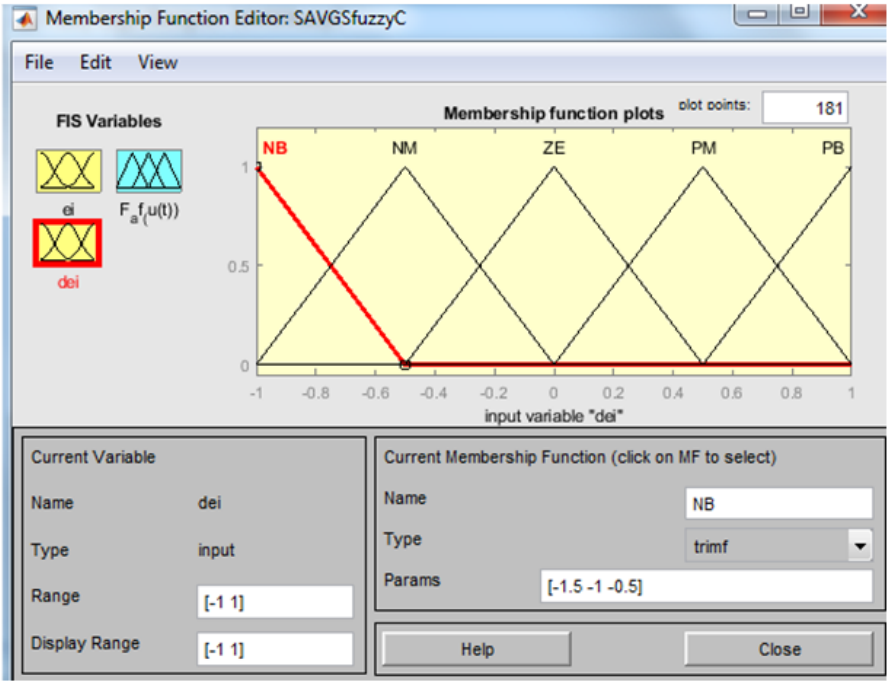

(b)

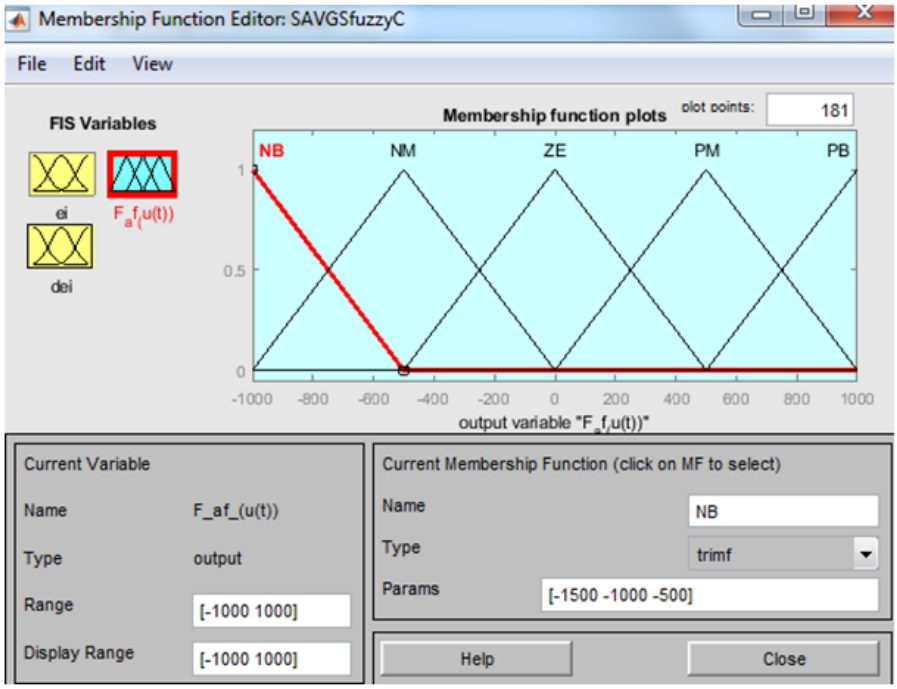

(c)

Figure 4.6: Membership function editor a) Error ($e_{(t)}$), b) Error rate ($\frac{de_{(t)}}{dt}$) c) Actuation signal (force $f_{(act)}$)

In summarizing, by constructing the fuzzy logic with well-defined fuzzy sets, a comprehensive rule-base, and a Mamdani-type inference system, the SAVGS is expected to perform optimally, maintaining better ride comfort and road handling by minimizing the impact of disturbances. The FLC's design enables adaptive control through linguistic rules, offering robust performance against the nonlinearities and uncertainties in the system.

Fuzzy Logic Controller Rule-Base for SAVGS system

The rule base for the Fuzzy Logic Controller (FLC) in the Suspension Active Vehicle Ground System (SAVGS) is constructed to simulate human decision-making in controlling the suspension system. The two inputs to the FLC are the vertical displacement error ($e_{(t)}$) and vertical rate error ($\frac{de_{(t)}}{dt}$), which respectively provide information on the displacement magnitude and speed/direction of the sprung mass endpoint. The output from the FLC is the actuation signal (force $f_{(act)}$), which adjusts based on these two inputs to maintain system stability and comfort. So the structure of the rule-base is discussed as follow.

Based on the system's response, the rule base is defined to achieve the following actions:

1. **When both the error and error rate are Negative**: Apply a Negative force to steer the system back towards equilibrium state.
2. **When the error is Negative and error rate is Positive:** Apply a positive force to continue correcting the displacement in the positive direction.
3. **When the error and error rate both are Positive:** Apply a Negative force to reduce the error and bring the system towards the equilibrium.
4. **When the error is Positive and error rate is Negative:** Apply a Positive force to continue reducing the error in the controlled manner.

This rile-base ensures that the controllers adjusts the force based on both the magnitude and direction of the errors, resulting in smooth transitions and reduces overshoot or undershoot. Having discussed the basic conditions the decision table (Rule-Base) can be constructed as follow with 25 rules for both the front and rear FLC used as it is considered it experiences the same road disturbance in front and rear sides except time delay.

The following table provides a decision matrix for the FLC, mapping the two fuzzy inputs to the desired actuator force output: which is expected to have a better performance compared to passive suspension system.

Table 4.1: Fuzzy Logic Controller Rule-Base

		$\frac{de_{(t)}}{dt}$				
$e_{(t)}$		NB	NM	Z	PM	PB
	NB	NB	NB	NM	Z	PM
	NM	NB	NM	NM	Z	PM
	Z	NM	NM	Z	PM	PB
	PM	NM	Z	PM	PM	PB
	PB	Z	PM	PM	PB	PB

In this table: Note that, NB stands for "Negative Big', NM stands for "Negative Medium", ZE stands for "Zero', PM stands for "Positive Medium", and PB stands for "Positive Big".

Each cell in the decision table represents a fuzzy rule in the FLC, where the combination of the inputs (error and error rate) maps to the output actuation signal (force). For instance when both the error ($e_{(t)}$) and error rate ($\frac{de_{(t)}}{dt}$) are "NB", the output actuation signal (force $f_{(act)}$) is "NB", indicating a strong negative force to counteract the large displacement and rate in the negative direction.

Now with this consistence Rule-Base we can see smoothed surface designed in figure 4.7 below.The Surface Viewer in MATLAB-Simulink is used to visualize the FLC's output behavior across all possible input combinations of designed Rule-bases. This viewer provides a three-dimensional surface plot of the actuating signal (force $f_{(act)}$) as a function of the two inputs, the error ($e_{(t)}$) and error rate ($\frac{de_{(t)}}{dt}$).The surface plot helps to confirm that the FLC's output varies smoothly and predictably in response to changes in the inputs, which is crucial for ensuring stable control performance.

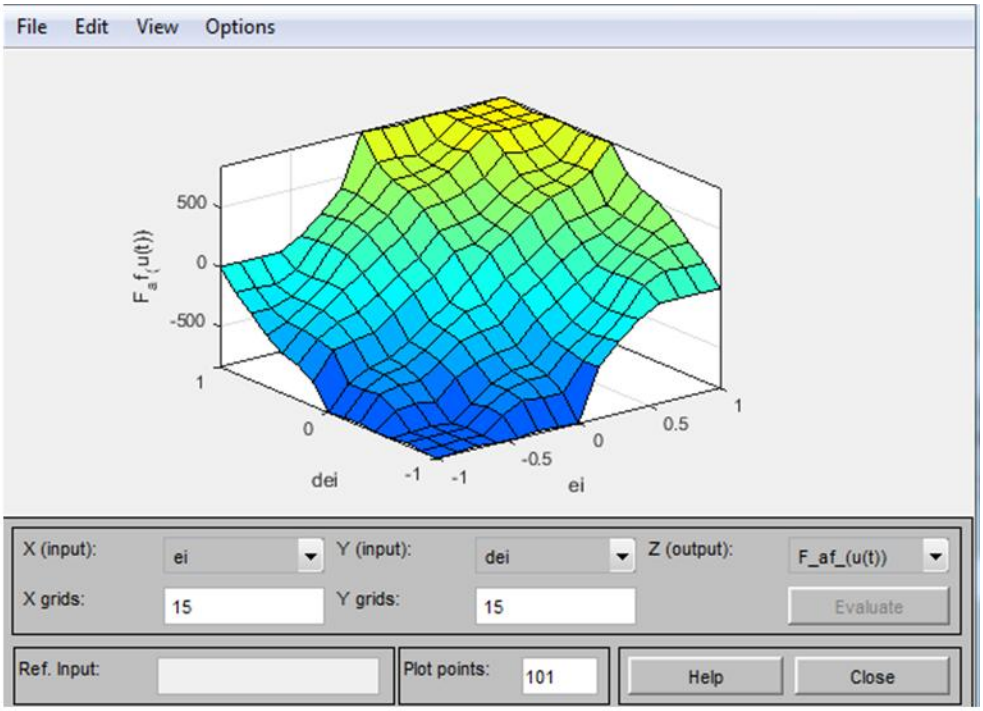

Figure 4.7: Designed Fuzzy Rule Surface (Surface Viewer)

The Surface Viewer acts as a read-only editor, allowing users to assess how the FLC will respond without altering the system or inference object. This visualization can assist in refining the membership functions and rule base if the control response is not optimal.

CHAPTER 5

SIMULATION AND RESULT

5.1 Over View

The dynamic behavior of both Passive suspension and the Fuzzy Logic Controller based Active suspension SAVGS systems for a full-car model is analyzed using MATLAB-Simulink. The purpose of this comparison is to evaluate the performance improvements of the FLC-based Active suspension SAVGS system over the traditional passive suspension system focusing on passenger comfort, suspension safety, and road handling capabilities. The tests were conducted under identical conditions, where the car experiences a single bump (acting as a speed breaker) at two different constant forward velocities: 20 km/hr and 50 km/hr and thirdly for pothole at 20km/hr.

5.2 Comparison of Passive vs. FLC-Based Active Suspension SAVGS systems

The comparison is done by implementing it on MATLAB-Simulink environment and the analysis is also done.

Evaluation Criteria: The performance of the suspension system is assessed/done based on the following criteria's:

- **Passenger Comfort:** Observed through, Amplitude of vertical acceleration of sprung mass, and Roll and Pitch acceleration of sprung mass.
- **Suspension Safety:** Evaluated by, Suspension travel (the range of motion in the suspension system) and Velocity at each front and rear wheels.
- **Road Handling:** assessed through, Tire deflection at each front and rear wheels, which indicate the ability of the tire to maintain contact with the road surface.

The goal of the FLC active suspension system (SAVGS) is to achieve reduced peak overshoot, faster settling times, and an overall smoother response to road disturbances when compared to the passive suspension system which is done in MATLAB-Simulink.

Simulation Setup: MATLAB-Simulink was used to create block diagrams for both Passive and Active suspension SAVGS systems and Road profile input (A single bump, acting as a speed breaker, was used as the road disturbance input for both simulations). The simulation time frame was conducted over a 10 second period and the simulations were carried out for two different vehicle speeds (20 km/hr and 50 km/hr) to assess performance under different forward velocities. The overall block diagram of the comparative model, including both the passive and FLC-Based active suspension SAVGS systems, is illustrated on figure 5.1 below.

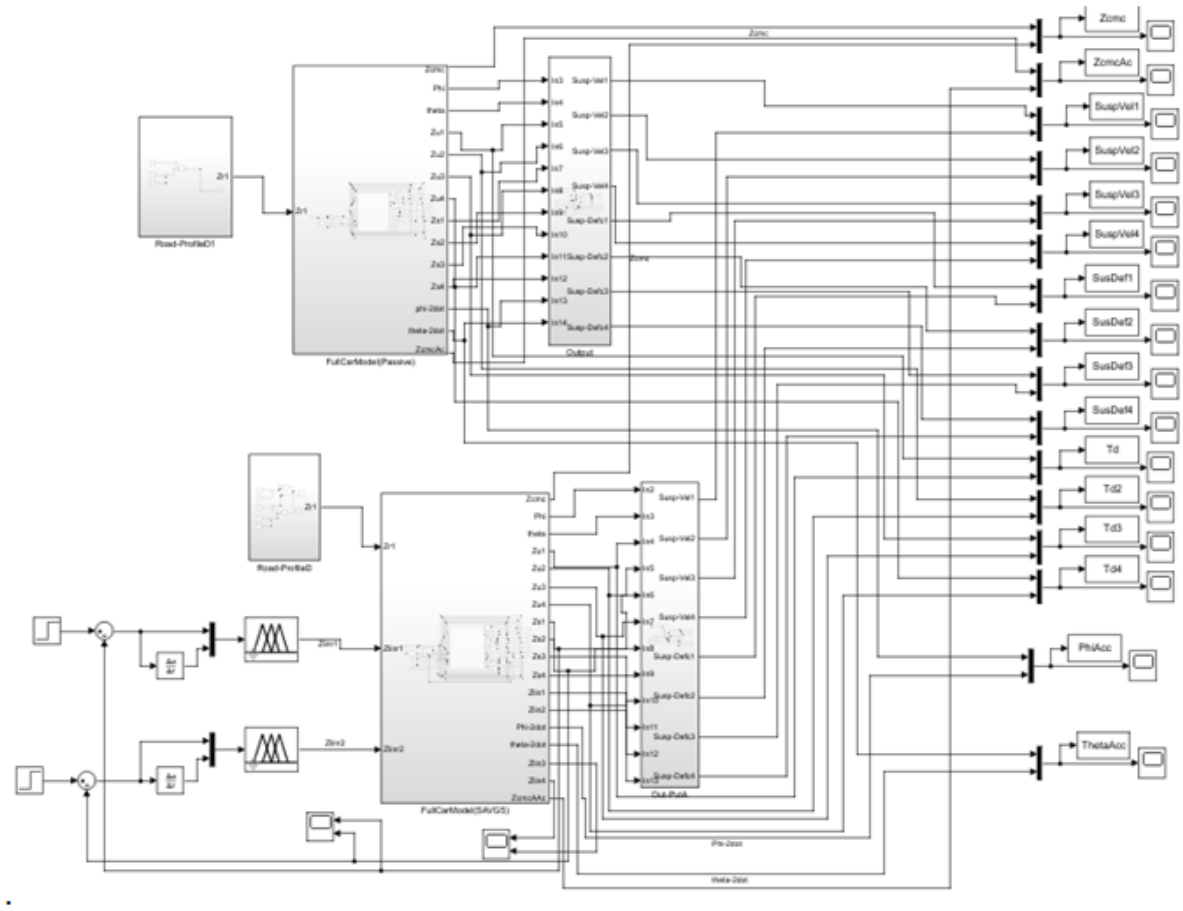

Figure 5.1: Comparative Simulink Model of Passive and FLC-Based Suspension SAVGS systems.

Result and Analysis

The results for both systems are illustrated in figure 5.2 and figure 5.3, showing the performance response of both Passive and FLC-Based Active suspension SAVGS systems over the same speed breaker road profile at 20 km/hr and 50 km/hr, respectively. Below in each figure there is a summary of the comparative findings.

1. Passenger Comfort

- **Vertical Acceleration:** The FLC-Based active Suspension SAVGS system lower amplitude of acceleration, indicating a smoother rides and improved comfort.
- **Roll and Pitch Acceleration:** With the FLC-Based active Suspension SAVGS system, both the roll and pitch accelerations were reduced, providing a more stable experience for passengers, particularly at the higher speed of 50 km/hr.

2. Suspension Safety

- **Suspension Travel and Velocity:** The FLC-Based active Suspension SAVGS system showed reduced suspension travels and velocities at both the front and rear wheels, highlighting an improvement in suspension stability and safety. This result suggests that the FLC active system can better manage the suspension's range of motions and movement speed, enhancing overall system durability.

3. Road Handling

- **Tire Deflection:** The FLC-Based Active suspension SAVGS system demonstrates less tire deflection than the passive suspension, particularly when encountering a bump at 50 km/hr. This improvement indicates better road contact and handling stability, reducing the likelihood of loss of traction.

Let's see each response in the following figures.

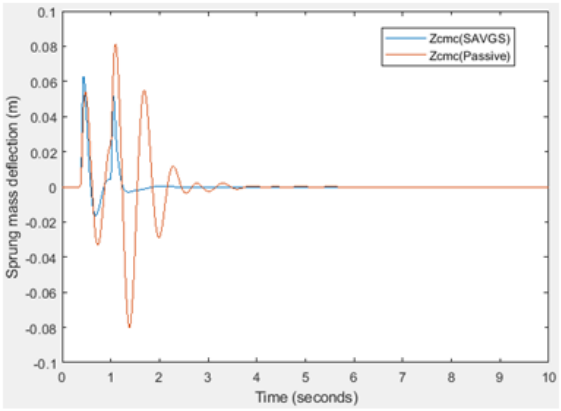

i) Sprung mass deflection

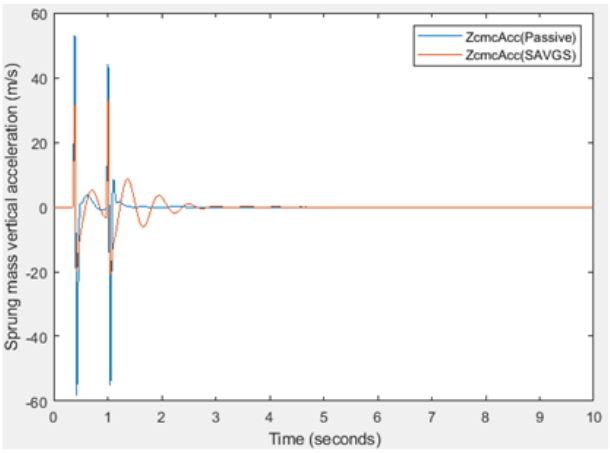

ii) Sprung mass vertical acceleration

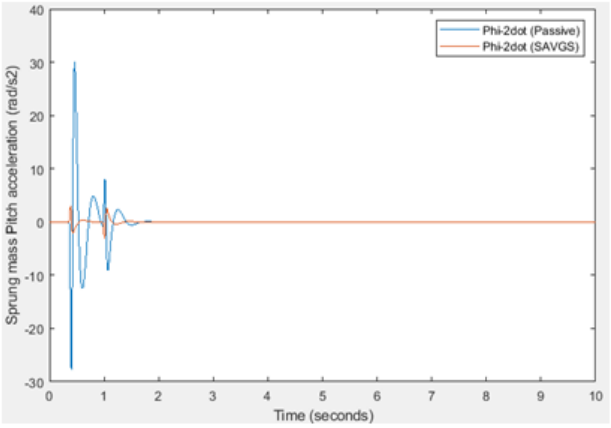

iii) Sprung mass Pitch acceleration

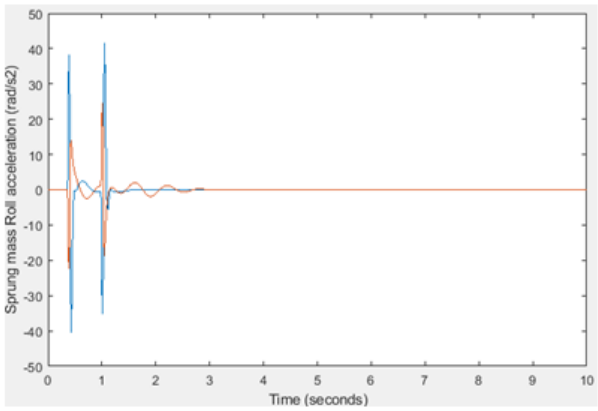

iv) Sprung mass Roll acceleration

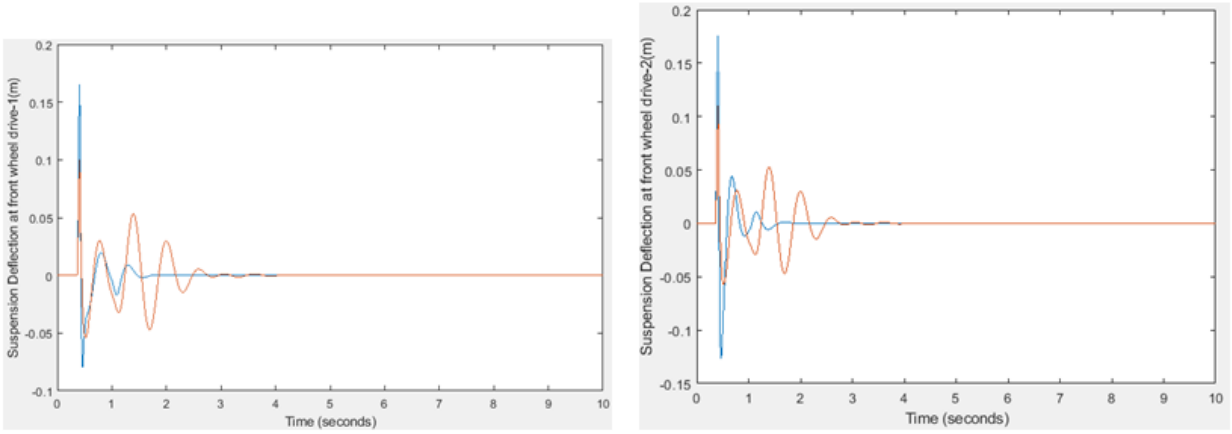

v) Suspension Deflection at front wheel drive (1 and 2)

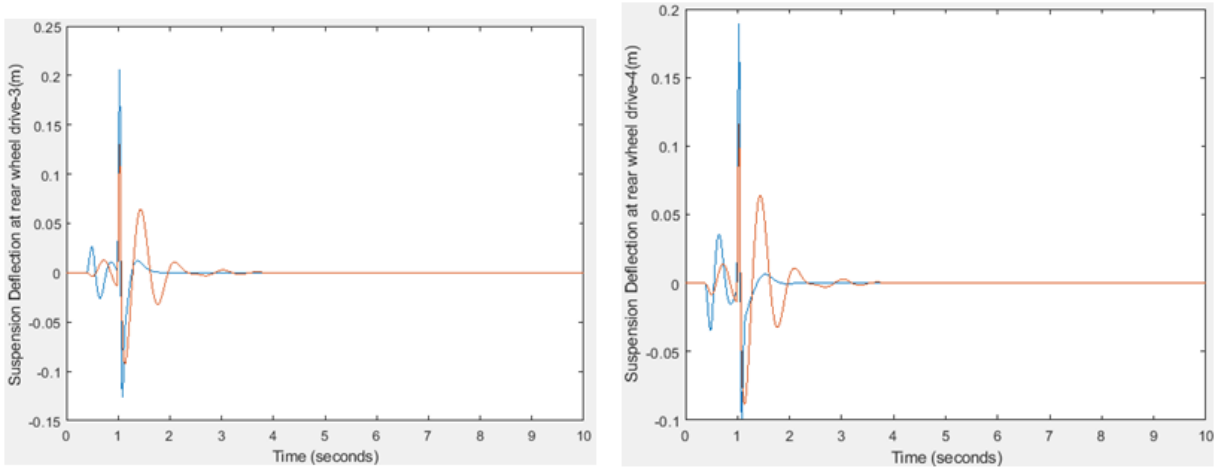

vi) Suspension Deflection at rear wheel drive (3 and 4)

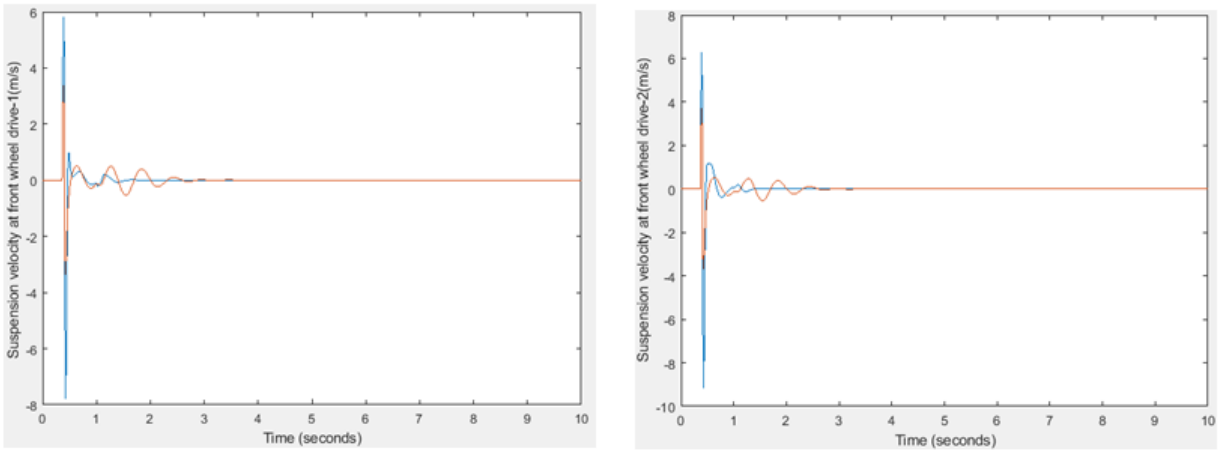

vii) Suspension velocity at front wheel drive (1 and 2)

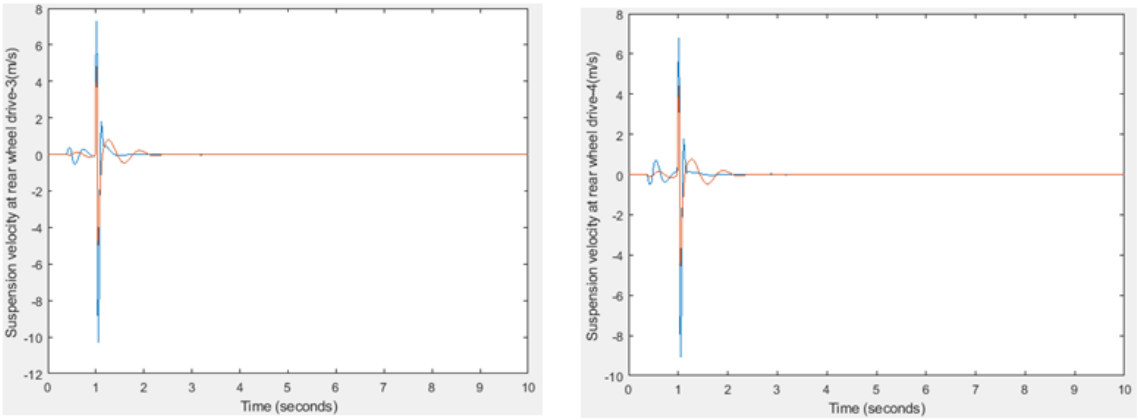

viii) Suspension velocity at rear wheel drive (3 and 4)

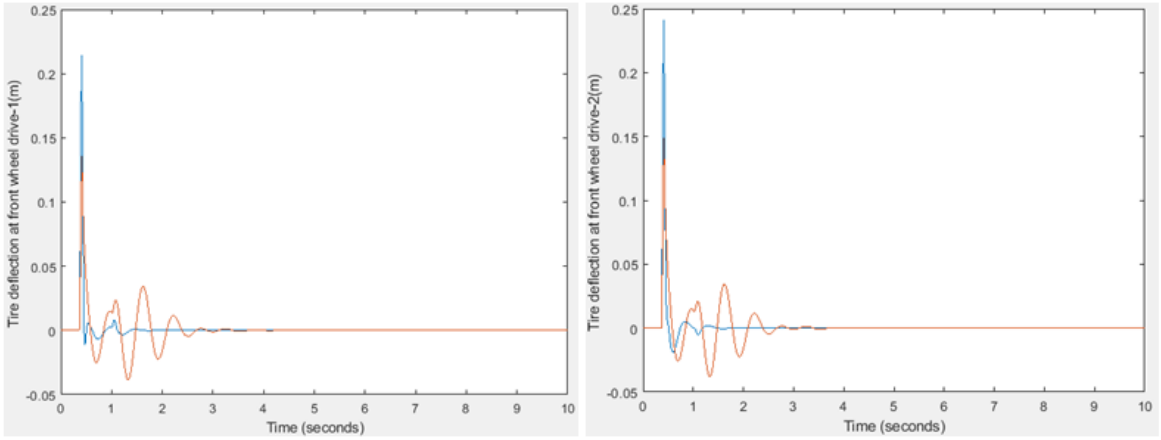

ix) Tire deflection at front wheel drive (1 and 2)

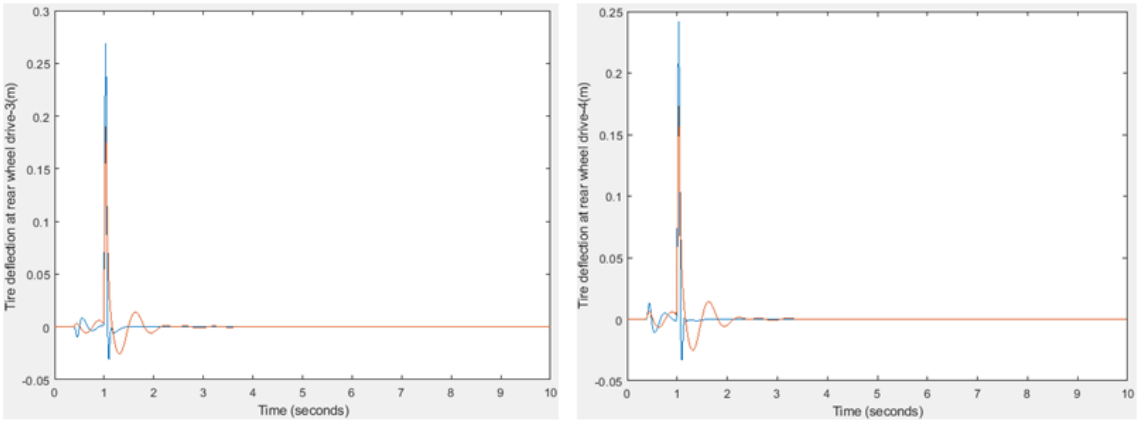

x) Tire deflection at rear wheel drive (3 and 4)

Figure 5.2: Passive and FLC-Based SAVGS systems Response to a road profile under 20 km/hr constant forward velocity of the car.

Quantitative Comparison

The following Table 5.1 and Table 5.2 both provides a quantitative comparison of a key performance matrices for the FLC-Based active suspension SAVGS against the passive suspension system. These tables summarize the improvement in Passenger Ride Comfort, Suspension Safety, and Road Handling in terms of percentage increase or decreases.

Let's see first the comparison of the 20 km/hr forward velocity response below in table 5.1.

Table5.1: Peak Overshoot comparison of Passive and FLC-Based SAVGS system Parameters at 20 km/hr forward velocity

NO	Measurement parameters	Passive Suspension	FLC(SAVGS)	FLC Vs. Passive Compared	Percentage improvement
	Passenger Ride Comfort				
1	Suspension Deflection, $\|Zcmc\|$(m)	0.0827	0.0511	0.0316 ↓	38.21%
2	Suspension Vertical Acceleration, $\|\ddot{Z}cmc\|$ ...(m/s2)	53.14	31.53	21.61 ↓	41.67%
3	Sprung Mass Pitch Acceleration, $\|\ddot{\varphi}\|$… (rad/s2)	30.02	2.937	27.083 ↓	90.21%
4	Sprung Mass Roll Acceleration, $\|\ddot{\theta}\|$… (rad/s2)	41.53	21.6	19.93 ↓	47.99%
	Suspension Safety				
5	Suspension Defl. at Front wheel Drive-1, $\|Zs1 - Zu1\|$… (m)	0.165	0.079	0.086 ↓	52.12%
6	Suspension Defl. at Front wheel Drive-2, $\|Zs2 - Zu2\|$… (m)	0.175	0.089	0.086 ↓	49.14%
7	Suspension Defl at Rear wheel Drive-3, $\|Zs3 - Zu3\|$… (m)	0.206	0.128	0.078 ↓	37.86%
8	Suspension Defl at Rear wheel Drive-4, $\|Zs4 - Zu4\|$… (m)	0.189	0.106	0.083 ↓	43.92%
9	Suspension Velocity at Front wheel Drive-1, $\|\dot{Z}s1 - \dot{Z}u1\|$… (m/s)	7.789	3.275	4.512 ↓	57.95%
10	Suspension Velocity at Front wheel Drive-2, $\|\dot{Z}s2 - \dot{Z}u2\|$… (m/s)	9.168	3.717	5.451 ↓	59.46%
11	Suspension Velocity at Rear wheel Drive-3, $\|\dot{Z}s3 - \dot{Z}u3\|$… (m/s)	10.29	4.755	5.535 ↓	53.79%

12	Suspension Velocity at Rear wheel Drive-4, $\|\dot{Z}s4 - \dot{Z}u4\|$… **(m/s)**	9.078	4.324	4.754 ↓	52.37%
	Road Holding				
13	Tire Deflection at Front Wheel Drive-1, $\|Zu1 - Zr1\|$… **(m)**	0.214	0.115	0.099 ↓	46.26%
14	Tire Deflection at Front Wheel Drive-2, $\|Zu2 - Zr2\|$… **(m)**	0.241	0.128	0.113 ↓	46.89%
15	Tire Deflection at Rear Wheel Drive-3$\|Zu3 - Zr3\|$… **(m)**	0.268	0.169	0.099 ↓	36.94%
16	Tire Deflection at Rear Wheel Drive-4, $\|Zu4 - Zr4\|$… **(m)**	0.241	0.153	0.091 ↓	37.76%

Table 5.1 Comparative result at 20 km/hr: Shows how the FLC-Based active suspension SAVGS system performs compared to the passive suspension system in low speed conditions and indicates significant improvement in comfort and stability due to smoother vertical acceleration and reduced suspension travels.

Now let's see the figure 5.3 at 50 km/hr forward velocity system response and followed by the quantitative comparison on table 5.2.

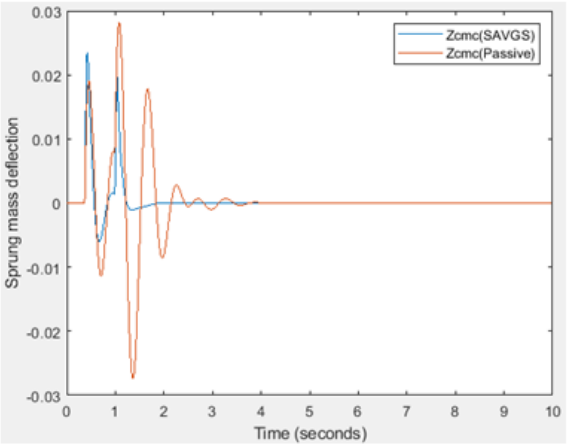

i) Sprung mass deflection

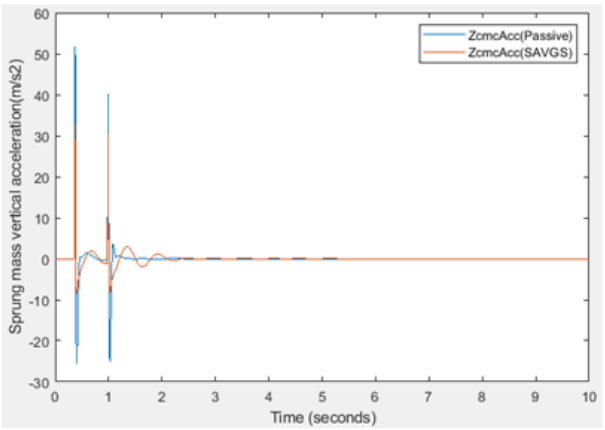

ii) Sprung mass vertical acceleration

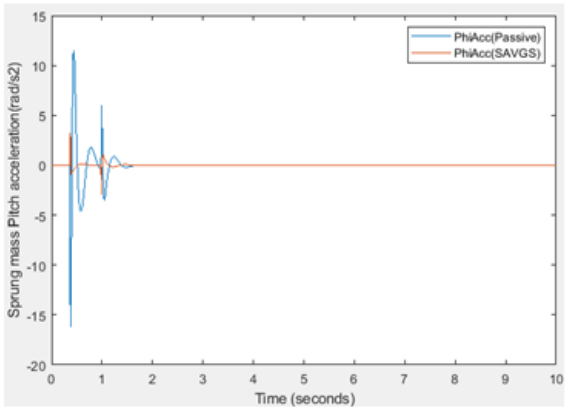

iii) Sprung mass Pitch acceleration

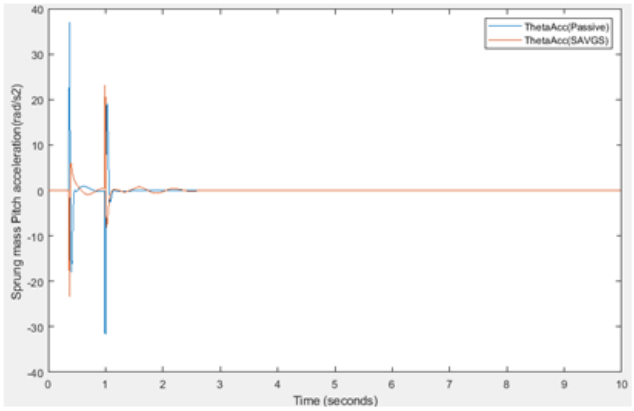

iv) Sprung mass Pitch acceleration

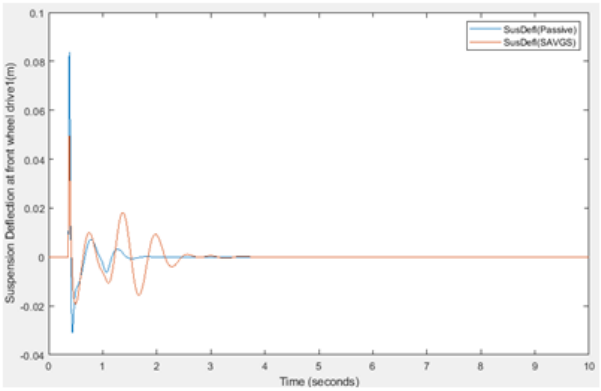

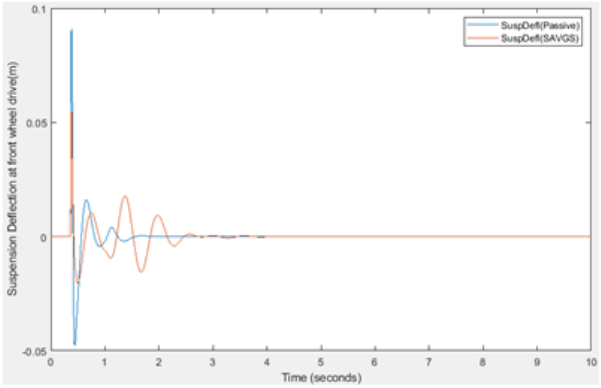

v) Suspension Deflection at front wheel drive

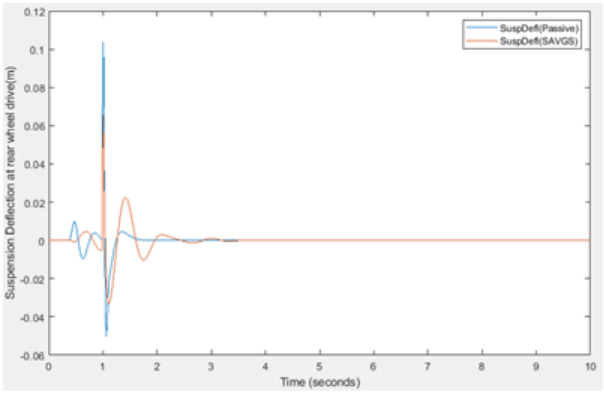

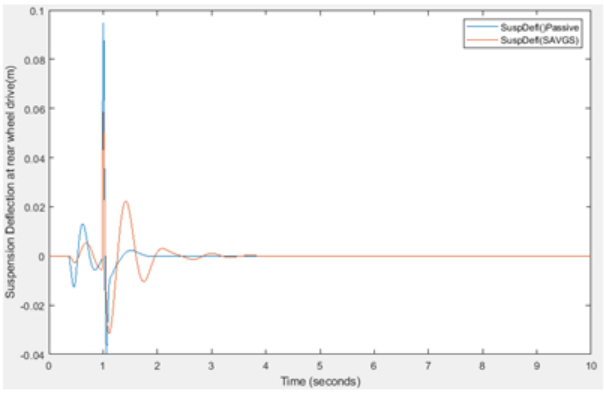

vi) Suspension Deflection at rear wheel drive

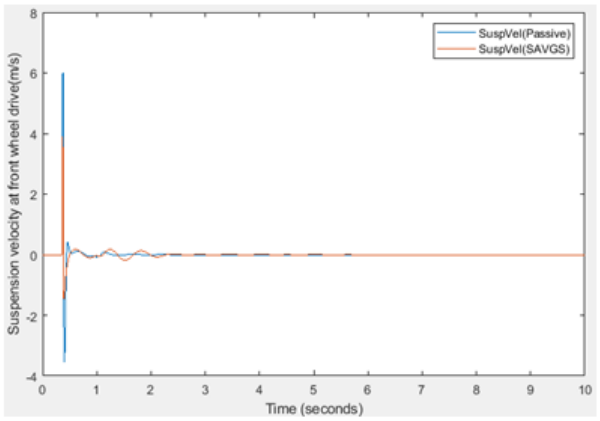

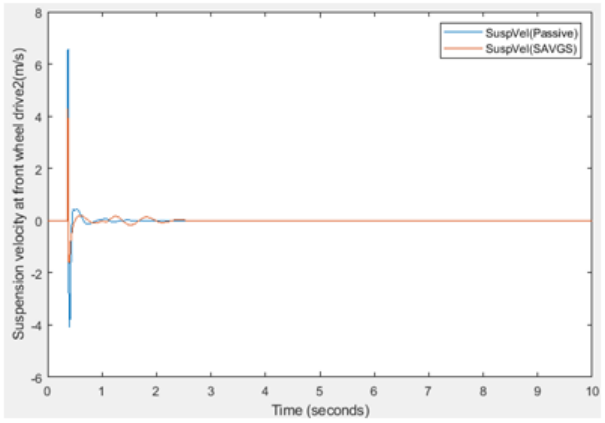

vii) Suspension velocity at front wheel drive

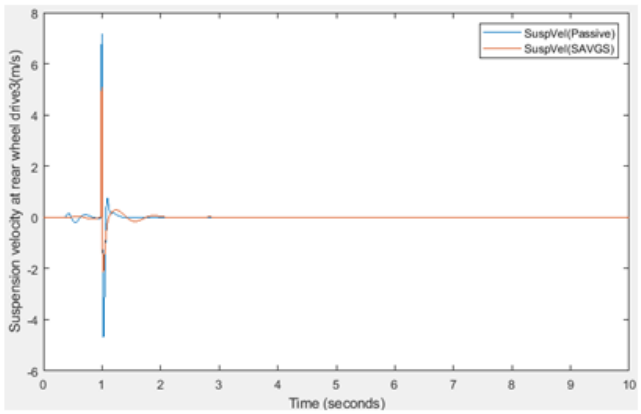

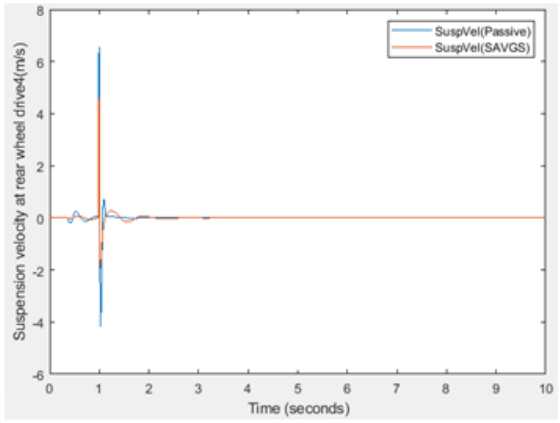

viii) Suspension velocity at rear wheel drive

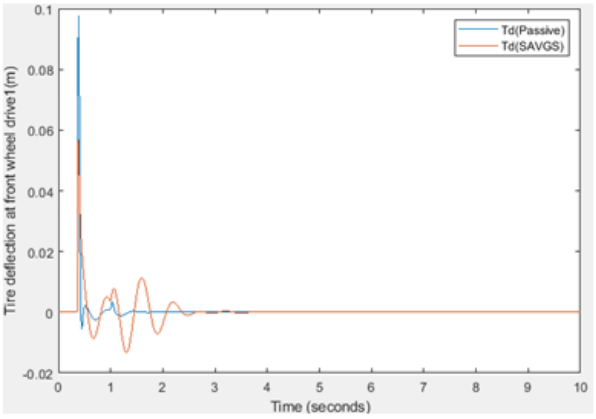

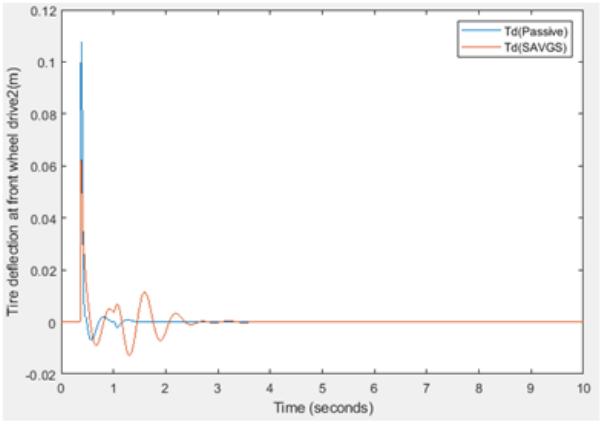

ix) Tire deflection at front wheel drive

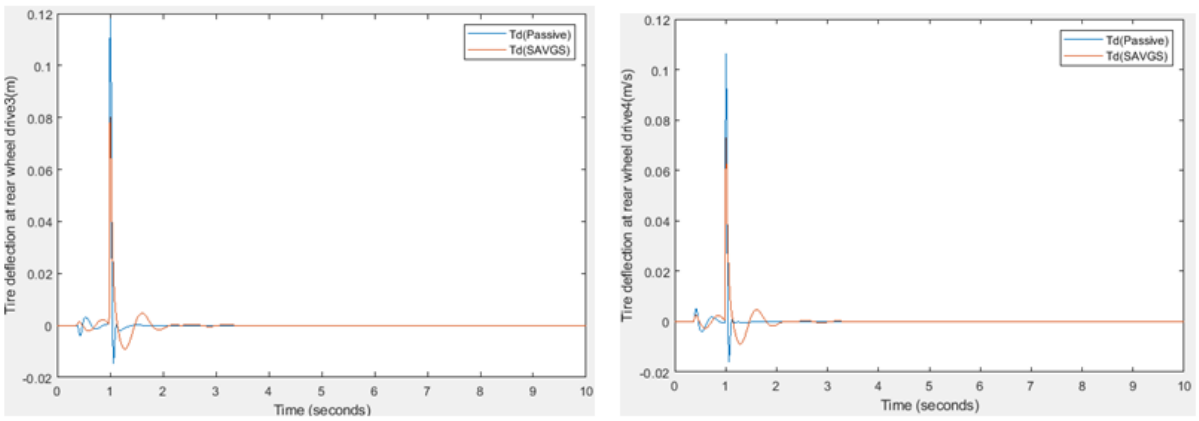

x) Tire deflection at rear wheel drive

Figure 5.3: Passive and FLC-Based SAVGS systems Response to a road profile under 50 km/hr constant forward velocity of the car.

Table 5.2: Peak Overshoot comparison of Passive and FLC-Based SAVGS system Parameters at 50 km/hr forward velocity.

NO	Measurement parameters	Passive Suspension	FLC(SAVGS)	FLC Vs. Passive Compared	Percentage improvement
	Passenger Ride Comfort				
1	Suspension Deflection,$\|Zcmc\|$ **(m)**	0.0382	0.0235	0.0147 ↓	38.48%
2	Suspension Vertical Acceleration, $\|\ddot{Z}cmc\|$ ... **(m/s2)**	51.72	30.86	20.86 ↓	40.33%
3	Sprung Mass Pitch Acceleration, $\|\ddot{\varphi}\|$**…** **(rad/s2)**	16.14	3.17	12.97 ↓	80.21%
4	Sprung Mass Roll Acceleration, $\|\ddot{\theta}\|$**…** **(rad/s2)**	36.92	23.2	9.8 ↓	75.38%
	Suspension Safety				
5	Suspension Defl at Front wheel Drive-1, $\|Zs1 - Zu1\|$**…** **(m)**	0.0837	0.0495	0.0342 ↓	40.86%
6	Suspension Defl at Front wheel Drive-2, $\|Zs2 - Zu2\|$**…** **(m)**	0.091	0.054	0.037 ↓	40.66%
7	Suspension Defl at Rear wheel Drive-3, $\|Zs3 - Zu3\|$**…** **(m)**	0.104	0.0652	0.039 ↓	37.5%
8	Suspension Defl at Rear wheel Drive-4, $\|Zs4 - Zu4\|$**…**	0.0945	0.0555	0.039 ↓	41.27%

	(m)				
9	Suspension Velocity at Front wheel Drive-1, $\lvert \dot{Z}s1 - \dot{Z}u1 \rvert$… **(m/s)**	6	3.6	2.4 ↓	40%
10	Suspension Velocity at Front wheel Drive-2, $\lvert \dot{Z}s2 - \dot{Z}u2 \rvert$… **(m/s)**	6.568	4.3	2.268 ↓	34.53%
11	Suspension Velocity at Rear wheel Drive-3, $\lvert \dot{Z}s3 - \dot{Z}u3 \rvert$… **(m/s)**	7.162	4.49	2.61 ↓	36.45%
12	Suspension Velocity at Rear wheel Drive-4, $\lvert \dot{Z}s4 - \dot{Z}u4 \rvert$ … **(m/s)**	6.171	4.23	1.97 ↓	31.92%
	Road Holding				
13	Tire Deflection at Front Wheel Drive-1, $\lvert Zu1 - Zr1 \rvert$… **(m)**	0.0975	0.0568	0.0407 ↓	41.74%
14	Tire Deflection at Front Wheel Drive-2, $\lvert Zu2 - Zr2 \rvert$… **(m)**	0.1078	0.0623	0.0477 ↓	43.36%
15	Tire Deflection at Rear Wheel Drive-3$\lvert Zu3 - Zr3 \rvert$… **(m)**	0.118	0.0801	0.0379 ↓	32.12%
16	Tire Deflection at Rear Wheel Drive-4, $\lvert Zu4 - Zr4 \rvert$… **(m)**	0.106	0.0729	0.0331 ↓	31.23%

Table 5.2 Comparison Results at 50 km/hr: Highlights performance enhancements of the FLC-Based active suspension SAVGS system at higher speed, where road disturbances are more pronounced and demonstrates improved tire-road contacts, reduces roll, and pitch accelerations, showcasing the FLC's effectiveness at managing larger road inputs and has better settling time and steady state errors.

Next let's consider if the road has potholes and observe how the FLC-Based active suspension SAVGS system responses compared to the passive suspension system in figure 5.4 at 20 km/hr forward velocity system response and followed by the quantitative comparison on table 5.3.

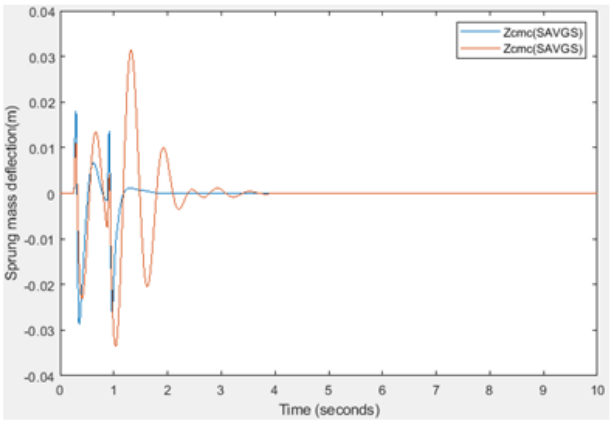

i) Sprung mass deflection

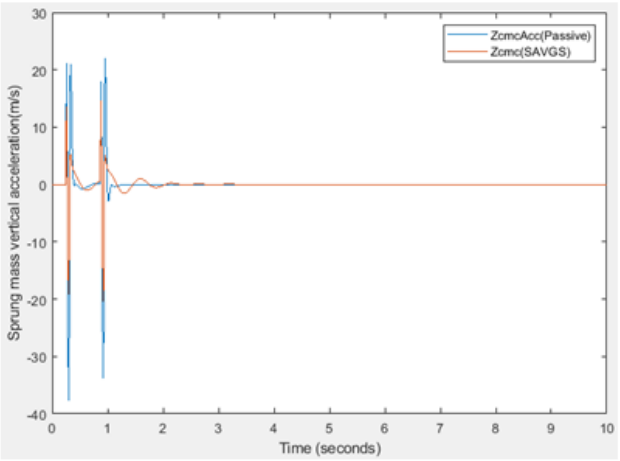

ii) Sprung mass vertical acceleration

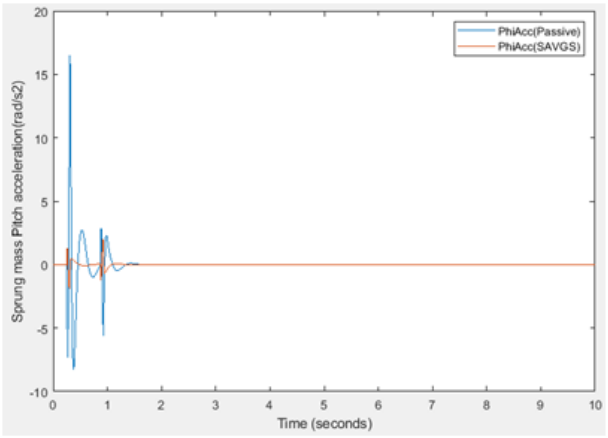

iii) Sprung mass Pitch acceleration

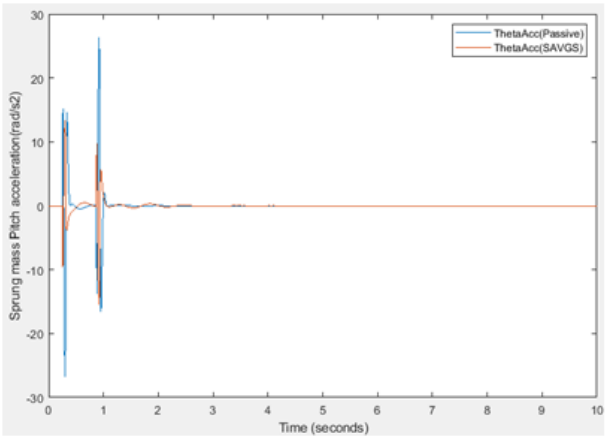

iv) Sprung mass Pitch acceleration

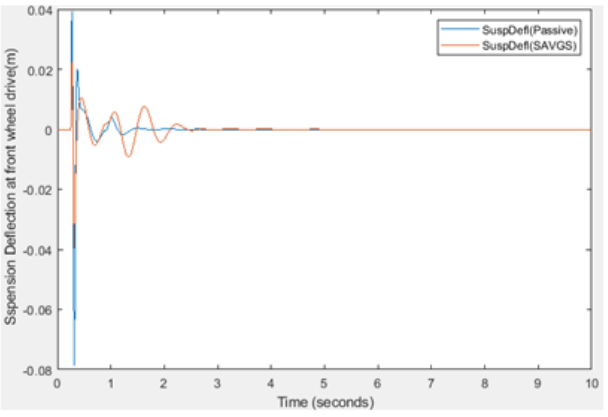

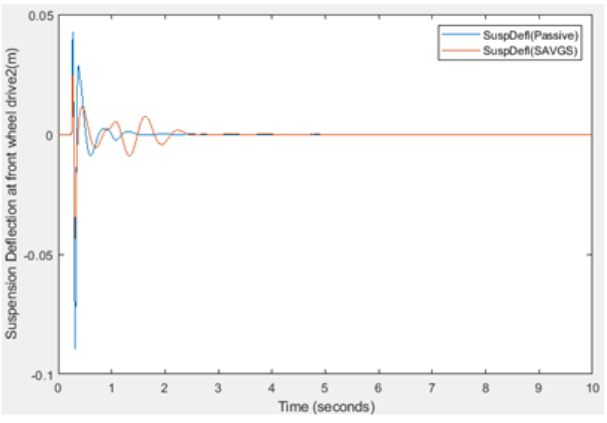

v) Suspension Deflection at front wheel drive

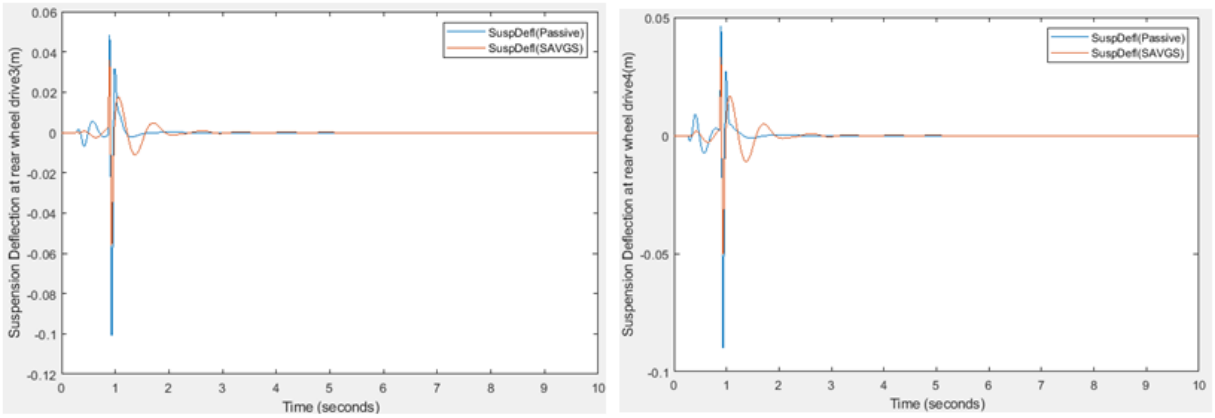

vi) Suspension Deflection at rear wheel drive

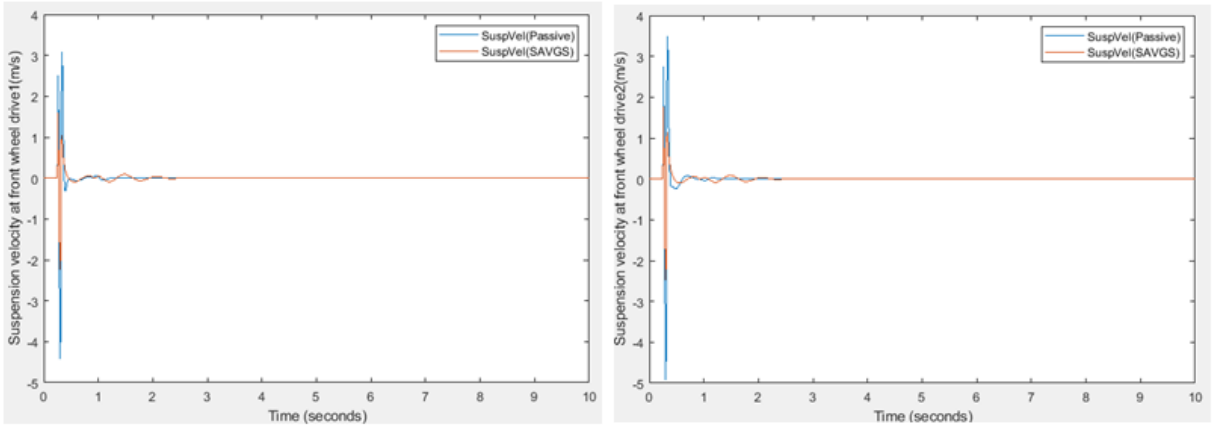

vii) Suspension velocity at front wheel drive

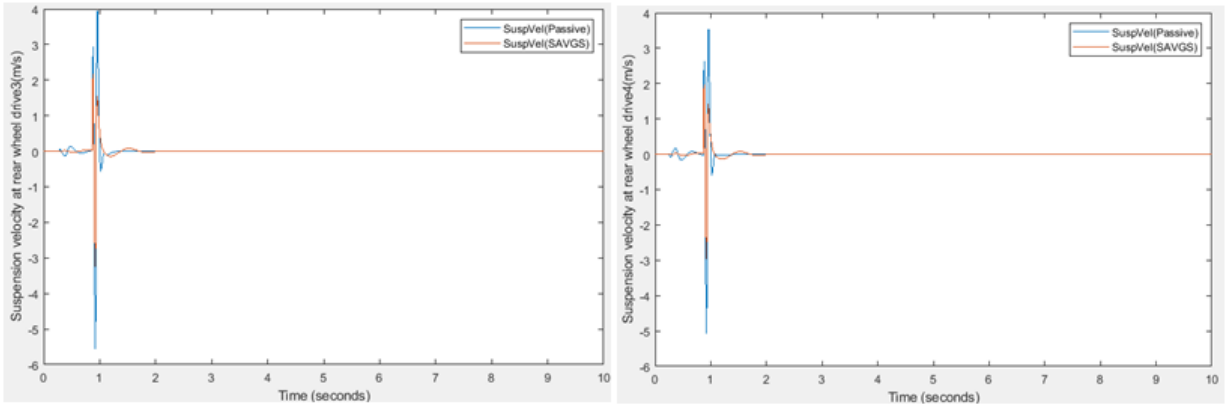

viii) Suspension velocity at rear wheel drive

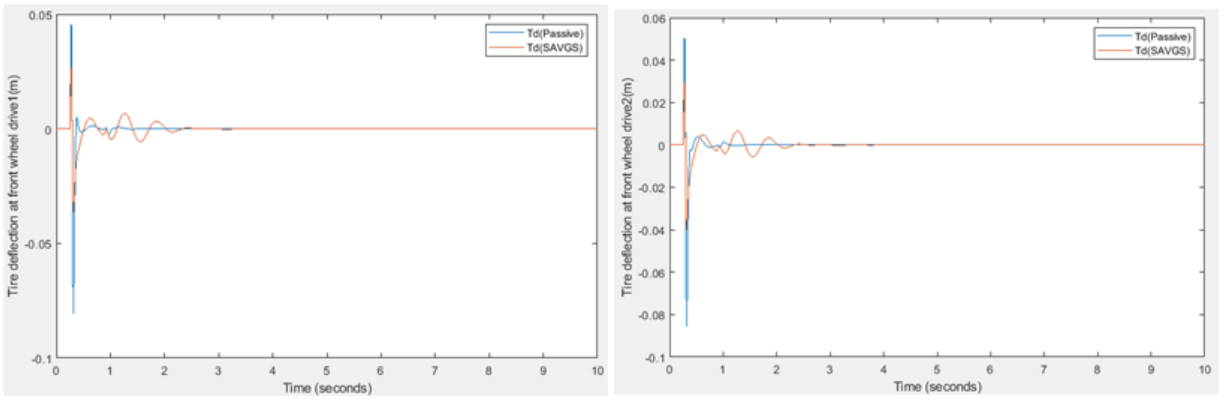

ix) Tire deflection at front wheel drive

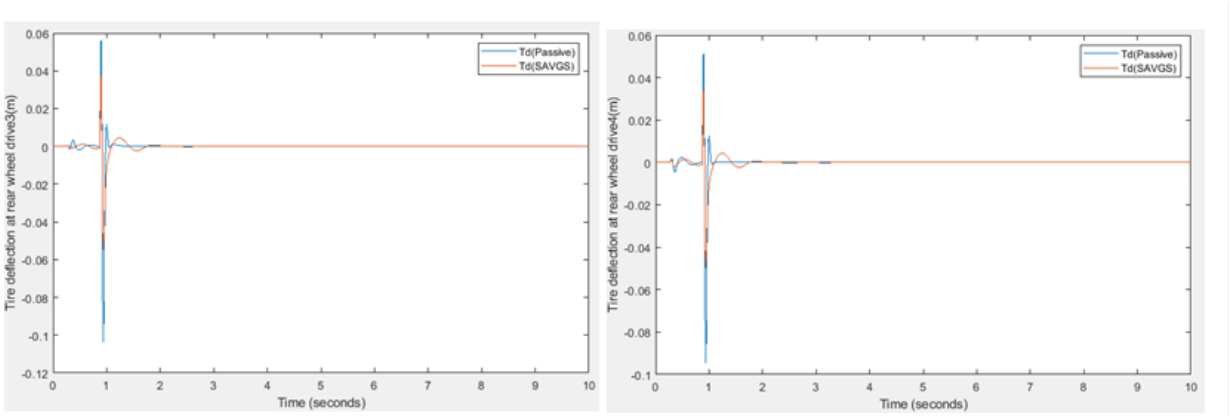

ix) Tire deflection at rear wheel drive

Figure 5.4: Passive and FLC-Based SAVGS systems Response to a pothole road profile under 20 km/hr constant forward velocity of the car.

Table 5.3: Peak Overshoot comparison of Passive and FLC-Based SAVGS system Parameters at 20 km/hr forward velocity for pothole road disturbance.

NO	Measurement parameters	Passive Suspension	FLC(SAVGS)	FLC Vs. Passive Compared	Percentage improvement
	Passenger Ride Comfort				
1	Suspension Deflection, $\|Zcmc\|$ **(m)**	0.0258	0.0137	0.0121	46.9%
2	Suspension Vertical Acceleration, $\|\ddot{Z}cmc\|$ ... **(m/s2)**	37.61	20.04	17.61↓	46.82%
3	Sprung Mass Pitch Acceleration, $\|\ddot{\varphi}\|$… **(rad/s2)**	16.52	1.99	14.53↓	87.54%
4	Sprung Mass Roll Acceleration,	26.79	15.48	11.31↓	42.22%

	$\lvert\ddot{\theta}\rvert$… (rad/s2)				
	Suspension Safety				
5	Suspension Defl at Front wheel Drive-1, $\lvert Zs1 - Zu1\rvert$… (m)	0.0787	0.0395	0.0392↓	49.81%
6	Suspension Defl at Front wheel Drive-2, $\lvert Zs2 - Zu2\rvert$… (m)	0.0896	0.0434	0.0462↓	51.56%
7	Suspension Defl at Rear wheel Drive-3$\lvert Zs3 - Zu3\rvert$… (m)	0.101	0.0559	0.0451↓	44.65%
8	Suspension Defl at Rear wheel Drive-4, $\lvert Zs4 - Zu4\rvert$… (m)	0.0901	0.0505	0.0396↓	43.95%
9	Suspension Velocity at Front wheel Drive-1, $\lvert \dot{Z}s1 - \dot{Z}u1\rvert$… (m/s)	4.41	2.235	2.175↓	49.32%
10	Suspension Velocity at Front wheel Drive-2, $\lvert \dot{Z}s2 - \dot{Z}u2\rvert$… (m/s)	4.92	2.46	2.46↓	50%
11	Suspension Velocity at Rear wheel Drive-3, $\lvert \dot{Z}s3 - \dot{Z}u3\rvert$… (m/s)	5.555	3.24	2.315↓	41.65%
12	Suspension Velocity at Rear wheel Drive-4, $\lvert \dot{Z}s4 - \dot{Z}u4\rvert$ … (m/s)	5.1	2.95	2.15↓	42.16%
	Road Holding				
13	Tire Deflection at Front Wheel Drive-1, $\lvert Zu1 - Zr1\rvert$… (m)	0.0806	0.0361	0.0445↓	55.22%
14	Tire Deflection at Front Wheel Drive-2, $\lvert Zu2 - Zr2\rvert$… (m)	0.0855	0.0398	0.0457↓	53.45%
15	Tire Deflection at Rear Wheel Drive-3$\lvert Zu3 - Zr3\rvert$… (m)	0.1035	0.0548	0.0487↓	47.05%
16	Tire Deflection at Rear Wheel Drive-4, $\lvert Zu4 - Zr4\rvert$… (m)	0.0943	0.0498	0.0445↓	49.12%

Here also the FLC-Based active suspension SAVGS system has got a better performance compared to passive suspension system with having lower suspension deflection and velocities with small overshoot and minimum settling time and small steady state error.

The **SAVGS (Series Active Variable Geometry Suspension)** system as it is a type of adaptive suspension technology designed to optimize vehicle handling, comfort, and stability by dynamically adjusting the suspension geometry based on driving conditions and her as we can see from the MATLAB-Simulink simulation for 20km/h and 50km/h using the designed FLC it enhances performance compared to the passive suspension system.

Additionally as seen from the simulation the **vertical deflection, vertical acceleration, roll acceleration, and pitch acceleration overshoots** are reduced compared to a passive suspension system, it indicates:

1. Improved Ride Comfort

- Lower **vertical deflection** means the suspension absorbs road irregularities better, reducing discomfort for passengers.
- Reduced **vertical acceleration** minimizes vibrations felt inside the vehicle, leading to a smoother ride.

2. Enhanced Vehicle Stability

- Lower **roll acceleration** means the vehicle experiences less body roll during cornering, improving handling and reducing the risk of rollover.
- Reduced **pitch acceleration** means the vehicle is more stable during braking and acceleration, preventing excessive nose-diving or lifting.

3. Better Road Holding and Control

- Less overshoot in suspension responses means **faster settling time**, improving the tire's contact with the road.
- Enhanced grip and traction improve the vehicle's ability to respond to steering inputs effectively.

4. Energy Efficiency and Durability

- A well-controlled suspension reduces excessive oscillations, minimizing energy dissipation and wear on suspension components.

So the Key Thing is; as these overshoots are reduced, the FLC based **SAVGS system outperforms the passive suspension**, offering a balance between ride comfort, handling, and stability while reducing unnecessary oscillations.

CHAPTER 6

CONCLUSION AND RECOMMENDATION

6.1 Conclusion

The simulation results suggest that the FLC active suspension system (SAVGS) offers substantial improvements over the passive suspension system across all evaluation criteria. The FLC system delivers better passenger comfort by minimizing peak accelerations, improved suspension safety by reducing suspension travel and velocity, and enhanced road holding through decreased tire deflection. These improvements were consistent across both test speeds, showing the robustness of the FLC-based system.

By integrating the FLC, the SAVGS system provides a more adaptive and responsive suspension, which can handle road disturbances more effectively than the passive system, leading to a smoother and safer ride experience, especially at higher speeds.

The study simulates the system's reaction to a disturbance input represented by a single bump (analogous to a speed breaker) and a pothole on a smooth road surface. The performance of the proposed active suspension system with the FLC is compared to a passive suspension system.

The simulation results indicate that the SAVGS exhibits improved performance concerning peak overshoot and settling time, suggesting that the active suspension system with the FLC offers superior ride comfort and handling capabilities compared to the passive suspension. Additionally, comparisons reveal that the FLC consistently outperforms the passive system across various performance metrics. The performance response at 20 kilometer per hour shows improvement in all the performance metrics, like in Passenger ride comfort is reduced in Vertical acceleration by 41.67% with reduced pitch and roll acceleration, Suspension safety is reduced in suspension deflection by 49.1% in front and 43.1% in rear sides with reduced velocity, and in road handling the tire deflection reduces by 46.3% at front and 36.9% at the rear sides of the car. Additionally he performance response at 50 kilometer per hour shows improvement in all the performance metrics, like in Passenger ride comfort is reduced in Vertical acceleration by 40.33% with reduced pitch and roll acceleration around 75-80%, Suspension safety is reduced in suspension deflection by 40.66% in front and 37.5% in rear sides with reduced velocity, and in road handling the tire deflection reduces by 41.74% at front and 31.23% at the rear sides of the car. So the designed FLC is in satisfying the performance matrices.

6.2 RECOMMENDATION

While this validates the effectiveness of an active suspension system using FLC in a full vehicle model, it is crucial to recognize that the current model is a linear simplification and may not accurately capture all vehicle dynamics. Future research should focus on creating a dynamic model that incorporates the full nonlinear behaviors of the suspension system.

One major advantage of simulating car suspension systems using computer models is the convenience, speed, and cost-effectiveness relative to developing and testing physical prototypes. Tools like MATLAB/Simulink facilitate thorough analysis of suspension performance until the research objectives are achieved. However, simulation results might not fully reflect real-world behavior, highlighting the importance of experimental validation.

To enhance the accuracy of the findings, it is advisable to conduct physical tests using a test rig to verify the simulation results. Prior to this, it is essential to investigate suitable sensors and actuators to ensure they meet the production prototype requirements, thereby facilitating a smooth transition from simulation to physical testing.

REFERENCE

[1] C. Arana, S. A. Evangelou, I. Asme, and D. Dini, “Series Active Variable Geometry Suspension application to chassis attitude control,” no. June, 2015.

[2] M. Yu *et al.*, “Model Identification and Control for a Quarter Car Test Rig of Series Active ScienceDirect Model Identification and Control for a Quarter Car Test Rig of Model Identification and Control for a Quarter Car Test Rig of Model Identification for a Quarter Car Test Rig of Series Active,” *IFAC-PapersOnLine*, vol. 50, no. 1, pp. 3376–3381, 2017.

[3] C. Cheng, S. A. Evangelou, C. Arana, and D. Dini, “Active Variable Geometry Suspension robust control for improved vehicle ride comfort and road holding Active variable geometry suspension robust control for improved vehicle ride comfort and road holding,” no. July, 2015.

[4] A. S. Gad, H. Elzoghby, W. A. H. Oraby, and S. El-demerdash, “Application of a Preview Control with an MR Damper Model Using Genetic Algorithm in Semi-Active Automobile Suspension,” no. October 2021, 2019.

[5] M. Yu, C. Cheng, S. A. Evangelou, S. Member, and D. Dini, “Robust Control for a Full-Car Prototype of Series Active Variable Geometry Suspension *.”

[6] N. S. Bhangal and K. A. Raj, “Fuzzy Control of Vehicle Active Suspension System,” vol. 5, no. 2, pp. 144–148, 2016.

[7] D. Wang, D. Zhao, M. Gong, and B. Yang, “Nonlinear Predictive Sliding Mode Control for Active Suspension System,” vol. 2018, 2018.

[8] M. Yu, S. Member, C. Arana, S. A. Evangelou, S. Member, and D. Dini, “Quarter-Car Experimental Study for Series Active Variable Geometry Suspension,” no. November, 2017.

[9] D. Version, “The Control of an Active Seat with Vehicle Suspension Preview Information,” vol. 24, no. 8, pp. 1412–1426, 2017.

[10] M. Gong, H. Wang, and X. Wang, “Active Suspension Control Based on Estimated Road Class for Off-Road Vehicle,” vol. 2019, 2019.

[11] R. Darus, “Modeling and control active suspension system for a full car model,” no. October, 2014.

[12] G. Ali and H. Nasser, “Vehicle Dynamics Response to Road Hump using a 10 Degrees of Freedom Full-Car Model Abstract :,” vol. 2, no. 1, 2015.

[13] T. D. Gillespie, “Fundamentals of Vehicle Dynamics.”

[14] C. Arana, S. A. Evangelou, and D. Dini, “crossmark,” *Control Eng. Pract.*, vol. 59, no. November, pp. 111–126, 2016.

[15] A. Sharkawy, A. S. Ali, N. M. Ghazaly, and G. Abdel-jaber, “PID CONTROLLER OF ACTIVE SUSPENSION SYSTEM FOR A QUARTER CAR,” no. December, 2015.

[16] L. Preserve, “Research and Simulation on New Active Suspension Control System,” 2013.

[17] S. K. Sharma, V. Pare, M. Chouksey, and B. R. Rawal, “Numerical Studies Using Full Car Model for Combined Primary and Cabin Numerical studies using full car model for combined primary and cabin suspension,” no. May, 2016.

[18] H. Du and N. Zhang, “with input constraint,” pp. 343–356, 2009.

[19] *No Title*. .

[20] H. Anant, N. Vivekanandan, and A. M. Fulambarkar, “Active Suspension System Based on Fuzzy Logic Controller for Quarter Car Model,” vol. 9, no. 43, pp. 323–334, 2016.

[21] *Introduction to Fuzzy Logic using MATLAB*. .

[22] M. Akpakpavi, “Modeling and Control of a Car Suspension System Using P , PI , PID , GA-PID and Auto- Tuned PID Controller in Matlab / Simulink,” vol. 3, no. 3, pp. 1506–1513, 2017.

[23] C. Mathworks, “Fuzzy Logic Toolbox ™ User ’ s Guide R 2018 a,” 2018.

[24] E. Alvarez-sánchez, “The 2013 Iberoamerican Conference on Electronics Engineering and Computer Science A quarter-car suspension system : car body mass estimator and sliding mode control,” *J. Mater. Process. Tech.*, vol. 7, pp. 208–214, 2013.

[25] R. Shakya, K. Rajanwal, S. Patel, and S. Dinkar, “Design and Simulation of PD , PID and Fuzzy Logic Controller for Industrial Application,” vol. 4, no. 4, pp. 363–368, 2014.

[26] J. R. Jang, “Fuzzy Logic Toolbox.”

[27] V. M. Peri, “FUZZY LOGIC CONTROLLER FOR AN AUTONOMOUS MOBILE ROBOT,” 2005.

Appendix A

State Space Equation for a Passive Suspension

$$\dot{X}(t) = AX(t) + f(t) \qquad , A = \begin{bmatrix} A11 & A12 \\ A21 & A22 \end{bmatrix}$$

$$A11 = \begin{bmatrix} 0 & 0 & 0 & 0 & 0 & 0 & 0 \\ 0 & 0 & 0 & 0 & 0 & 0 & 0 \\ 0 & 0 & 0 & 0 & 0 & 0 & 0 \\ 0 & 0 & 0 & 0 & 0 & 0 & 0 \\ 0 & 0 & 0 & 0 & 0 & 0 & 0 \\ 0 & 0 & 0 & 0 & 0 & 0 & 0 \\ 0 & 0 & 0 & 0 & 0 & 0 & 0 \end{bmatrix} \quad A12 = \begin{bmatrix} 1 & 0 & 0 & 0 & 0 & 0 & 0 \\ 0 & 1 & 0 & 0 & 0 & 0 & 0 \\ 0 & 0 & 1 & 0 & 0 & 0 & 0 \\ 0 & 0 & 0 & 1 & 0 & 0 & 0 \\ 0 & 0 & 0 & 0 & 1 & 0 & 0 \\ 0 & 0 & 0 & 0 & 0 & 1 & 0 \\ 0 & 0 & 0 & 0 & 0 & 0 & 1 \end{bmatrix}$$

$$A21 = \begin{bmatrix} \frac{2(-KfTfTf-KrTrTr)}{Ir} & 0 & 0 & \frac{-1}{Ir} & \frac{-1}{Ir} & \frac{-1}{Ir} & \frac{-1}{Ir} \\ 0 & \frac{2(-KfAfAf-KrBrBr)}{Ip} & \frac{2(-KfAf+KrBf)}{Ip} & \frac{-1}{Ip} & \frac{-1}{Ip} & \frac{-1}{Ip} & \frac{-1}{Ip} \\ 0 & \frac{2(-KfAf+KrBr)}{ms} & \frac{2(-Kf-Kr)}{ms} & \frac{-1}{ms} & \frac{-1}{ms} & \frac{-1}{ms} & \frac{-1}{ms} \\ \frac{KfTf}{muf} & \frac{KfAf}{muf} & \frac{Kf}{muf} & \frac{-1-Ktf}{muf} & 0 & 0 & 0 \\ \frac{-KfTf}{muf} & \frac{KfAf}{muf} & \frac{Kf}{muf} & 0 & \frac{-1}{muf} & 0 & 0 \\ \frac{KrTr}{mur} & \frac{-KrBr}{mur} & \frac{Kr}{mur} & 0 & 0 & \frac{-1-Ktr}{mur} & 0 \\ \frac{-KrTr}{mur} & \frac{-KrBr}{mur} & \frac{Kr}{mur} & 0 & 0 & 0 & \frac{-1-Ktr}{mur} \end{bmatrix}$$

$A22$

$$= \begin{bmatrix} \frac{2(-bfTfTf-brTrTr)}{Ir} & 0 & 0 & \frac{-1}{Ir} & \frac{-1}{Ir} & \frac{-1}{Ir} & \frac{-1}{Ir} \\ 0 & \frac{2(-CfAfAf-CrBrBr)}{Ip} & \frac{2(-CfAf+CrBr)}{Ip} & \frac{-1}{Ip} & \frac{-1}{Ip} & \frac{-1}{Ip} & \frac{-1}{Ip} \\ 0 & \frac{2(-CfAf+CrBr)}{ms} & \frac{2(-Cf-Cr)}{ms} & \frac{-1}{ms} & \frac{-1}{ms} & \frac{-1}{ms} & \frac{-1}{ms} \\ \frac{CfTf}{muf} & \frac{CfAf}{muf} & \frac{Cf}{muf} & \frac{-1}{muf} & 0 & 0 & 0 \\ \frac{-CfTf}{muf} & \frac{bfa}{muf} & \frac{Cf}{muf} & 0 & \frac{-1}{muf} & 0 & 0 \\ \frac{CrTr}{mur} & \frac{-CrBr}{mur} & \frac{Cr}{mur} & 0 & 0 & \frac{-1}{mur} & 0 \\ \frac{-CrTr}{mur} & \frac{-CrBr}{mur} & \frac{Cr}{mur} & 0 & 0 & 0 & \frac{-1}{mur} \end{bmatrix}$$

$$f(t) = \begin{bmatrix} 0 & 0 & 0 & 0 \\ 0 & 0 & 0 & 0 \\ 0 & 0 & 0 & 0 \\ 0 & 0 & 0 & 0 \\ 0 & 0 & 0 & 0 \\ 0 & 0 & 0 & 0 \\ 0 & 0 & 0 & 0 \\ 0 & 0 & 0 & 0 \\ 0 & 0 & 0 & 0 \\ 0 & 0 & 0 & 0 \\ \frac{Ktf}{muf} & 0 & 0 & 0 \\ 0 & \frac{Ktf}{muf} & 0 & 0 \\ 0 & 0 & \frac{Ktr}{mur} & 0 \\ 0 & 0 & 0 & \frac{Ktr}{mur} \end{bmatrix} \begin{bmatrix} \dot{Z}r1 \\ \dot{Z}r2 \\ \dot{Z}r3 \\ \dot{Z}r4 \end{bmatrix}$$

Appendix B

State Space Equation for an Active (SAVGS) Suspension

$$\dot{X}(t) = AX(t) + Bu(t) + f(t) \qquad , A = \begin{bmatrix} A11 & A12 \\ A21 & A22 \end{bmatrix}$$

$$Bu(t) = \begin{bmatrix} 0 & 0 & 0 & 0 \\ 0 & 0 & 0 & 0 \\ 0 & 0 & 0 & 0 \\ 0 & 0 & 0 & 0 \\ 0 & 0 & 0 & 0 \\ 0 & 0 & 0 & 0 \\ 0 & 0 & 0 & 0 \\ \frac{Tf}{Ir} & \frac{-Tf}{Ir} & \frac{Tr}{Ir} & \frac{-Tr}{Ir} \\ \frac{a}{Ip} & \frac{a}{Ip} & \frac{-b}{Ip} & \frac{-b}{Ip} \\ \frac{1}{ms} & \frac{1}{ms} & \frac{1}{ms} & \frac{1}{ms} \\ \frac{-1}{muf} & 0 & 0 & 0 \\ 0 & \frac{-1}{muf} & 0 & 0 \\ 0 & 0 & \frac{-1}{mur} & 0 \\ 0 & 0 & 0 & \frac{-1}{mur} \end{bmatrix} \begin{bmatrix} u1 \\ u2 \\ u3 \\ u4 \end{bmatrix}$$

The Dynamic state equation function Build in MATLAB-Simulink of SAVGS

```
function
[Zcmc_2dot,Phi_2dot,theta_2dot,Zu1_2dot,Zu2_2dot,Zu3_2dot,Zu4_2dot,Zs1,Zs2,Zs
3,Zs4,Zlin1_dot,Zlin2_dot,Zlin3_dot,Zlin4_dot] =
fcn(Zcmc_dot,Zcmc,Phi_dot,Phi,...

theta_dot,theta,Zu1dot,Zu1,Zu2dot,Zu2,Zu3dot,Zu3,Zu4dot,Zu4,Zr1,Zr2,Zr3,Zr4,Z
lin1,Zlin2,Zlin3,Zlin4,U1,U2,U3,U4)

bf=1.1;
br=1.2;
Tf=1.405;
Tr=1.43;
Ms=1350;
Ip=2100;
Ir=460;
mu1=60;
mu2=60;
mu3=60;
mu4=60;
Keq1=60000;
Keq2=60000;
Keq3=20700;
Keq4=20700;
```

```
Ceq1=5000;
Ceq2=5000;
Ceq3=4000;
Ceq4=4000;
Kt1=275000;
Kt2=275000;
Kt3=275000;
Kt4=275000;
Ct1=300;
Ct2=300;
Ct3=300;
Ct4=300;
Rsdf=0.72;
Rsdr=0.88;
Zlin1_dot=(1/Rsdf)*(Zcmc_dot-bf*theta_dot-0.5*Tf*Phi_dot-Zu1dot);
Zlin2_dot=(1/Rsdf)*(Zcmc_dot-bf*theta_dot+0.5*Tf*Phi_dot-Zu2dot);
Zlin3_dot=(1/Rsdr)*(Zcmc_dot+br*theta_dot-0.5*Tr*Phi_dot-Zu3dot);
Zlin4_dot=(1/Rsdr)*(Zcmc_dot+br*theta_dot+0.5*Tr*Phi_dot-Zu4dot);

Zs1=Zcmc-bf*theta-0.5*Tf*Phi;
Zs2=Zcmc-bf*theta+0.5*Tf*Phi;
Zs3=Zcmc+br*theta-0.5*Tr*Phi;
Zs4=Zcmc+br*theta+0.5*Tr*Phi;

Zcmc_2dot=(Keq1*(Zu1-(Zs1))+Ceq1*(Zu1dot-(-bf*theta_dot-
0.5*Tf*Phi_dot+Zcmc))+...
         Keq2*(Zu2-(Zs2))+Ceq2*(Zu2dot-(-
bf*theta_dot+0.5*Tf*Phi_dot+Zcmc))+...
         Keq3*(Zu3-(Zs3))+Ceq3*(Zu3dot-(br*theta-0.5*Tr*Phi+Zcmc_dot))+...
         Keq4*(Zu4-(Zs4))+Ceq4*(Zu4dot-
(br*theta+0.5*Tr*Phi+Zcmc_dot))+U1+U2+U3+U4)/Ms;

Phi_2dot=(0.5*Tf*(Keq2*(Zu2-(Zs2)))+0.5*Tf*(Ceq2*(Zu2dot-(-
bf*theta_dot+0.5*Tf*Phi_dot+Zcmc_dot)))-...
         0.5*Tf*(Keq1*(Zu1-(Zs1)))-0.5*Tf*(Ceq1*(Zu1dot-(-bf*theta_dot-
0.5*Tf*Phi_dot+Zcmc_dot)))+...
         0.5*Tr*(Keq4*(Zu4-(Zs4)))+0.5*Tr*(Ceq4*(Zu4dot-
(br*theta_dot+0.5*Tr*Phi_dot+Zcmc_dot)))-...
         0.5*Tr*(Keq3*(Zu3-(Zs3)))-0.5*Tr*(Ceq3*(Zu3dot-(br*theta_dot-
0.5*Tr*Phi_dot+Zcmc_dot)))+Tf*U1-Tf*U2+Tr*U3-Tr*U4)/Ir;

theta_2dot=(-bf*(Keq1*(Zu1-(Zs1)))-bf*(Ceq1*(Zu1dot-(-bf*theta_dot-
0.5*Tf*Phi_dot+Zcmc_dot)))-...
         bf*(Keq2*(Zu2-(Zs2)))-bf*(Ceq2*(Zu2dot-(-
bf*theta_dot+0.5*Tf*Phi_dot+Zcmc_dot)))+...
         br*(Keq3*(Zu3-(Zs3)))+br*(Ceq3*(Zu3dot-(br*theta_dot-
0.5*Tr*Phi_dot+Zcmc_dot)))+...
         br*(Keq4*(Zu4-(Zs4)))+br*(Ceq4*(Zu4dot-(br*theta_dot
+0.5*Tr*Phi_dot+Zcmc_dot)))+bf*U1+bf*U2-br*U3-br*U4)/Ip;

Zu1_2dot=(-Keq1*(Zu1-(Zs1)-Zlin1)-Ceq1*(Zu1dot-(-bf*theta_dot-
0.5*Tf*Phi_dot+Zcmc_dot)-Zlin1_dot)+Kt1*(Zr1-Zu1)-Ct1*Zu1dot-U1)/mu1;

Zu2_2dot=(-Keq2*(Zu2-(Zs2)-Zlin2)-Ceq2*(Zu2dot-(-
bf*theta_dot+0.5*Tf*Phi_dot+Zcmc_dot)-Zlin2_dot)+Kt2*(Zr2-Zu2)-Ct2*Zu2dot-
U2)/mu2;
```

```
Zu3_2dot=(-Keq3*(Zu3-(Zs3)-Zlin3)-Ceq3*(Zu3dot-(br*theta_dot-
0.5*Tr*Phi_dot+Zcmc_dot)-Zlin3_dot)+Kt3*(Zr3-Zu3)-Ct3*Zu3dot-U3)/mu3;

Zu4_2dot=(-Keq4*(Zu4-(Zs4)-Zlin4)-Ceq4*(Zu4dot-
(br*theta_dot+0.5*Tr*Phi_dot+Zcmc_dot)-Zlin4_dot)+Kt4*(Zr4-Zu4)-Ct4*Zu4dot-
U4)/mu4;
```